KONINKLIJK BELGISCH INSTITUUT VOOR NATUURWETENSCHAPPEN
OD NATUUR – BEHEERSEENHEID VAN HET MATEMATISCH MODEL

MOnitoring en MOdellering van het cohesieve sedimenttransport en evaluatie van de effecten op het mariene ecosysteem ten gevolge van bagger- en stortoperatie (MOMO)

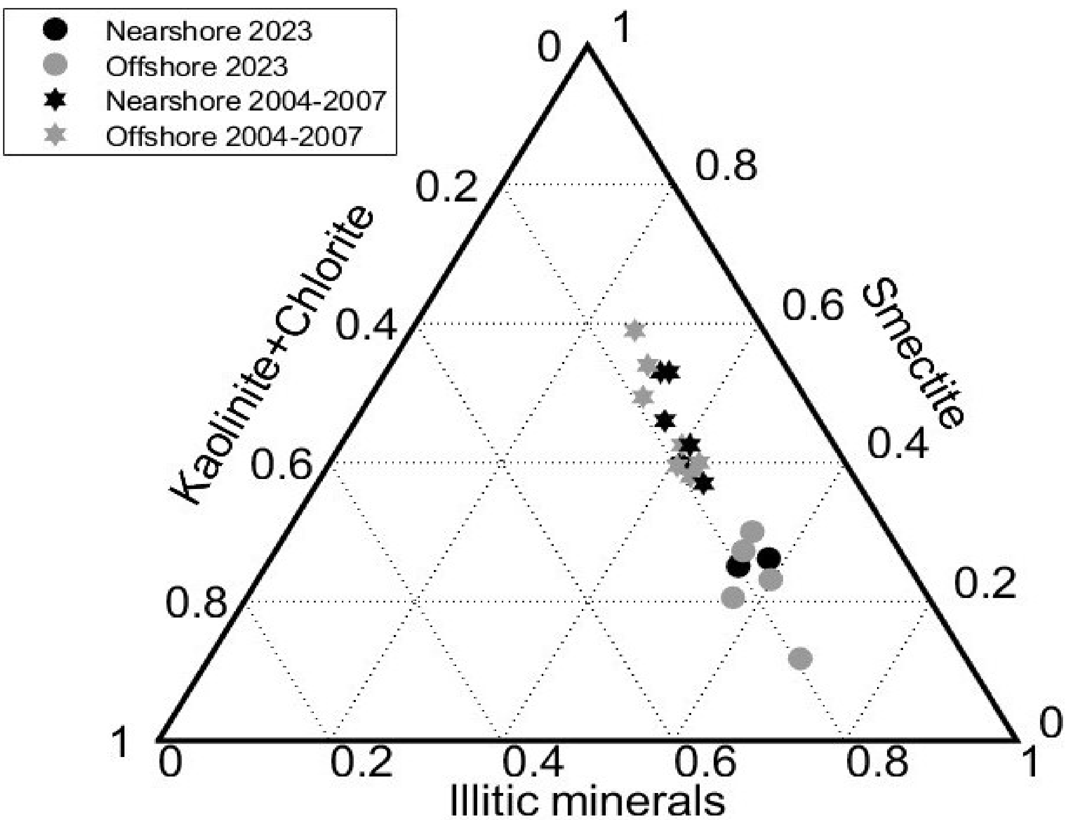

Activiteitsrapport (1 juli - 31 december 2024)

Michael Fettweis, Saumya Silori, Duc Tran, Xavier Desmit

MOMO/10/MF/202502/NL/AR/6

KBIN-OD Natuur - BMM
Vautierstraat 29
B–1000 Brussel
België

Inhoudstafel

1. Inleiding

1.1. Voorwerp van deze opdracht

Het MOMO-project (monitoring en modellering van het cohesieve sedimenttransport en de evaluatie van de effecten op het mariene ecosysteem ten gevolge van bagger- en stortoperatie) maakt deel uit van de algemene en permanente verplichtingen van monitoring en evaluatie van de effecten van alle menselijke activiteiten op het mariene ecosysteem waaraan België gebonden is overeenkomstig het verdrag inzake de bescherming van het mariene milieu van de noordoostelijke Atlantische Oceaan (1992, OSPAR-Verdrag). De OSPAR Commissie heeft de objectieven van haar Joint Assessment and Monitoring Programme (JAMP) gedefinieerd tot 2021 met de publicatie van een holistisch "quality status report" van de Noordzee en waarvoor de federale overheid en de gewesten technische en wetenschappelijke bijdragen moeten afleveren ten laste van hun eigen middelen.

De menselijke activiteit die hier in het bijzonder wordt beoogd, is het storten in zee van baggerspecie waarvoor OSPAR een uitzondering heeft gemaakt op de algemene regel "alle stortingen in zee zijn verboden" (zie OSPAR-Verdrag, Bijlage II over de voorkoming en uitschakeling van verontreiniging door storting of verbranding). Het algemene doel van de opdracht is het bestuderen van de cohesieve sedimenten op het Belgisch Continentaal Plat (BCP) en dit met behulp van zowel numerieke modellen als het uitvoeren van metingen. De combinatie van monitoring en modellering zal gegevens kunnen aanleveren over de transportprocessen van deze fijne fractie en is daarom fundamenteel bij het beantwoorden van vragen over de samenstelling, de oorsprong en het verblijf ervan op het BCP, de veranderingen in de karakteristieken van dit sediment ten gevolge van de bagger- en stortoperaties, de effecten van de natuurlijke variabiliteit, de impact op het mariene ecosysteem in het bijzonder door de wijziging van habitats, de schatting van de netto input van gevaarlijke stoffen op het mariene milieu en de mogelijkheden om deze laatste twee te beperken.

Een samenvatting van de resultaten uit de vergunningsperioden 2017-2021 en 2022-2026 kan gevonden worden in het "Vooruitgangsrapport (juni 2019) over de effecten op het mariene milieu van baggerspeciestortingen" (Lauwaert et al. 2019), het "Syntheserapport over de effecten op het mariene milieu van baggerspeciestortingen" (Lauwaert et al., 2021) en het Vooruitgangsrapport (juni 2024) over de effecten op het mariene milieu van baggerspeciestortingen" (Fettweis et al., 2024) die gepubliceerd werden conform art. 10 van het K.B. van 12 maart 2000 ter definiëring van de procedure voor machtiging van het storten in de Noordzee van bepaalde stoffen en materialen.

1.2. Algemene doelstellingen

Het onderzoek uitgevoerd in het MOMO project kadert in de algemene doelstellingen om de baggerwerken op het BCP en in de kusthavens te verminderen, om de effecten van het storten van baggerspecie te kwantificeren en om een gedetailleerd inzicht te verwerven van de fysische processen die plaatsvinden in het mariene kader waarbinnen deze baggerwerken worden uitgevoerd. Dit impliceert enerzijds beleidsondersteunend onderzoek naar de vermindering van de sedimentatie op de baggerplaatsen en het evalueren van alternatieve stortmethoden. Anderzijds is vernieuwend onderzoek noodzakelijk om beter de effecten van het storten van baggerspecie in te schatten. Dit onderzoek is specifiek gericht op het dynamische gedrag van slib in de waterkolom en op de bodem en de interacties tussen fysische en biologische processen en zal uitgevoerd worden met behulp van modellen, in situ metingen en remote sensing data.

De specifieke acties die binnen dit onderzoek uitgevoerd worden om de algemene doelstellingen in te vullen zijn:

1. Streven naar een efficiënter stortbeleid door een optimalisatie van de stortlocaties.

2. Continue monitoring van het fysisch en biogeochemisch milieu waarbinnen de baggerwerken worden uitgevoerd (Taak 1) en aanpassing van de monitoring aan de nog op te stellen targets voor het bereiken van de goede milieutoestand (GES), zoals gedefinieerd zal worden binnen MSFD;

3. Uitbouw en optimalisatie van het numerieke modelinstrumentarium, ter ondersteuning van het onderzoek (Taak 2.1).

1.3. Algemeen Onderzoek 2012-2026

Het onderzoek heeft als doel om de effecten van baggerspeciestortingen op het mariene ecosysteem (fysische en biogeochemische aspecten) te onderzoeken. Hiervoor worden in situ metingen verzameld, gebruik gemaakt van remote sensing data en worden numerieke modellen ingezet. Voor de vergunningsperiode 2022-2026 worden volgende taken voorzien:

1) In situ en remote sensing metingen en data-analyse
De monitoring van effecten van baggerspeciestortingen gebeurd met behulp van een vast meetstation in de nabijheid van MOW1, en met meetcampagnes met de RV Belgica (een 10-tal meetcampagnes voor het verzamelen van traject informatie, profielen en de calibratie van sensoren; en een 10-tal campagnes voor het onderhoud van het meetstation te MOW1). De geplande monitoring is gericht op het begrijpen van processen, zodoende dat de waargenomen variabiliteit en de effecten van baggerspeciestortingen in een correct kader geplaatst kunnen worden. Een belangrijk deel is daarom gericht op zowel het uitvoeren van de in situ metingen, het garanderen van kwalitatief hoogwaardige data en het archiveren, rapporteren en interpreteren ervan. Remote sensing data afkomstig van onder andere satellieten worden gebruikt om een ruimtelijk beeld te bekomen.

2) Uitbouw en optimalisatie van het modelinstrumentarium
Het tijdens de voorbije jaren verbeterde en aangepaste slibtransportmodel zal verder worden ontwikkeld. Dit zal parallel gebeuren met de nieuwe inzichten die voorvloeien uit de metingen en de procesgerichte interpretatie van de metingen.

3) Ondersteunend wetenschappelijke onderzoek
Monitoring gebaseerd op wetenschappelijke kennis is essentieel om de effecten van menselijke activiteiten (hier het storten van baggerspecie) te kunnen inschatten en beheren. Om te kunnen voldoen aan de door OSPAR opgelegde verplichtingen van monitoring en evaluatie van de effecten van menselijke activiteiten is het ontwikkelen van nieuwe monitorings- en modelleractiviteiten nodig. Dit houdt in dat onderzoek dat de actuele stand van de wetenschappelijke kennis weerspiegelt wordt uitgevoerd en dat de hieruit voortvloeiende nieuwe ontwikkelingen geïntegreerd zullen worden in zowel de verbetering van het modelinstrumentarium als voor het beter begrijpen van het kustnabije ecosysteem.

1.4. Onderzoek Januari 2022 – December 2024

Voor de periode 2019-2021 werd rekening gehouden werd met de aanbevelingen voor de minister ter ondersteuning van de ontwikkeling van een versterkt milieubeleid zoals geformuleerd in het "Syntheserapport over de effecten op het mariene milieu van baggerspeciestortingen (2021)" dat uitgevoerd werd conform art. 10 van het K.B. van 12 maart 2000 ter definiëring van de procedure voor machtiging van het storten in de

Noordzee van bepaalde stoffen en materialen.

Taak 1: In situ en remote sensing metingen en data-analyse

Taak 1.1 Langdurige metingen te MOW1 en W05

Sinds eind 2009 worden er continue metingen uitgevoerd te MOW1 met behulp van een meetframe (tripode). Met dit frame worden stromingen, slibconcentratie, korrelgrootte-verdeling van het suspensiemateriaal, saliniteit, temperatuur, waterdiepte en zeebodem altimetrie gemeten. Om een continue tijdreeks te hebben, wordt gebruik gemaakt van 2 tripodes. Na ongeveer 1 maand wordt de verankerde tripode voor onderhoud aan wal gebracht en wordt de tweede op de meetlocatie verankerd. Op de meetdata wordt een kwaliteitsanalyse uitgevoerd, zodat de goede data onderscheiden kunnen worden van slechte of niet betrouwbare data.

Veranderingen in kustnabije ecosystemen zijn dikwijls gecorreleerd met veranderingen van de helderheid van het water of de concentratie aan particulair suspensiemateriaal (SPM) en dus ook met het gehalte aan particulair organisch materiaal. De zone waar de invloed van het minerale en kustnabij suspensiemateriaal overgaat in een zone met dominantie van organisch suspensiemateriaal van mariene origine is van bijzonder belang. De monitoring wordt uitgebreid met de verankering van een meetboei in locatie W05 (51°N 24.96’, 2°E 48.7’). W05 is één van de drie monitoringspunten waar waterstalen en sensormetingen maandelijks worden uitgevoerd.

Taak 1.2 Calibratie van sensoren tijdens in situ metingen

Tijdens meetcampagnes met de R/V Belgica zullen een voldoende aantal 13-uursmetingen uitgevoerd worden met als hoofddoel het kalibreren van optische of akoestische sensoren en het verzamelen van verticale profielen. De metingen zullen plaatsvinden in het kustgebied van het BCP (MOW1, W05). De optische metingen (Optical Backscatter Sensor) zullen gekalibreerd worden met de opgemeten hoeveelheid materie in suspensie (gravimetrische bepalingen na filtratie) om te komen tot massa concentraties

Taak 1.3 Bio-geo-chemische monitoring van het SPM (BGCMonit)

SPM bestaat uit minerale deeltjes van fysicochemische (b.v. kleimineralen, kwarts, veldspaat) en biogene oorsprong (b.v. calciet, aragoniet, opaal), levend (bacteriën, fyto- en zoöplankton) en niet-levend organisch materiaal (b.v. fecale pellets, detritus, exopolymeren), en partikels van menselijke oorsprong (microplastiek). Het SPM kan door hydrofobe organische polluenten of metalen gecontamineerd zijn. De samenstelling en concentratie van het SPM inclusief de hydrofobe polluenten verandert in functie van de tijd en de locatie. Deze variaties worden beïnvloed door de interacties tussen de fysische processen (getij, meteo, klimaat), biologische cycli (algenbloei), chemische processen (koolstofcyclus) en menselijke activiteiten (aanvoer van nutriënten, bagger- en stortactiviteiten, offshore constructies). De samenstelling van het particulair en opgelost suspensiemateriaal zal bepaald worden tijdens meetcampagnes met de RV Belgica tijdens een 10-tal campagnes per jaar. Naast de totale hoeveelheid aan SPM worden ook de concentraties aan verschillende organische bestanddelen (POC, PON, TEP, chlorofyl en phaeofytine) bepaald. De opgeloste stoffen zijn inorganische nutriënten, DOC, DIC en alkaliniteit. Stalen van suspensiemateriaal zullen genomen worden met de centrifuge om de samenstelling ervan te bepalen.

Taak 1.4: Archivering en verwerking van de data

De meetdata worden gearchiveerd en er wordt een kwaliteitsanalyse uitgevoerd, zodat de goede data onderscheiden kunnen worden van slechte of niet betrouwbare data. Slechte data kunnen bv optreden doordat het instrument slecht heeft gewerkt en verkeerd werd ingesteld. Niet betrouwbare data zijn typisch geassocieerd met bv biofouling. De data en metadata worden gearchiveerd. De metingen worden verwerkt en geïnterpreteerd. En zullen dienen als basis voor het verder gebruik bij wetenschappelijke vraagstellingen.

Taak 2: Uitbouw en optimalisatie van het modelinstrumentarium

Taak 2.1: Opstellen van een slibtransportmodel voor het BCP met Coherens V2

Een slibtransportmodel zal worden geïmplementeerd met de software Coherens V2. De software laat toe om rekening te houden met gemengde sedimenten en dus met de interactie tussen zand en slib en laat morfologische berekeningen toe door een verbeterde implementatie van het schema voor het massabehoud en gebruik van lagen met gemengde sedimenten. Verdere aanpassingen en verbeteringen aan het model zullen worden uitgevoerd, meer bepaald:

- Kritische bodemschuifspanning voor erosie van gemengde sedimenten,
- Formulering voor de bodemschuifspanning,
- Koppeling van het model met het TILES voxel model voor een betere voorstelling van de bodemkarakteristieken.

Taak 2.2: Validatie van het slibtransportmodel voor het jaar 2013 (stortproef)

Een eerste toepassing van het model kan het jaar 2013 zijn, waarin de terreinproef voor alternatieve stortplaats alsook een intensieve monitoring plaatsvond. Deze laatste zal gebruikt worden voor de validatie van het model. Verder zal het model vergeleken worden met andere modellen van het BCP.

Taak 2.3: Optimalisatie baggerwerken

Een operationeel stortmodel zal worden opgezet in overleg met aMT. Dit model zal geïntegreerd worden in de binnen BMM-OD Natuur beschikbare operationele modellen. Het model zal gebruikt worden om in functie van de voorspelde fysische (wind, stroming, golven, sedimenttransport, recirculatie), economische (afstand, grootte baggerschip) en ecologische aspecten op korte termijn een keuze te kunnen maken tussen de beschikbare stortlocaties. Een eerste test hiervoor werd uitgevoerd in Van den Eynde en Fettweis (2011) waarin werd aangetoond dat door een optimale positie te kiezen voor het storten van baggerspecie in functie van de meteorologische omstandigheden, een vermindering van de aanslibbing van de vaargeulen en haven van Zeebrugge kan worden verwacht.

Het model zal worden gebruikt voor de optimalisatie van de baggerwerken. Verschillende simulaties kunnen worden uitgeoefend waarbij de invloed van de verschillende mogelijke stortplaatsen kunnen worden geëvalueerd.

Taak 2.4: Flocculatiemodel

De inzichten die voortvloeien uit de in situ data (Taken 1.4, 3.1 en 3.2) zullen worden geïntegreerd in een numeriek model dat het verband tussen SPM, TEP en flocculatie langsheen temporele (getij, seizoenen) en geografische (waterkolom, onshore-offshore) schalen combineert. Het model zal worden opgezet als 1D verticaal en zal gekoppeld worden met het 2 klassen populatie model van Lee et al. (2011). Hierdoor zal de verticale verdeling van de minerale en de organische fractie van het SPM en hun interactie kunnen worden voorspeld.

Taak 3: Ondersteunend wetenschappelijk onderzoek

Monitoring gebaseerd op wetenschappelijke kennis is essentieel om de effecten van menselijke activiteiten (hier het storten van baggerspecie) te kunnen inschatten en beheren. Om te kunnen voldoen aan de door OSPAR opgelegde verplichtingen van monitoring en evaluatie van de effecten van menselijke activiteiten is een verdere implementatie van huidige en het ontwikkelen van nieuwe monitoringsactiviteiten nodig.

Meer specifiek gericht op de activiteit 'storten van baggerspecie' worden hier – wat het fysische milieu betreft - turbiditeit, samenstelling van de zeebodem, bathymetrie en hydrografische condities beoogt. Deze taak speelt hierop in door de ontwikkeling en de implementatie van nieuwe tools die de actuele stand van de wetenschappelijke kennis weerspiegelen teneinde de mathematische modellen te optimaliseren en verfijnen.

Taak 3.1: SPM samenstelling - minerale fractie

Door de aanwezigheid van gemengde sedimenten in de zeebodem (zand en slib) zal tijdens sterke stroming en of hoge golven ook een gemengde minerale fractie in suspensie komen. Dit heeft twee consequenties voor monitoring. Ten eerste reageren akoestische en optische sensoren verschillend op zand en slib, zodat de verzamelde tijdreeksen een grotere onnauwkeurigheid hebben tijdens zo'n momenten (Fugate & Friedrichs, 2002; Baschek et al., 2017; Schwarz et al, 2017; Fettweis et al., 2019). Ten tweede bevatten zandkorrels geen mineraal-gebonden organisch materiaal en stalen genomen tijdens dit soort momenten kunnen dus de onzekerheid van het SPM-POM model vergroten. Indien er geen rekening gehouden wordt hiermee zal de SPM concentratie onder- of overschat worden alsook de afgeleid organische fracties. Doel is om de zand en slibfractie te identificeren door gebruik te maken van innovatieve meettechnieken (Pearsons et al., 2021) die optische en akoestische sensoren combineren. Het ultieme doel is om te komen tot tijdreeksen van zand- en slibconcentratie te MOW1.

Uit visuele inspecties van de bodemsamenstelling te MOW1 tijdens de laatste jaren blijkt dat het sediment zandiger is geworden. De hypothese is, dat dit verband houdt met erosie van de vooroever na de strandopspuitingen die de voorbije jaren werden uitgevoerd. Aan de hand van de boven aangehaalde methode zal nagegaan worden of er een trend naar zandaanrijking kan vastgesteld worden in de omgeving van MOW1.

Taak 3.2: SPM samenstelling - organische fractie

Het semi-empirisch POM-SPM model (Fettweis et al., 2022) zal verfijnd worden met de nieuwe data verzameld in taak 1.3. Hierdoor zal de inschatting van de minerale en de vers en mineraal-gebonden organische fractie nauwkeuriger kunnen worden gedaan.

Op basis van dit POM-SPM model kan de samenstelling van het suspensiemateriaal (minerale fractie, vers en mineraal gebonden POC, PON en TEP) worden berekend voor de tijdreeksen te MOW (vanaf 2005) en voor de satellietdata (vanaf 1997). Dit zal toelaten om de geografische en temporele variabiliteit van de transitiezone tussen het kustgebonden turbiditeitsmaximum en de offshore wateren te kwantificeren. De dynamica van het suspensiemateriaal in beide gebieden is verschillend, wat consequenties heeft naar de modellering ervan. Verder kan uit de lange tijdsreeksen gekeken worden of het gebruik van de stortplaatsen, meer bepaald S1, geleid heeft tot een zeewaartse uitbreiding van het turbiditeitsmaximum.

Taak 3.3: Trends in SPM concentratie

Om significante statistische trends te kunnen documenteren in SPM concentratie over de laatste decades, zijn metingen nodig die een lange tijdspanne omvatten en een groot gebied omvatten. Deze data zijn helaas niet beschikbaar. Wat er wel beschikbaar is zijn de tripode metingen te MOW1 (vanaf 2005) en op andere locaties, de puntmetingen verzameld met onderzoeksschepen in het Belgisch Deel van de Noordzee sinds ongeveer 1970 (cf. Belspo 4DEMON project) en satellietbeelden (vanaf 1997). De tripode data geven de temporele variabiliteit weer, maar zijn heel beperkt wat ruimtelijke spreiding betreft. De 4DEMON en satellietbeelden zijn beschikbaar over een lange periode en over een groot gebied, maar kunnen de temporele schaal niet oplossen. Om deze heterogene datasets samen te kunnen gebruiken, zal gekeken worden naar de statistische verschillen tussen de datasets en naar een manier om deze te combineren. Doel is om mogelijke trends in de SPM concentratie te identificeren en deze te linken aan natuurlijke veranderingen of aan menselijke activiteiten.

De trendanalyse van de historische data zal de basis vormen om de verandering van de SPM concentratie in de nabijheid van de nieuwe stortplaats ZBW te kwantificeren.

Taak 4: Rapportage en outreach

Om de zes maanden zal er een activiteitenrapport worden opgesteld dat de onderzoeksresultaten beschrijft. Jaarlijks wordt er een 'factual data' rapport opgesteld van de verzamelde meetgegevens. De resultaten uit het onderzoek zullen tevens worden voorgesteld op workshops, conferenties en in de wetenschappelijke literatuur.

1.5. Aanpassing onderzoeksplan naar aanleiding van de niet beschikbaarheid van de RV Belgica

Het onderzoek uitgevoerd door het KBIN heeft als doel om de effecten van baggerspeciestortingen op het mariene ecosysteem (fysische en biogeochemische aspecten) te onderzoeken. Hiervoor worden in situ metingen verzameld, gebruik gemaakt van remote sensing data en worden numerieke modellen ingezet. Door het wegvallen van de RV Belgica sinds juni 2024 tot vermoedelijk 2026 kan het verzamelen van in situ data (monitoring) enkel deels worden uitgevoerd. Ter verantwoording van het begrootte budget voor 2024 en 2025 wordt er een overzicht over de geplande activiteiten met betrekking tot de in situ monitoring gegeven als ook extra taken beschreven die verantwoorden waarvoor het voorziene budget zal gebruikt worden.

Taak 1: In situ en remote sensing metingen en data-analyse

<u>Taak 1.1 Langdurige metingen te MOW1 en W05</u>

De Zeetijger zal ingezet worden voor het voortzetten van de langdurige meting met behulp van een meetframe (tripode) te MOW1. Het uitbreiden van de langdurige monitoring met een meetboei te W05 zal worden uitgevoerd.

<u>Taak 1.5 Analysemethode TEP</u>

De analysemethode voor de TEP (transparant exoplymeric particle) werd recent verbeterd (zie activiteitsrapport MOMO/10/MF/202410/AR/5). TEP-concentratie wordt bepaald met behulp van de kationische kleurstof Alciaan Blauw. In de literatuur wordt vermeld dat dit soort kleurstoffen zich kunnen hechten aan kleimineralen, waardoor de TEP-concentratie mogelijks verkeerd wordt bepaald. Er zal daarom onderzocht worden of de aanwezigheid van kleimineralen (zie hieronder) in het SPM een invloed kan hebben op de TEP-concentratie.

Taak 3: Ondersteunend wetenschappelijk onderzoek

<u>Taak 3.4 SPM-samenstelling – mineralogie en interactie met organisch materiaal</u>

Deze taak zal worden aangevuld met een mineralogische analyse van het suspensiemateriaal. We zullen hiervoor materiaal gebruiken dat in 2023 werd verzameld met een centrifuge (RV Belgica). Een mineralogische karakterisatie (bulk en kleimineralogie) van het suspensiemateriaal werd in 2004-2007 uitgevoerd en diende als basis voor een herkomstonderzoek van het slib op het BCP. Met deze nieuwe analyse willen we nagaan of er zich veranderingen hebben voorgedaan en indien ja, waarom.
Mineralen en organisch materiaal vertonen beide cohesieve eigenschappen en interacties kunnen leiden tot organo-minerale associaties. In natuurlijke systemen komen mineralen en organisch materiaal altijd samen voor en zijn organo-minerale associaties op moleculaire tot mm-schaal alomtegenwoordig. Deze interacties vinden op verschillende manieren plaats, variërend van de sorptie van kleine en grotere organische moleculen aan

oppervlakken door bijvoorbeeld waterstofbruggen of van der Waals-krachten, tot intercalatie in expandeerbare kleimineralen, de occlusie in kleine kleimineraalaggregaten (flocculi), het incorporeren van grote organische deeltjes (bijvoorbeeld fytoplankton, bacteriën) in vlokken en de vorming van biofilms. In mariene sedimenten en in het suspensiemateriaal wordt het gehalte aan organische materiaal voornamelijk bepaald door de mineralen en de beschikbaarheid van organisch materiaal. Met behulp van de mineralogische karakteristieken zal een betere beschrijving van de stabiliteit van de organische fractie kunnen worden bepaald.

Taak 3.5: Trends in SPM concentratie en stortoperaties

Doel van dit onderzoek is om mogelijke trends in de SPM concentratie te identificeren en deze te linken aan natuurlijke veranderingen of aan menselijke activiteiten. Deze bestaande taak zal worden aangevuld met een onderzoek op het effect van stortplaats ZBW. Onderzoeksvragen zijn 1) of de herlocatie van de stortplaats ZBW tot een vermindering van de aanslibbing (SPM concentratie) in de haven van Zeebugge heeft geleid en 2) wat de veranderingen in SPM concentratie ter hoogte van ZBW is. Hiervoor zullen tripode en remote sensing data worden gebruikt.

1.6. Gerapporteerde en uitgevoerde taken

Periode Januari 2022 - Juni 2022

Taak 1.1: De meetreeks te MOW1 werd verdergezet.

Taak 1.2: Calibratie van OBS sensoren werd uitgevoerd tijdens RV Begica campagnes 2022/01, 2022/03, 2022/06, 2022/09 en 2022/14.

Taak 3.1: De akoestische en optische sensoren werden gebruikt om veranderingen in sedimentsamenstelling te zien te MOW1. Eerste resultaten worden getoond in hoofdstuk 2.

Taak 3.2: Intensieve bio-geochemische monitoring werd uitgevoerd te MOW1, W05 en W08 tijdens RV Belgica campagnes 2022/01, 2022/03, 2022/07, 2022/11, 2022/14). Eerste resultaten worden besproken in hoofdstuk 3.

Periode Juli 2022 - December 2022

Taak 1.1: De meetreeks te MOW1 werd verdergezet.

Taak 1.2: Calibratie van OBS sensoren werd uitgevoerd tijdens RV Begica campagnes 2022/17, 2022/19, 2022/21, 2022/24, 2022/28 en 2022/32.

Taak 2.4: De interactie van phytoplankton en SPM resulteert in de vorming van grotere vlokken met hogerer valsnelheden. In een labo experiment werd de flocculatie bestudeerd tussen klei en phytoplankton deeltjes. Een twee-klassen flocculatiemodel werd opgesteld om de experimentele data kwantitatief te analyseren, zie paper in appendix 1.

Taak 3.2: Intensieve bio-geochemische monitoring werd uitgevoerd te MOW1, W05 en W08 tijdens RV Belgica campagnes 2022/17, 2022/19, 2022/21, 2022/24, 2022/28 en 2022/32). Eerste resultaten worden besproken in hoofdstuk 3.

Taak 3.3: Het informatieverlies van niet continue tijdreeksen werd bepaald. Dit zal de basis vormen voor de trendanalyse in SPM concentratie over een langere periode, zie hoofdstuk 2.

Periode Januari 2023 - Juni 2023

Taak 1.1: De meetreeks te MOW1 werd verdergezet.

Taak 1.2: Calibratie van OBS sensoren werd uitgevoerd tijdens RV Begica campagnes 2023/01, 2023/04, 2023/06, 2023/08 en 2023/10.

Taak 2.4: Een 2D horizontaal flocculatiemodel werd gevalideerd voor het BCP (zie appendix 3). De resultaten tonen het nut van een flocculatiemodel voor grootschalig SPM transport modellering. Tegelijkertijd onderstrepen ze tekortkomingen die het gevolg zijn van de transitie tussen kust en offshore en die zich uiten in verschillende SPM dynamica (zie ook hoofdstuk 2). Dit dient

	opgenomen te worden in toekomstige modelleringen.
Taak 3:	De resultaten beschreven in hoofdstuk 2 hebben mogelijks consequenties voor het storten van baggerspecie. Zij tonen immers aan dat er een duidelijk verschil tussen een kustnabije zone die gedomineerd wordt door minerale deeltjes en een offshore zone die vooral uit organische deeltjes bestaat. Er is geen (of weinig) uitwisseling tussen deze twee zones, zie hoofdstuk 3.
Taak 3.1:	Analysen werden uitgevoerd gebaseerd op akoestische en optische sensoren van de tripode te MOW1 om de slib en zand fractie van het SPM te bepalen.
Taak 3.2:	De biogeochemische monitoring werd verdergezet te MOW1, W05 en W08 tijdens RV Belgica campagnes 2023/01, 2023/04, 2023/06, 2023/08 en 2023/10.

<u>Periode Juli 2023 – December 2023</u>

Taak 1.1:	De meetreeks te MOW1 werd verdergezet.
Taak 1.2:	Calibratie van OBS sensoren werd uitgevoerd tijdens RV Belgica campagnes 2023/17 en 2023/25.
Taak 1.3:	De biogeochemische monitoring werd verdergezet te MOW1, W05 en W08 tijdens RV Belgica campagnes 2023/17 en 2023/25.
Taak 2.4:	De interactie tussen phytoplankton en minerale partikels werd verdergezet, resultaten werden voorgesteld op de INTERCOH conferentie (zie Appendix 1).
Taak 3.1:	De analysen gebaseerd op akoestische en optische sensoren van de tripode te MOW1 om de slib en zand fractie van het SPM te bepalen, werden verdergezet. Eerste resultaten werden op de INTERCOH conferentie voorgesteld (zie Appendix 1)
Taak 3.2:	De verandering in samenstelling van het SPM werd bestudeerd over de waterkolom, conclusies met betrekking tot de gehele waterkolom in turbide gebieden worden besproken in hoofdstuk 2 (en Appendices 2-12) en werden voorgesteld op de INTERCOH conferentie (zie Appendix 1).

<u>Periode Januari 2024 – Juni 2024</u>

Taak 1.1:	De meetreeks te MOW1 werd verdergezet.
Taak 1.2:	Calibratie van OBS sensoren werd uitgevoerd tijdens RV Belgica campagnes 2024/01 en 2024/03.
Taak 1.3:	De biogeochemische monitoring werd verdergezet te MOW1, W05 en W08 tijdens RV Belgica campagnes 2024/01 en 2024/03.
Taak 3.1:	De analysen gebaseerd op akoestische en optische sensoren van de tripode te MOW1 om de slib en zand fractie van het SPM te bepalen worden besproken in hoofdstuk 2 voor de langdurige meetreeks te MOW1. De mineralogische samenstelling van het SPM werd bepaald in 4 locaties (MOW1, W03, W05 en W08).
Taak 3.2:	Er werd gewerkt aan een klimatologie van de biogeochemische parameters (particulair en opgelost) langsheen de kust-offshore gradiënt.

<u>Periode Juli 2024 – December 2024</u>

Taak 1.1:	De meetreeks te MOW1 werd enkel verdergezet tot september 2024, wegens het niet beschikbaar zijn van de Belgica.
Taak 1.2:	idem voor de calibratie van de OBS sensoren.
Taak 1.3:	idem voor de biogeochemisch monitoring te MOW1, W05 en W08.
Taak 2.4:	De interactie van biologische en minerale bestanddelen werd gemodelleerd in een 0D flocculatiemodel. Het model simuleert de fytoplankton groei en de productie van organisch material, inclusief de 'transparent exopolymer particles' (TEP) en is gekoppeld aan het 'two-class population balance equation' flocculatie model zie Appendix 1;
Taak 3.1:	Akoestische en optische sensoren van de tripode te MOW1 om de slib en zand fractie van het SPM te bepalen. Resultaten werden voorgesteld op de PECS concferentie, zie Appendices 2 en 3.
Taak 3.2:	De studie van de biogeochemische karakterisatie van particulaire en opgeloste parameters op het BCP werd afgewerkt. Een uitgebreid verslag ervan zal in het

komende rapport worden opgenomen, een samenvatting van de resultaten is te vinden in hoofdstuk 3.

Er werd meegewerkt aan een review paper over SPM dynamica, zie Appendix 4.

Taak 3.4: SPM-samenstelling – mineralogie en interactie met organisch materiaal. De taak werd uitgevoerd, zie hoofdstuk 2.

1.7. Publicaties

Hieronder wordt een overzicht gegeven van publicaties met directe betrokkenheid van het KBIN waar resultaten en data uit het MOMO project in worden gebruikt.

Activiteits-, Meet- en Syntheserapporten

Fettweis M, Silori S, Tran D, Desmit X. 2025. MOMO activiteitsrapport (1 juli - 31 december 2024). BMM-rapport MOMO/10/MF/202502/NL/AR/6, 34pp + app.

Fettweis M, Tran D, Knockaert M, Desmit X. 2024. MOMO activiteitsrapport (1 januari - 30 juni 2024). BMM-rapport MOMO/10/MF/202410/NL/AR/5, 27pp.

Fettweis M, Silori S, Desmit X. 2024. MOMO activiteitsrapport (1 juli - 31 december 2023). BMM-rapport MOMO/10/MF/202403/NL/AR/4, 29pp + app.

Fettweis M, Desmit X. 2023 MOMO activiteitsrapport (1 januari - 30 juni 2023). BMM-rapport MOMO/10/MF/202310/NL/AR/3, 28pp + app.

Fettweis M, Desmit X. 2023 MOMO activiteitsrapport (1 juli – 31 december 2022). BMM-rapport MOMO/10/MF/202303/NL/AR/2, 27pp + app.

Fettweis M, Baeye M, Desmit X. 2022 MOMO activiteitsrapport (1 januari – 30 juni 2022). BMM-rapport MOMO/10/MF/202210/NL/AR/1, 21pp + app.

Thesis

Brysse F. 2024. Optimalisatie en validatie van de 'Multiskan Skyhigh spectrofotometer' voor analyse van transparante exopolymeerpartikels (TEP) in zeewater. VIVES Hogeschool Campus Roeselare, Bachelor thesis in de agro- en biotechnologie, 55pp + app.

Conferenties/Workshops

Tran D, Verney R, Fettweis M. 2024. New insights into near-bed SPM concentration and sand/mud fraction. AGU Meeting, 9-13 December, Washington DC (USA).

Baeye M, Fettweis M, Verney R. 2024. On the effects of SPM composition on the inherent acoustic and optical particle properties of the SPM. Physics of Estuaries and Coastal Seas, 23-27 September, Bordeaux (France).

Tran D, Verney R, Fettweis M. 2024. New insights into near-bed SPM concentration and sand/mud fraction in the use of Sediment Composition Index. Physics of Estuaries and Coastal Seas, 23-27 September, Bordeaux (France).

Terseleer N, Kerimoglu O, Lee BJ, Fettweis M, Desmit X. 2024. A coupled biogeochemical-flocculation model to unravel suspended particulate matter dynamics on the Belgian shelf. Symposium on Advances in Marine Ecosystem Modelling Research, 8-11 July, Plymouth (UK).

Fettweis M. 2024. A universe of particles in a sip of water: Composition, concentration and size along the land-ocean transition. Geo-Colloquium University Kiel, 18 June, Kiel (Germany).

Fettweis M. 2024. Jerico Research Infrastructure @ RBINS. Conference on EU Research Infrastructures – Belgian Presidency EU2024. 4-5 June, Brussels (Belgium).

Desmit X, Terseleer Lillo N, Fettweis M, Kallend A, Sabbe K, Dujardin J, De Rijcke M. 2024 Impact of plankton-mineral interactions on the carbon cycle in the Southern North Sea. Particles in Belgium workshop, 3 May, VLIZ, Ostend.

Silori S, Fettweis M, Desmit X, Terseleer N, Riethmüller R, Schartau M. 2024. Vertical profiles of Chlorophyll and SPM at seasonal and tidal scales in a turbid, well-mixed coastal zone. Particles in Belgium workshop, 3 May, VLIZ, Ostend.

Tran D, Fettweis M. 2024 Characterizing the composition of sand and mud suspension in coastal and estuarine environments using combined optical and acoustic measurements. Particles in Belgium workshop, 3 May, VLIZ, Ostend.

Fettweis M, Delhaye L, Lee BJ, Riethmüller R, Schartau M, Silori S, Desmit X. 2023. Vertical

variations of suspended particle composition reflect particle dynamics. INTERCOH, 18-22 September, Inha University, Incheon (Korea).

Ho QN, Fettweis M, Hur J, Lee SD, Lee BJ. 2023. The role of microalgae in cohesive sediment flocculation: Insights from stochastic modeling and laboratory experiments. INTERCOH, 18-22 September, Inha University, Incheon (Korea).

Huynh TT, Fettweis M, Lee BJ. 2023. Application of an 1-DV TCPBE model with Bayesian calibration to diagnose the flocculation potential in the laboratory experiments and field measurement. INTERCOH, 18-22 September, Inha University, Incheon (Korea).

Pham TTTP, Ho QN, Lee SD, Fettweis M, Lee BJ. 2023. Isolation and characterization of the molecular composition of algal dissolved organic matter. INTERCOH, 18-22 September, Inha University, Incheon (Korea).

Tran D, Desmit X, Verney R, Fettweis M. 2023. Application of sediment composition index to predict suspended particulate matter concentration in the North Sea. INTERCOH, 18-22 September, Inha University, Incheon (Korea).

Kallend A, Dujardin J, De Rijcke M, Fettweis M, Sabbe K, Vyverman W, Desmit X. 2023. Interactions between phytoplankton, marine gels and suspended particulate matter in a dynamic, shallow coastal system before and during the phytoplankton spring bloom. ASLO Aquatic Sciences Meeting, 4–9 June, Palma de Mallorca (Spain).

Schartau M, Fettweis M, Desmit X, Terseleer N, Riethmüller R. 2023. From brown to blue water: Unraveling spatio-temporal variations in organic matter composition of suspended particulate matter. ASLO Aquatic Sciences Meeting, 4–9 June, Palma de Mallorca (Spain).

Baeye M, Delhaye L, Fettweis M. 2022. Acoustic and optical turbidity response to altering particle size distribution during extreme events. EuroSea/OceanPredict workshop, 29 June – 1 July, Exeter (UK).

Fettweis M, Desmit X, Terseleer N, Parmentier K, Van der Zande D, Schartau M, Lee BJ, Riethmüller R. 2022. The characteristics of the organic matter in biomineral flocs. Ocean Science Meeting, 24 February – 4 March, Honolulu (USA).

<u>Peer reviewed artikels</u>

Huynh TT, Kim J, Lee SD, Fettweis M, Bi Q, Kim SS, Lee SY, Choi YY, Lee BJ. 2024. Spatiotemporal dynamics of suspended particulate matter in the water environment: A review. *Water* 16, 3613.

Desmit X, Schartau M, Terseleer N, Van der Zande D, Riethmüller R, Fettweis M. 2024. The transition between coastal and offshore areas in the North Sea unraveled by the suspended particle composition. Science of the Total Environment 915, 169966. doi:10.1016/j.scitotenv.2024.169966

Escobar S, Bi Q, Fettweis M, Monbaliu J, Wongsoredjo S, Toorman E. 2023. A 2DH flocculation model for coastal domains. Ocean Dynamics 73, 333-358. doi:10.1007/s10236-023-01554-y

Fettweis M, Riethmüller R, Van der Zande D, Desmit X. Water quality monitoring in coastal seas: How significant is the information loss of patchy time series? Science of the Total Environment 873, 162273. doi:10.1016/j.scitotenv.2023.162273.

Fettweis M, Schartau M, Desmit X, Lee BJ, Terseleer N, Van der Zande D, Parmentier K, Riethmüller R. 2022. Organic matter composition of biomineral flocs and its influence on suspended particulate matter dynamics along a nearshore to offshore transect. Journal of Geophysical Research Biogeosciences, 126, e2021JG006332. doi:10.1029/2021JG006332

Ho NQ, Fettweis M, Hur J, Desmit X, Kim JI, Jung DW, Lee SD, Lee S, Choi YY, Lee BJ. 2022. Flocculation kinetics and mechanisms of microalgae- and clay-containing suspension in different microalgae growth phases. Water Research 226, 119300. doi:10.1016/j.watres.2022.119300

Ho QN, Fettweis M, Spencer KL, Lee BJ. 2022. Flocculation with heterogeneous composition in water environments: A review. Water Research. 118147. doi:10.1016/j.watres.2022.118147

2. Clay minerals and the stability of organic carbon in suspension along coastal to offshore transects

Minerals and organic matter (OM) are the major constituents of suspended particulate matter (SPM) in aquatic systems. Marine OM constitutes a mixture of plankton (phytoplankton, bacteria, etc.), exudates, detritus, faecal pellets, organic molecules originating from diverse autochthonous and allochthonous sources and organo-mineral associations (Arndt et al., 2013; Keil & Mayer, 2014). The lability of the OM ranges from high, for example living cells, to low, for example organo-mineral associations (Ittekkot, 1988; Mayer, 1994; Etcheber et al., 2007; Singh et al., 2016; Hemingway et al., 2019). The relative content of these different forms of OM varies temporally and spatially, due to biogeochemical and physical processes.

In marine systems, minerals and OM come mostly together and organo-mineral interactions on molecular to mm scale are ubiquitous. Clay minerals are the major mineral component in organo-mineral associations. The primary interaction between them takes place on molecular to nano scale; they have been well described in reviews (for example Mitchell & Sogai, 2005; Keil and Mayer, 2014; Deng et al., 2022; Zhao et al., 2023). These interactions occur in a variety of ways that goes from the adsorption of small and larger organic molecules onto surfaces by, for example, hydrogen bonds or van der Waals forces, to intercalation into expandable clay minerals and the occlusion into small clay mineral aggregates (flocculi). The resultant organo-mineral associations serve as building blocks or primary particles at a higher level of complexity known as biomineral flocs (Maggi, 2009; Lee et al., 2012; Shen et al., 2019). The interactions between organic molecules and minerals through adsorption/desorption kinetics show that a transition between the dissolved (organic molecules) and the particulate phase occurs (Kleber et al., 2021). Both the particulate (POM) and the dissolved organic matter (DOM) fractions are therefore not necessarily constant in composition and concentration (Middelburg et al., 1993; Blattmann et al., 2019).

The OM plays an important role in many coastal and estuarine processes, such as the formation of biomineral deposits and the sequestration of carbon; the variation in water clarity and its influence on primary production; flocculation and the settling of biomineral flocs; or the transport of pollutants (see for example Pedersen & Calvert, 1990; Mayer, 1994; Chen et al, 2016; Singh et al., 2016; Blattmann et al., 2019; Hemingway et al., 2019; Opdal et al., 2019; Fettweis et al., 2022). The interactions of minerals and OM may stabilize part of the organic carbon or prevent further degradation (Hemingway et al., 2019). Organo-mineral association and other stable OM are found in marine sediments. Before being sequestered, they have been transported in suspension; an accurate estimation of this OM fraction in the SPM is up to now lacking.

We argue in this study that the organic matter in suspension can be classified into three groups: A mineral-associated, a slowly degrading or non-metabolizable, and a fresh and consumable fraction that encompasses the living cells and their exudates. This classification reflects the various organo-mineral interactions better than the two types of POM (mineral-associated and fresh) that were put forward by Schartau et al. (2019) in their semi-empirical POM-SPM model. We propose to split their 'mineral-associated' fractions into a slowly degrading fraction (POC_{slow}) and a truly mineral-associated fraction ($POC_{mineral}$). The latter comprises the POC that is preserved from degradation through sorption of organic molecules to mineral surfaces and the intercalation into expandable clay minerals, and which depends mainly on the specific surface area of minerals (Keil & Mayer, 2014). We further argue that the mineral-associated POC fraction can be interpreted as DOC, it is thus a kind of pseudo POC, and the result of analysis methods. This could explain the variation in POC/DOC ratios as a function of SPM concentrations (Herman & Heip, 1999). The aim of our study is to estimate the content of the three POC groups in the SPM by collecting SPM from water samples and by analysing the POC and DOC concentration and the mineral composition.

2.1. Methods

2.1.1. Sampling

The samples were taken in 12 stations all located along a cross-shore transect that ranges from the high turbid nearshore to the low turbid offshore in the English Channel and the southern North Sea in spring (March-April) and winter (December) 2023, see Figure 2.1. The coordinates and the sampling date and time can be found in Table 2.1. The Belgian stations MOW1, W05, W08 and Codevco and the UK stations West Gabbard and Sizewell are in the Southern Bight of the North Sea; stations Scenes and BS1 in the Seine Bay (France), stations HB2, HB1 and Helgoland in the German Bight and station Dogger Bank in the central North Sea.

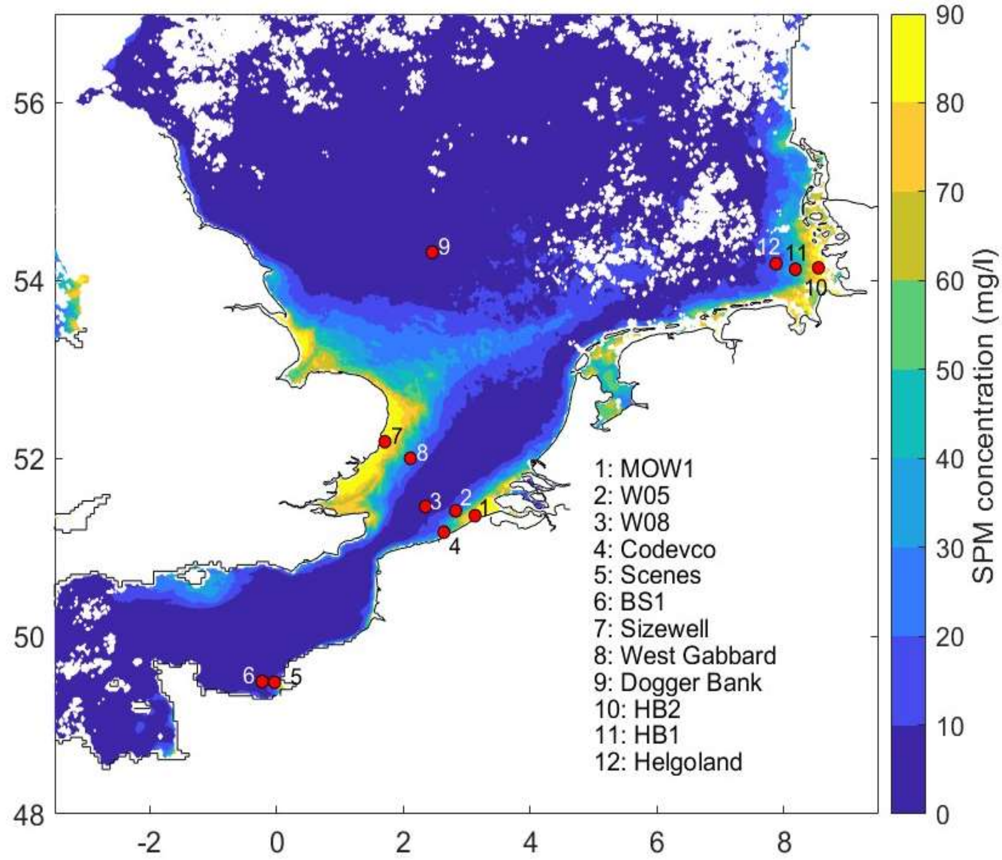

Figure 2.1. Map of sampling stations in the North Sea and the English Channel. The background displays the averaged near surface SPM concentrations computed using the algorithm of Nechad et al. (2010) from Sentinel-3/OLCI images between November 2019 and March 2020.

The sampling was done with Niskin bottles and a centrifuge with a water inlet at about 4 m below the surface. The data set from Niskin bottles consists of 1.5 or 2 hourly samples at the surface and near the bed collected during 13 full tidal cycles and 8 half tidal cycles, and 2 times 2 samples in one location. To compare both samples, we will use here only the surface samples from the water samples. The centrifuge was collecting SPM during the full or half tidal cycle in all stations except for Dogger bank where the collection was done during transit (started 3 hours before arrival until 3 after leaving the station). For station MOW1, W05 and W08 additional water samples data are available: MOW1 100 full tidal cycles since 2004, W05 40 full and half tidal cycles since 2018 and W08 37 full and half tidal cycles since 2019.

Table 2.1: Date (dd/mm) and time (hh:mm, UTC) of sampling and coordinates of the sampling stations.

	spring 2023	winter 2023	Latitude	Longitude
1 MOW1	06/04 06:45 - 19:00	13/12 09:00 - 21:00	51°N 21.3’	003°E 11.9’
2 W05	04/04 17:45 - 23:30	14/12 16:20 - 22:15	51°N 24.6’	002°E 49.5’
3 W08	05/04 15:30 - 21:00	15/12 18:20 - 16/12 00:30	51°N 27.5’	002°E 20.9’
4 Codevco	04/04 10:20 - 14:30	16/12 12:40 - 16:45	51°N 10.2’	002°E 38.4’
5 Scenes	26/03 15:20 - 27/03 03:00	06/12 11:30 - 23:00	49°N 28.8’	000°W 01.9’
6 BS1	27/03 11:00 - 23:00	-	49°N 29.4’	000°W 13.6’
7 Sizewell	29/03 16:00 - 30/03 04:00	08/12 05:00 - 17:00	52°N 11.2’	001°E 42.6’
8 West Gabbard	28/03 20:45 - 29/03 07:00	07/12 14:15 - 20:00	52°N 00.0’	002°E 06.6’
9 Dogger Bank	30/03 16:30 - 18:30	09/12 06:20 - 08:10	54°N 19.1’	002°E 27.4’
10 HB2	02/04 01:30 - 13:30	10/12 07:00 - 19:00	54°N 08.6’	008°E 33.0’
11 HB1	02/04 22:00 - 03/04 04:00	11/12 01:00 - 13:00	54°N 07.6’	008°E 11.1’
12 Helgoland	31/03 12:30 - 01/04 00:30	11/12 19:15 - 12/12 01:00	54°N 11.4’	007°E 52.8’

2.1.2. SPM, POC and DOC analysis

At every sampling occasion, three subsamples for SPM concentration were taken and filtered on board using pre-combusted (405°C, 24 hr.), rinsed, dried for 24 hr. at 105°C and pre-weighted 47 mm GF/C filters. After sampling the filters were rinsed with ultrapure water (resistivity 18.2 MΩ cm normalized at 25°C) and immediately stored at −20°C, before being dried for 24 hr. at 50°C and weighted to obtain the concentration. The uncertainty (expressed as the RMSE of the triplicates divided by the mean value) decreases with increasing concentration from 8.5% (SPM concentration <5 mg/l) to 6.7% (<10 mg/), 3.5% (10–50 mg/l), and 2.1% (>100 mg/l) and represent the random error related to the lack of precision during filtrations. The samples for POC were filtered on board using 25 mm GF/C filters (pretreated as above for SPM), stored immediately at −20°C, before being analysed using a Thermo Finnigan Flash EA1112 elemental analyser (for details see Ehrhardt and Koeve, 1999). The analytical uncertainty is 12%. The filtrates for the surface samples were collected in sample tubes for DOC and analysed using standard spectrophotometric methods with a Skalar autoanalyzer, for details see van der Zee & Chou (2005).

2.1.3. Semi-empirical POC-SPM model

A characteristic feature of the SPM is that the organic matter content decreases exponentially with increasing SPM concentration and reaches an asymptotic value at high SPM concentration, which is about 3% for the POC in the North Sea; at SPM concentration around 1 mg/l the POC content reaches values up to about 30% (Fettweis et al. 2022). Schartau et al. (2019) proposed a semi-empirical model of the POM content of the SPM (measured as Loss on Ignition) as a function of SPM concentration, which allowed to calculate the POM concentration when SPM concentration is known. The conceptual basis of the POM-SPM model is that the POM concentration can be written as the sum of two fractions, a fresh and labile fraction (POM_{fresh}) and a less reactive and more refractory fraction (POM_{ref}). The first boundary condition of the model is that, when the SPM concentration approaches zero, the POM content of SPM converges to one, and POM is assumed to be mainly POM_{fresh}. The second one is that, at high SPM concentrations, the POM content converges towards an invariant POM fraction of the SPM, which is assumed to be mainly refractory POM (POM_{ref}). The remaining POM is described as a time varying fraction of the SPM, which can be attributed to the buildup (primary production) and decay (remineralization) of POM_{fresh}. The model was later extended for the POC, the particulate organic nitrogen and the transparent exopolymer particle contents of the SPM (Fettweis et al. 2022). When calibrated with observational data, the model can estimate the compositional changes of the POC fraction as a function of the SPM concentration.

2.1.4. Grain size, mineralogy and mineral-associated OC

2.1.4.1. Grain size analysis

The grain-size volume distribution of the samples was measured with laser diffraction using a Malvern Mastersizer-S in water with ultrasound sonication and after a thorough chemical treatment to remove the cementing agents such as the often poorly crystalline calcite cements by a moderate oxalic acid buffering solution, the organics with peroxide/hypochlorite and the free (Fe-)oxides and -hydroxides with the Citrate-Bicarbonate-Dithionite method (modified after Jackson 1975). Crystalline calcite and opal are preserved.

2.1.4.2. Mineralogical analysis method

For bulk mineralogy, a representative portion of each sample was mixed with a 10% internal standard (ZnO) and 4 ml of ethanol. This mixture was milled for 5 min. using a McCrone micronizing mill and afterwards recuperated in porcelain cups (Środoń et al. 2001). The material was passed through a 250 µm sieve, side-loaded into alumina diffractometer holders to optimize the random orientation of crystallites. Bulk powders were measured by X-ray diffraction from 5 to 65° 2θ with steps of 0.02° lasting 2 s per step. Bulk powder diffraction patterns were analysed and quantified using the Quanta software (© Chevron ETC) which combines summation of pure reference standards and the use of a ZnO internal standard.

Proven robust quantitative clay mineral analyses have been used following the approach outlined by Drits et al. (1997), Sakharov et al. (1999), Środoń et al. (2001) and Zeelmaekers et al. (2015). All collected samples were subjected to a systematic preparation procedure to characterize both bulk mineral composition and clay mineral composition <2µm using X-ray diffraction analysis.

Approximately 100 g of each sample was dried at 60 °C and subsequently gently powdered and homogenized in a mortar. For clay mineral analysis, 15 g of powdered sample was subjected to a chemical preparation (modified after Jackson 1975) during which carbonate cements, organic matter and free Fe-(hydr)oxides were removed using respectively acetic acid/Na-acetate buffer solution, 30% H_2O_2 solution and Na-dithionite in a Na-citrate-bicarbonate environment respectively. Subsequently, clay material <2µm was extracted using a Thermo-Scientific SL-40R centrifuge and Ca-saturated using $CaCl_2$. Clay slides were prepared by sedimenting 160 mg of clay material <2µm on a glass slide. Both bulk powders and clay slides were measured using a Philips PW1050/37 goniometer connected to a PW1830 generator equipped with Cu-Kα radiation and PW3011/00 proportional detector in Bragg-Brentano θ–2θ setup. Clay slides were measured in air-dry conditions and saturated with ethylene glycol, each time from 2 to 47° 2θ with steps of 0.02° lasting 2 s per step. Clay slides were also exposed to 550 °C heating during 1 h and measured from 2 to 15° 2θ. Diffraction patterns of oriented slides were analysed and quantified using the Sybilla clay modeling software (© Chevron ETC) (Adriaens et al. 2014; Zeelmaekers et al. 2015).

2.1.4.3. *Mineral-associated OC content based on the mineral SSA*

A strong positive correlation between the mineral specific surface area (SSA) and the OC content in sediments has been reported (Mayer 1994; Keil & Mayer 2014). Different techniques are used to determine the SSA, such as the gas adsorption method (including the N_2 method), the ethylene glycol monoethyl ether method, and the methylene blue method (Macht et al. 2011; Zhu et al. 2015). The variation in methods and in experimental conditions impact the SSA. However, studies consistently show that smectite has the highest SSA, followed by illite, kaolinite, and chlorite, see Table 2.2. By comparison, fine sand and silt sized minerals have SSA of 0.1 and 1 m^2/g, respectively. The OC content per SSA (mg/m^2) has been reported as 0.5-1 mg OC/m^2 SSA (Keil & Mayer 2014) and 0.86 mg OC/m^2 Mayer (1994). Based on the mineral composition we have calculated the OC associated with the minerals per g of SPM using the average values of SSA (Table 2.2) and OC content per SSA.

Table 2.2: Specific surface area (m^2/g) of different clay minerals.

	Smectite	Illite	Kaolinite+Chlorite
Zhao et al. (2023)	500-800	60-120	10-20
Macht et al. (2011)	346±37	83±5	-
White (2005)	750	100-200	5-40
Kohnke (1986)	500-800	60-200	20-40
Fripiat (1964)	700-800	100-200	5-20
Greene-Kelly (1962)	600-700	150-250	15-25

2.2. Results

2.2.1. *Primary particle size*

The primary particle size distribution is unimodal in winter in all stations, the median size is between 3.5 and 5.4 µm, showing that the SPM is composed of fine mineral particles (see Table 2.3). In spring, all stations except the coastal-offshore transect HB2, HB1 and Helgoland, have a bimodal distribution, see Figure 2.2. The first mode corresponds to the winter one, whereas the second one is one order of magnitude larger (30-50 µm). These samples were taken during the spring phytoplankton bloom and the second mode probably corresponds to the diatom skeletons, which have sizes of such magnitude. The vanishing of that second mode before the winter may be due to a combination of biogenic silica settling and dissolution.

2.2.2. *Mineralogy*

The bulk mineralogical composition of the SPM samples consists mainly of non-clay minerals (quartz and feldspars), biogenic minerals (carbonates and opal) and clay minerals, see Figure 2.3 and Tables 2.4 and 2.5. The other minerals in Figure 2.3 are apatite, halite, rutile, anatase, pyrite and marcasite and are typical accessory minerals that occur in low quantities (<5%). The amorphous silica (opal) is from diatoms and is highest in spring, where it reached up to 20% of the SPM in station W05. Changes in mineral composition are observed along the nearshore to offshore transects. We see generally an increase of the non-clay mineral (quartz and feldspar) fraction towards the offshore, which points to a dependence on the relative dominance of sandy or muddy lithologies. The latter is more abundant in nearshore areas. The clay mineral content was during both campaigns higher in the turbid nearshore stations Sizewell (41%), MOW1 (35%), Scenes (35%) and in the German Bight stations HB2, HB1 and Helgoland (37%) than in the low turbid Belgian stations W05, W08 and Codevco (22%). In the remaining stations the clay mineral content was more variable between both campaigns (Dogger Bank: 19-47% and West Gabbard: 17-40%). The biogenic mineral fraction (carbonates and opal) increased generally towards the offshore, where it reached up to 50%. It was always high (42-50%) in stations MOW1, W05 and W08, and always low at Sizewell, Dogger Bank and HB2 (<30%). In the other stations the content was significantly higher in spring than in winter.

Table 2.3: The 10%, 50% and 90% percentile (in µm) of the primary particle size distribution in spring and winter 2023.

	spring 2023			winter 2023		
	D10 (µm)	D50 (µm)	D90 (µm)	D10 (µm)	D50 (µm)	D90 (µm)
MOW1	2.30	6.07	15.62	1.59	3.46	6.94
W05	2.23	5.44	16.67	2.35	4.94	9.98
W08	1.76	4.04	9.99	2.34	5.33	11.88
Codevco	1.91	4.32	10.09	-	-	-
Scenes	2.22	5.87	17.37	1.96	4.27	9.00
BS1	2.07	4.43	8.98	-	-	-
Sizewell	2.28	5.67	14.41	2.13	4.70	9.43
West Gabbard	2.15	5.34	15.27	2.49	5.39	11.11
Dogger Bank	2.57	14.75	56.02	1.82	3.85	7.54
HB2	2.23	5.08	11.34	2.23	5.11	11.13
HB1	2.12	4.41	8.66	2.02	4.26	8.39
Helgoland	1.88	3.76	7.07	2.11	4.82	11.31

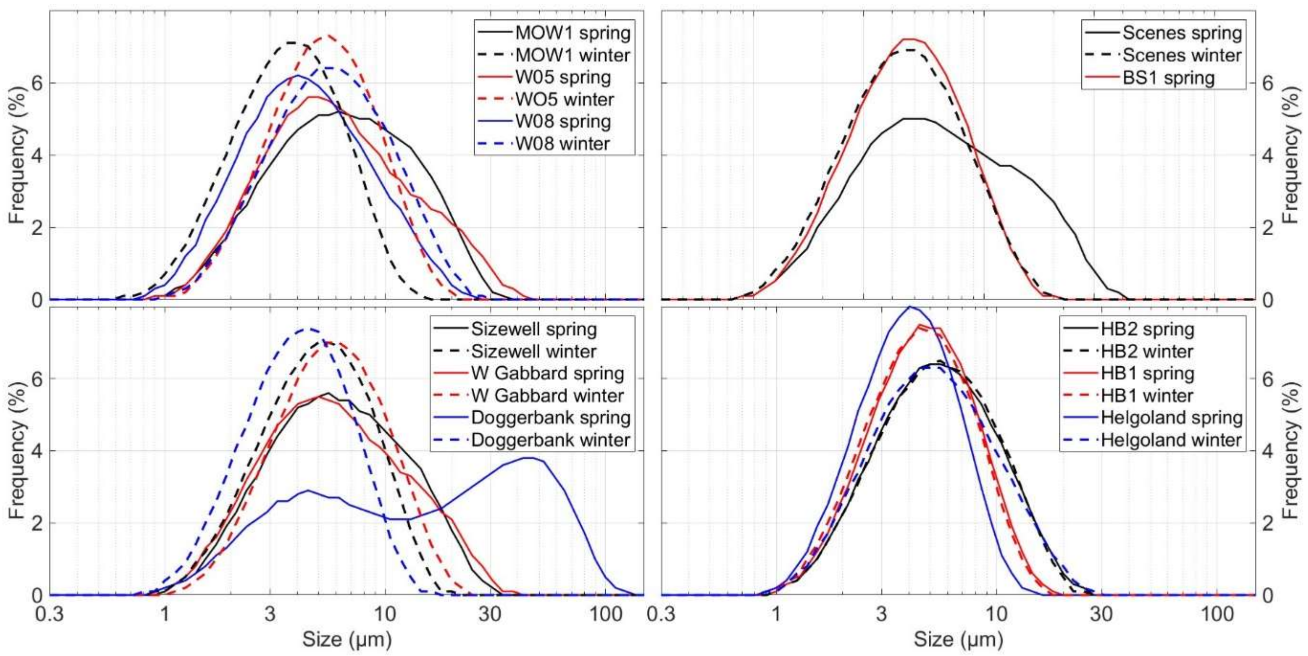

Figure 2.2: Primary particle size distribution of the SPM in spring and winter 2023.

Table 2.4: : Bulk mineralogy (sum=100%) and total OC (%) of the SPM in spring 2023 (K-feldspar, plagioclase, amphibole, chlorite, kaolinite, aragonite, dolomite, gypsum, anastase, marcasite).

	quartz	K-feld	plagio	amph	2:1 clays	chlor	kaol	calcite	arag	dolom	apatite	gyps	halite	rutile	anast	pyrite	marc	opal	TOC
MOW1	17.3	3.2	1.9	0.40	27.7	1.1	4.5	28.2	3.4	1.1	0.5	0	0.9	0.2	0.3	0.2	0	9.2	3.4
W05	21.7	4.0	2.6	0	15.7	0.5	2.3	23.0	4.2	0.8	0.5	0.4	4.0	0.2	0.3	0.0	0	19.7	11.3
W08	22.1	3.6	2.0	0	20.6	0.5	3.8	21.3	5.4	0.9	0.4	0	3.9	0.3	0.4	0.3	0	13.2	9.2
Codevco	18.3	2.4	2.2	0	19.0	0.6	3.2	31.0	4.4	0.9	0.4	0	3.6	0.2	0.3	0.1	0	13.5	6.7
Scenes	28.2	4.3	2.2	0	31.0	1.3	5.8	16.4	1.7	1.7	0.9	0	2.1	0.3	0.5	0.2	0	3.6	1.8
BS1	13.8	2.9	1.6	0	22.8	0.8	4.0	34.7	5.1	0.9	0.5	0	2.7	0.1	0.3	0.1	0	9.7	4.1
Sizewell	21.4	4.3	2.5	0.28	38.0	2.3	8.6	15.0	0.5	1.9	0.7	0	1.3	0.3	0.5	0.3	0.24	2.3	1.5
W Gabbard	20.1	2.7	2.6	0	18.2	0.8	2.9	36.1	4.5	1.3	0.6	0	2.2	0.1	0.2	0.1	0	7.5	2.1
Dogger Bank	18.0	4.0	3.2	0	31.6	2.0	5.1	15.4	2.4	1.4	0.5	0	2.2	0.3	0.4	0.3	0	13.2	2.9
HB2	17.4	3.9	2.9	0	35.0	2.0	5.4	14.4	2.0	1.3	0.3	0	2.4	0.3	0.4	0.5	0	11.7	3.0
HB1	14.0	2.5	1.7	0	22.7	0.7	3.6	36.1	5.1	1.0	0.4	0	2.3	0.1	0.3	0.1	0	9.4	3.7
Helgoland	15.4	3.7	2.6	0	33.0	1.7	5.9	15.7	2.6	1.2	0.5	0	2.8	0.3	0.4	0.1	0	14.2	4.8

Table 2.5: : Bulk mineralogy (sum=100%) and total OC (%) of the SPM in winter 2023 (K-feldspar, plagioclase, amphibole, chlorite, kaolinite, aragonite, dolomite, gypsum, anastase, marcasite).

	quartz	K-feld	plagio	amph	2:1 clays	chlor	kaol	calcite	arag	dolom	apatite	gyps	halite	rutile	anast	pyrite	marc	opal	TOC
MOW1	13.6	2.6	1.4	0	31.3	0.8	4.3	29.1	3.9	1.1	0.7	0	2.1	0.2	0.3	0	0	8.7	2.7
W05	21.7	3.5	2.9	0	16.9	0.5	2.1	34.5	6.6	1.1	0.6	0	2.8	0.2	0.3	0	0	6.4	1.9
W08	22.2	3.1	2.7	0	18.2	0.8	2.8	31.5	8.6	1.4	0.6	0	3.2	0.2	0.2	0	0	4.7	2.0
Codevco	-	-	-	-	-	-	-	-	-	-	-	-	-	-	-	-	-	-	-
Scenes	15.0	3.0	1.8	0	23.3	0.8	3.5	34.2	4.8	1.3	0.6	0	2.8	0.2	0.3	0.1	0	8.4	3.4
BS1	-	-	-	-	-	-	-	-	-	-	-	-	-	-	-	-	-	-	-
Sizewell	26.4	4.7	3.2	0	33.3	1.4	7.0	14.1	1.2	2.2	0.9	0	1.8	0.3	0.5	0.2	0	2.9	1.4
W Gabbard	23.7	5.3	2.1	0.5	31.1	1.6	7.7	17.4	1.4	1.9	0.6	0	2.4	0.3	0.5	0.2	0.23	3.0	1.5
Dogger Bank	18.3	4.2	3.5	0	37.1	1.7	8.2	13.9	1.3	2.5	1.0	0	3.4	0.3	0.4	0	0	4.1	2.9
HB2	21.7	4.5	3.8	0	31.9	1.8	5.0	13.1	1.7	2.1	0.6	0	2.4	0.3	0.4	0.5	0	10.3	2.8
HB1	22.8	4.5	4.1	0	30.8	1.7	4.4	14.0	1.7	2.2	0.7	0	3.0	0.3	0.4	0.5	0	9.1	3.0
Helgoland	18.0	4.0	3.3	0	29.1	1.5	4.3	20.2	2.3	2.0	0.6	0	4.2	0.3	0.4	0.2	0	9.8	3.4

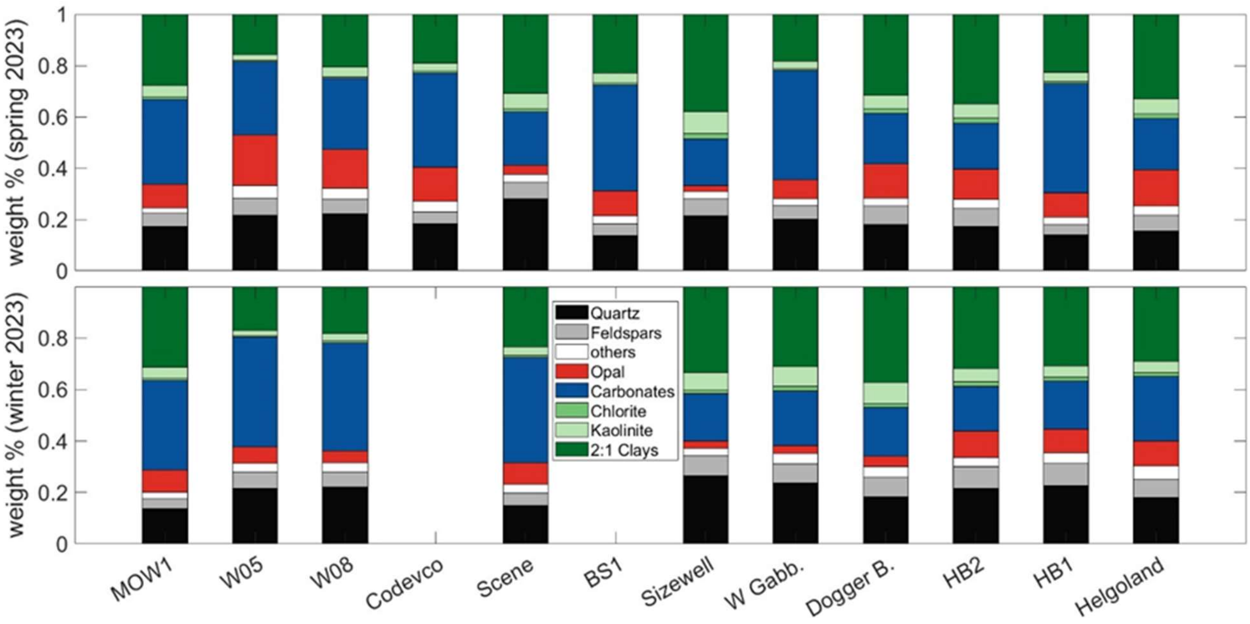

Figure 2.3: Bulk mineralogy of the SPM in spring (above) and winter 2023 (below), see Tables S3 and S4 in supplementary material for details.

The quantitative clay composition of the SPM consists of smectite, interstratified illite-smectite with about (65-75% illite), illite, kaolinite and chlorite (see Tables 2.6 and 2.7). In the ternary diagram, smectite, illitic minerals (sum of illite and interstratified illite-smectite) and kaolinite+chlorite form the endmember compositions (Figure 2.4). The clay mineral composition in all stations is on average 33.8±8.8% (interstratified illite-smectite), 25.5±6.0% (smectite), 16.6±5.1% (illite), 14.5±4.2% (kaolinite) and 2.1±0.6% (chlorite). The outliers in clay mineral composition are W08 in winter (low smectite content), Dogger Bank winter (high kaolinite+chlorite content) and Helgoland, Sizewell and BS1 in spring (high smectite content).

Table 2.6: Quantitative clay mineralogical composition of the clay minerals in the SPM in spring 2023.

	Illite	Illite/Smectite	Smectite	Kaolinite	Chlorite
MOW1	22.9	32.1	25.1	17.4	2.5
W05	14.4	39.8	30.1	13.7	2.1
W08	26.5	30.2	20.6	19.8	3.0
Codevco	24.1	30.4	27.3	15.4	2.8
Scenes	26.0	21.8	28.6	20.8	2.9
BS1	10.7	39.4	37.9	10.1	1.9
Sizewell	16.9	34.7	30.7	15.2	2.5
West Gabbard	20.6	33.4	27.5	16.2	2.4
Dogger Bank	20.6	34.5	31.3	10.8	2.7
HB2	17.8	44.5	20.3	14.8	2.7
HB1	16.8	37.0	29.2	14.9	2.2
Helgoland	15.0	27.4	37.5	18.0	2.0

Table 2.7: Quantitative clay mineralogical composition of the clay minerals in the SPM in winter 2023.

	Illite	Illite/Smectite	Smectite	Kaolinite	Chlorite
MOW1	13.2	44.8	26.2	13.9	1.9
W05	16.6	43.2	23.2	15.1	2.0
W08	19.6	49.2	11.8	16.8	2.5
Codevco	-	-	-	-	-
Scenes	17.4	40.2	25.0	15.3	2.1
BS1	-	-	-	-	-
Sizewell	11.6	33.1	37.3	16.4	1.7
West Gabbard	14.6	37.4	24.9	21.1	1.9
Dogger Bank	28.4	27.9	17.0	23.1	3.6
HB2	14.4	44.5	25.9	13.0	1.8
HB1	14.4	44.9	22.3	13.0	1.8
Helgoland	15.8	40.5	29.0	12.8	1.8

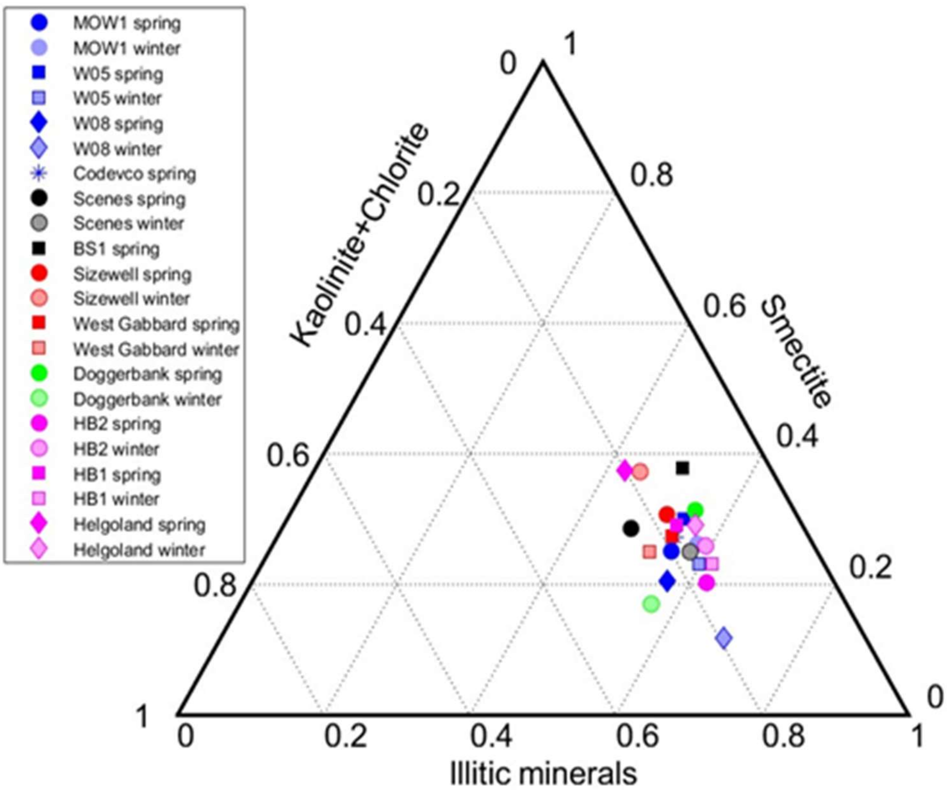

Figure 2.4: Ternary diagram of the quantitative clay composition (<2µm) of the SPM in the North Sea with smectite, illitic minerals (illite and interstratified illite-smectite) and kaolinite and chlorite as endmember compositions, see Table 2.6 and 2.7 for details.

2.2.3. OC content of the SPM

2.2.3.1. OC content derived from SSA and water samples

The OC content attached to minerals, called ‘$POC_{mineral}$ content’, has been calculated using the SSA of the minerals (Table 2.2), the clay mineral fraction (Tables 2.4 and 2.5) and the clay mineral composition (Tables 2.6 and 2.7). This $POC_{mineral}$ content is compared with the mean surface POC content of the SPM (i.e., the POC:SPM ratio) obtained from water samples and called 'sample POC' (Table 2.8). The table shows that the sample POC content is always higher than the $POC_{mineral}$ content. The highest sample POC contents occur in spring during the phytoplankton bloom and can reach up to 12% at the Dogger Bank station; in winter, the sample POC content is lower but remains about 5-10 times higher than the $POC_{mineral}$ content. The highest SSA derived OC content is found in the samples with highest smectite content.

Table 2.8: POC content of the SPM (in %) derived from the mineral SSA ($POC_{mineral}$) and from the ratio of POC:SPM concentration from water sample (sample-POC). The standard deviation for $POC_{mineral}$ is based on the uncertainties in surface area and OC content of clay minerals found in the literature (see §2.1.4.3). The geometric mean and standard deviation of the POC content are obtained from averaging all data collected during a full or ½ tidal cycle.

	spring 2023		winter 2023	
	$POC_{mineral}$ (%)	sample-POC (%)	$POC_{mineral}$ (%)	sample-POC (%)
MOW1	0.71±0.27	2.11*/2.7	0.86±0.33	2.81*/1.1
W05	0.46±0.18	5.12*/1.7	0.43±0.17	2.79*/1.1
W08	0.48±0.18	10.92*/1.6	0.39±0.16	3.61*/1.2
Codevco	0.51±0.20	7.54*/1.6	-	2.85*/1.1
Scene	0.82±0.32	2.95*/1.5	0.62±0.24	5.75*/1.2
BS1	0.77±0.30	3.50*/1.5	-	-
Sizewell	1.18±0.45	2.33*/1.3	1.10±0.43	2.60*/1.4
West Gabbard	0.50±0.19	3.34*/1.3	0.88±0.34	4.62*/1.4
Dogger Bank	0.96±0.37	11.82*/1.2	0.82±0.31	5.07*/1.4
HB2	0.90±0.35	4.00*/1.2	0.91±0.35	3.81*/1.3
HB1	0.64±0.25	3.58*/1.3	0.80±0.31	5.44*/1.5
Helgoland	1.05±0.41	5.27*/1.8	0.85±0.33	6.12*/1.4

2.2.3.2. Modeled POC content

The POC_{ref} and POC_{fresh} contents have been calculated using the semi-empirical POC-SPM model and the parameters given in Fettweis et al. (2022) applied to the SPM concentrations analysed from the water samples, see Table 2.9. Whereas the refractory POC (POC_{ref}) content is quasi constant, the POC_{fresh} content varies with season (higher in spring) and SPM concentration. From the turbid inshore towards clearer offshore waters, the relative proportion of the POC_{fresh} versus the POC_{ref} content increases. Accordingly, at low SPM concentration the POC_{fresh} content is high, whereas at high SPM concentrations the POC_{ref} content dominates.

2.2.3.3. Variability of DOC and POC concentrations

The tidal averaged sample-POC and DOC concentrations are given in Table 2.10 and the sample-POC:DOC ratios are shown in Figure 2.5. Additional sample-POC and DOC concentrations (2019-2023) from stations MOW1, W05 and W08 have been included in the figure. The figure shows that DOC concentrations exceed the POC concentration at low SPM concentration, while above about 30 mg/l the POC concentration is higher.

Table 2.9: Estimates of POC_{ref} and POC_{fresh} content (in %) of the SPM using the semi-empirical model of Fettweis et al. (2022). The values have been calculated using the measured SPM concentrations and are given as the geometric mean and standard deviation during a full or ½ tidal cycle.

	spring 2023			winter 2023		
	SPM (mg/l)	POC_{ref} (%)	POC_{fresh} (%)	SPM (mg/l)	POC_{ref} (%)	POC_{fresh} (%)
MOW1	121*/1.9	2.94*/2.4	0.27*/2.4	83*/2.0	3.01*/3.2	0.10*/3.2
W05	20*/2.1	2.94*/2.9	1.42*/2.9	9.6*/1.1	3.00*/1.3	0.79*/1.3
W08	5.1*/1.9	2.94*/2.4	4.01*/2.4	4.6*/1.1	3.00*/1.2	1.54*/1.2
Codevco	15*/1.3	2.94*/2.4	1.86*/2.4	14*/1.3	3.00*/1.5	0.60*/1.5
Scene	18*/1.6	2.91*/2.0	1.42*/2.0	8.7*/1.3	3.01*/1.4	0.92*/1.4
BS1	8.2*/1.8	2.92*/2.2	2.71*/2.2	-	-	-
Sizewell	31*/1.4	2.92*/1.6	0.91*/1.6	31*/1.4	3.01*/2.3	0.28*/2.3
West Gabbard	7.7*/1.5	2.92*/1.8	2.85*/1.8	7.2*/1.2	3.01*/1.3	1.08*/1.3
Dogger Bank	1.8*/1.3	2.93*/1.4	6.64*/1.4	3.4*/1.3	3.01*/1.3	2.05*/1.3
HB2	21*/1.2	2.93*/1.3	1.36*/1.3	22*/1.3	3.01*/2.8	0.37*/2.8
HB1	11*/1.3	2.93*/1.4	2.28*/1.4	5.3*/1.9	3.01*/2.3	1.37*/2.3
Helgoland	3.9*/1.8	2.93*/2.2	4.59*/2.2	3.4*/1.3	3.01*/1.6	2.00*/1.6

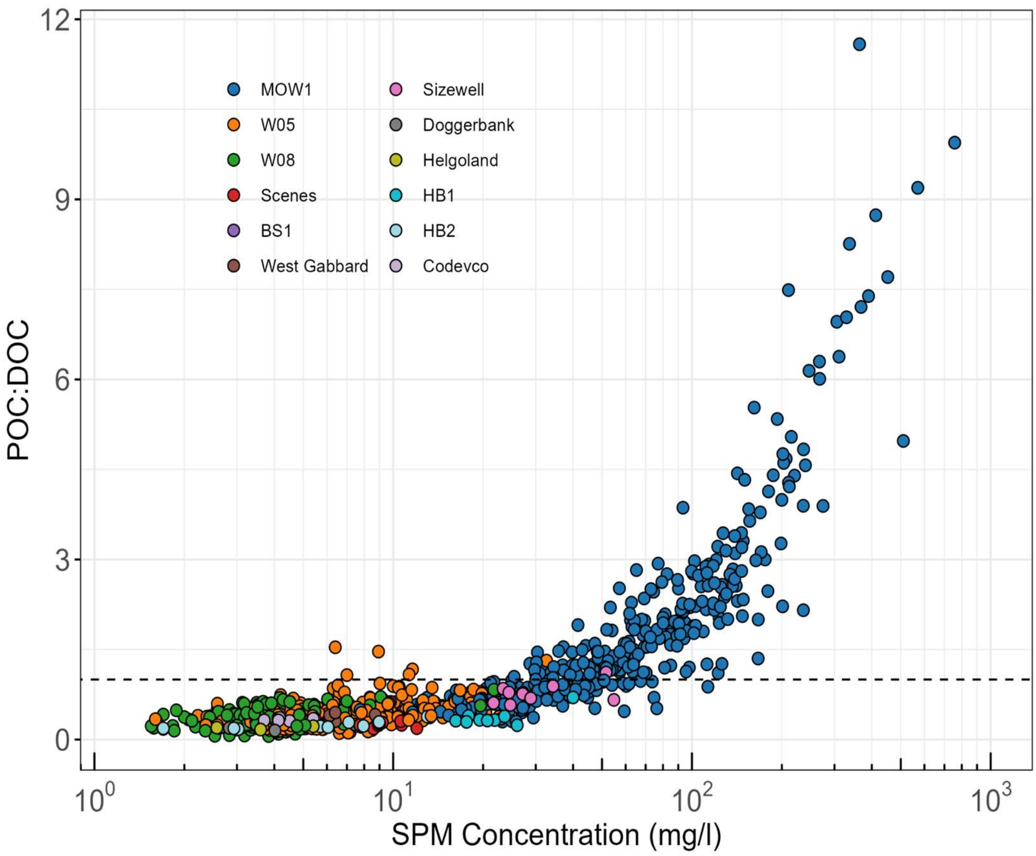

Figure 2.5: Sample-POC:DOC ratio (1:1 dashed line shown) as a function of SPM concentration. Additional data have (2019-2023) been added for stations MOW1, W05, and W08.

Table 2.10: Sample-POC and DOC concentrations (in mg/l) analysed from water samples. The (geometric for POC, arithmetic for DOC) mean and standard deviation of the POC and DOC concentration is from the averaging of all data collected during a full or ½ tidal cycle.

	spring 2023		winter 2023	
	sample-POC (mg/l)	DOC (mg/l)	sample-POC (mg/l)	DOC (mg/l)
MOW1	4.90*/2.5	1.61±0.15	2.32*/2.0	1.48±0.18
W05	0.82*/1.4	1.31±0.03	0.25*/1.2	0.82±0.01
W08	0.56*/1.2	1.09±0.13	0.17*/1.1	0.69±0.04
Codevco	1.04*/1.3	1.42±0.09	0.39*/1.3	1.02±0.07
Scene	0.53*/1.4	-	0.50*/1.2	2.06±0.65
BS1	0.29*/1.4	-	-	-
Sizewell	0.71*/1.3	-	0.79*/1.2	1.05±0.10
West Gabbard	0.26*/1.4	-	0.33*/1.2	0.93±0.06
Dogger Bank	0.21*/1.5	-	0.17*/1.1	0.99±0.10
HB2	0.80*/1.2	-	0.83*/1.3	2.40±0.43
HB1	0.39*/1.2	-	0.29*/1.4	1.26±0.10
Helgoland	0.20*/1.3	-	0.20*/1.1	1.02±0.03

2.3. Discussion

We have derived the POC content of the SPM using three methods. The bulk POC content (sample-POC) is calculated from water samples (POC and SPM concentration) and provides a value that is based on the filterability of the particles (particles >0.7µm) and can be seen as a reference for the total POC content of the SPM. The SSA-derived OC is the mineral-associated fraction ($POC_{mineral}$) as described by Keil and Mayer (2014). This fraction is likely to be incorporated in marine sediments (Mayer 1995; Middelburg & Meysman 2007). The $POC_{mineral}$ fraction is, however, not necessarily constant in composition as it may occur in an actively reversible sorption equilibrium (Blattmann et al. 2019; Kleber et al. 2021). With the SPM-POC model, two fractions are obtained, one that contains the fresh and consumable fraction that encompasses the living cells and their exudates (Fettweis et al. 2022). This POC_{fresh} fraction has a seasonal cycle driven by phytoplankton production - and hence light, nutrient availability and temperature - and a large fraction of it is rapidly recycled (Muylaert et al. 2006; Schartau et al. 2019). The other fraction, POC_{ref}, contains the mineral-associated fraction and a fraction with a longer, but variable, turnover time. It may consist amongst others of POC that is protected by occlusion into small clay mineral aggregates (flocculi) and other slowly degradable OM. The partitioning of organic carbon into two pools has been widely used in the literature, however, no clear definition exists on what constitutes labile or refractory material as it depends on the interactions between the OM and the environment. Therefore, many authors consider the degradability of the POC as a continuum between two different extremes: fast degradation within hours to days and preservation on geological time scales (Middelburg et al. 1993; Mayer 1995; Dauwe et al. 1999; Liu & Xue, 2020; Baltar et al. 2021). Our approach makes a distinction within the non-fresh fraction. The $POC_{mineral}$ fraction is the most refractory one and is only varying with the mineral composition of the SPM (considering that available mineral surfaces are always saturated with their associated OM). The POC fraction that remains after subtraction of the $POC_{mineral}$ from the bulk POC concentration can be split into a fresh and labile fraction (POC_{fresh}) and a fraction that is slowly degradable (POC_{slow}). The total POC concentration can then be written as:

$$POC = POC_{mineral} + POC_{slow} + POC_{fres}$$

Hereunder we explore three questions: 1) How does the $POC_{mineral}$ content vary with SPM concentration, i.e., in the cross-shore axis; 2) Is the $POC_{mineral}$ the missing DOC at high SPM concentration? and 3) What is the mineralogical variability of SPM in time; and

2.3.1. $POC_{mineral}$ content along a nearshore to offshore transect

The dynamic nature of shelf seas is responsible for variations in SPM concentration (Figure 2.1) and POC content (Desmit et al. 2024). The $POC_{mineral}$ content of the SPM in the measuring stations as a function of SPM concentration is shown in Figure 2.6. The large spread in the data is related to the heterogeneity in clay mineral content (% of clay in SPM) and clay mineral composition (types of clay). This variability may occur on spatial and temporal scales, for instance when comparing Helgoland to the nearshore HB2, or HB1 in winter and in spring. Despite the large spreading, an increase in $POC_{mineral}$ content with increasing SPM concentration can be observed in most areas, with the exceptions of Dogger Bank, Helgoland and HB1 in winter. Irion et al. (1987) report that dumping operations resulted in mud accumulation SE of Helgoland, which might explain the peculiar result from Helgoland and/or HB1. The differences between regions, for example the lower increase in $POC_{mineral}$ content in the Belgian stations (MOW1-W05-W08 and Codevco) when compared to the German and UK stations indicates the heterogeneity of SPM composition in the study area, and underlines that the SPM in the North Sea has different provenances (Adriaens et al., 2018). A detailed mineralogical composition in space and time is therefore needed to differentiate accurately between the more refractory POC fractions ($POC_{mineral}$ and POC_{slow}).

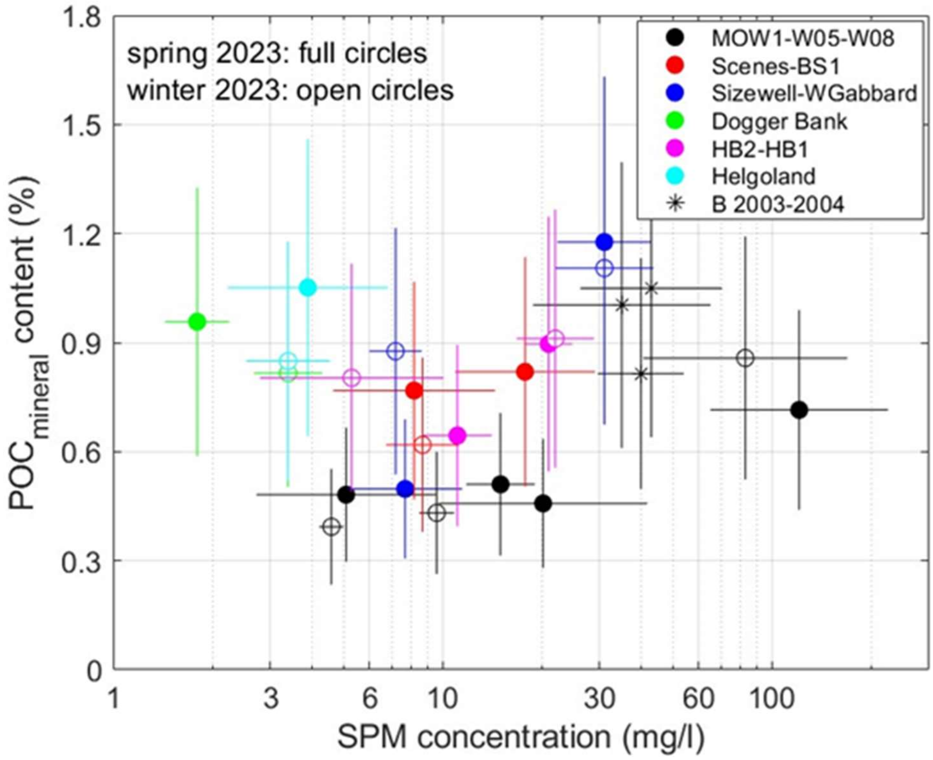

Figure 2.6: $POC_{mineral}$ content of the SPM derived from mineral SSA as a function of SPM concentration. The vertical error bars are the standard deviation from the SSA of the minerals (Table 1) and the horizontal ones the standard deviation from the full or half tidal averaging. 'B 2003-2004' are additional data from the Belgian part of the North Sea, see § 2.3.3.

A typical feature of shelf seas is the persistence of a horizontal cross-shore gradient, with higher SPM concentrations in the shallow coastal waters and lower concentrations offshore. Desmit et al. (2024) confirmed the concept of 'line of no return' of Postma (1984) by using the POM composition and content of the SPM. Such a line is located at some distance from the coast and functions as a zone with low cross transport of SPM. The data from the Belgian (MOW1, W05, W08), UK (Sizewell, West Gabbard) and German (HB2, HB1) stations show a decrease in clay mineral content towards the offshore and confirm that a transition zone exists, not only in the POC content and composition but also in the mineral content and composition. The line of no return can be interpreted as the outer limit to a transition zone where similar concentrations of POM_{fresh} and POM_{ref} prevail (Desmit et al. 2024), changes in phytoplankton order richness take place (Jung et al., 2017) and lowering of the mineral specific surface area per unit of SPM occur. We can distinguish two $POC_{mineral}$ contents: one offshore and one inshore the transition zone, see Table 2.11. The POC is thus less refractory offshore than nearshore.

Table 2.11: Averaged $POC_{mineral}$ content (± uncertainty) in cross-shore direction for 4 regions in the North Sea and English Channel based on Fig. 5 (data 2023).

	high turbid	low turbid
Belgian transect	0.79±0.22	0.45±0.09
UK, F and G transect	0.98±0.17	0.58±0.13
Helgoland	-	0.90±0.20
Dogger Bank	-	0.89±0.24

2.3.2. *$POC_{mineral}$ and DOC*

The traditional classification of organic matter into particulate and dissolved components is based on size and filtration properties. However, this classification can be distorted by the interaction of smaller dissolved molecules with mineral particles (Keil et al., 1994). These molecules, though intrinsically bound to be dissolved or colloidal, may be retained on filters due to their association with minerals, increasing the measured amount of POC. From a compositional point of view, only POC_{fresh} and POC_{slow} depend on phytoplankton production, remineralization, erosion or terrestrial input as opposed to $POC_{mineral}$, which depends only on the mineral composition. This effect is likely to be pronounced in nearshore turbid waters, which have higher mineral particle concentrations compared to clearer offshore waters.

Offshore waters generally exhibit sample-POC/DOC ratios well below 1, indicating a dominance of the DOC fraction (Osterholz et al., 2021), whereas ratios greater than 1 are often reported in turbid waters (Abril et al., 2002; Zhao and Gao, 2019). Herman & Heip (1999) demonstrated systematic variation in sample-POC/DOC ratios as a function of SPM concentrations in European estuaries, suggesting significant exchange between particulate and dissolved pools through adsorption and desorption processes. Similarly, along the Belgian transect, sample-POC/DOC ratios greater than 1 are frequently observed at MOW1 (Figure 2.5) but become less common at comparatively deeper and less turbid stations like W05 and W08. The OC adsorbed onto mineral particles is dynamically exchanging with the DOC, and thus influencing its fate and concentration. Clearly, such adsorption stabilizes the organic compound and may delay its degradation and loss (Keil et al., 1994; Hemingway et al., 2019), although some transformation of the adsorbed OC continuously occur (Kleber et al., 2021). The desorption of organic compounds can lead to their further transformation and replacement by other organic compounds present in the marine system (Blattmann et al., 2019). However, this process is not sufficient to explain the variation in POC/DOC along the SPM concentration gradient as suggested by Herman & Heip (1999) for estuaries. Subtracting $POC_{mineral}$ (estimated from the specific surface area of minerals) from the sample-POC and adding it to the DOC concentration results in a lower POC/DOC ratio, however, it still remains 2-4 times higher nearshore than offshore. This higher nearshore $(POC\text{-}POC_{mineral})/(DOC+POC_{mineral})$ ratio can be further explained by phytoplankton production, advection and diffusion, density gradients and seabed erosion. The production of POC and DOC is higher nearshore because of a higher phytoplankton production due to higher nutrient concentration. This higher DOC production will be affected by down-gradient diffusion, tidal or wind-driven advection and by the occurrence of a horizontal density gradient, initiated by fresh water inflow by rivers that causes a net particle transport towards the coast (see Desmit et al., 2024). For the Belgian nearshore, additional input of POC results from the erosion of OM rich muddy sediments (see Adriaens et al., 2018).

2.3.3. Temporal variability of SPM mineralogy in the Belgian coastal zone

The SPM concentration and composition is highly variable and depends on hydrodynamics, wind, waves, season, seafloor composition and human activities. Seasonal changes drive biological processes that change the POC content, of which a major part is POC_{fresh}. Spring-neap cycles, storm frequency and wind direction, have an influence on the transport, resuspension or erosion of the seabed and may alter the mineral composition. For the Belgian nearshore area Adriaens et al. (2018) concluded that the SPM originates from the erosion and resuspension of the muddy seafloor, which has the same clay mineral composition as the SPM. This conclusion was supported by 15 centrifuge samples that have been collected during four sampling campaigns in 2003, 2004 and 2007 in the Belgian part of the North Sea (Zeelmaekers, 2011). The clay minerals were analyzed using the method described above, bulk mineralogy was only determined on five samples and SPM concentration on only three. In Figure 2.7, these clay mineral compositions are presented with the 2023 data. The figure shows that the sum of kaolinite and chlorite remains constant (about 20%), but that there are large variations in the smectite and illitic minerals content. In the older data the smectite content is between 39% and 53% while in 2023 smectites represent only between 12% and 26%. A lower smectite content decreases the SSA significantly and thus the $POC_{mineral}$ content. The older data align with the UK, German and French data from 2023, see Figure 2.6. The reason for the difference between 2023 and 2003-2007 could be an increase of the SPM transport from the English Channel towards the North Sea caused by higher frequency of S, SW and W weather types. An increase of southwesterly winds in the Southern Bight of the North Sea has been reported by van den Eynde et al. (2012). Fettweis et al. (2012) have argued that changes in the frequency of these weather types change the SPM concentration distribution and thus possibly also the SPM mineral composition. SPM from the English Channel contain 10–30% less smectite than the 2003-2007 SPM samples and have a higher carbonate content due to the erosion of cretaceous cliffs (Adriaens et al., 2018). The latter is supported by the higher carbonate content (35%) in the recent samples from the Belgian part of the North Sea than in the samples from 2003-2007 (29%).

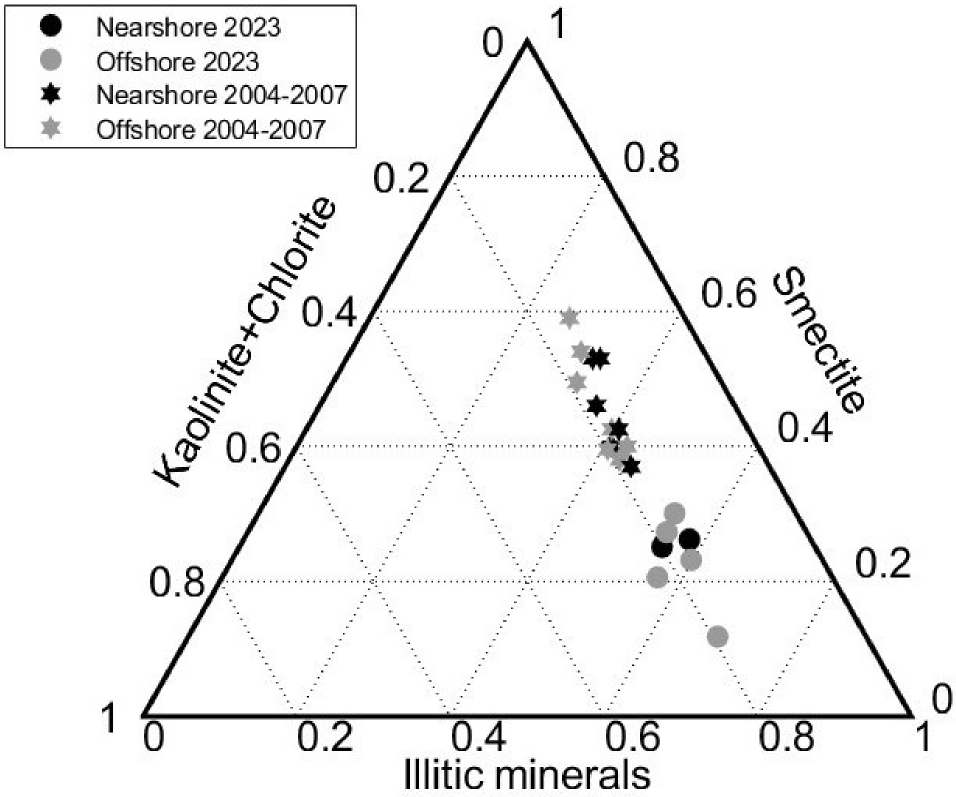

Figure 2.7: Ternary diagram of the longer-term quantitative clay composition (<2µm) of the SPM limited to the Belgian part of the North Sea with smectite, illitic minerals (illite+interstratified illite-smectite) and kaolinite+chlorite as endmember compositions. We compare 15 samples from 2004-2007 with the 7 samples from 2023 (stations MOW1, W05, W08 and Codevco).

2.3.4. Consequences for dredging and dumping

In situ SPM concentration data at MOW1 have shown that the residual alongshore flow changes the SPM concentration, see Figure 2.8. At MOW1 the SPM concentration is generally higher when the currents are directed in the same direction as the alongshore flow. Thus for ebb, the highest SPM concentration is recorded during SW-ward directed and for flood during NE-ward directed residual alongshore flow. On a regional scale, these changes are caused by a shift of the coastal turbidity towards the NE resulting in an increase of SPM concentration in the North Sea and a decrease of it in the Strait of Dover (Fettweis et al., 2012). The changes in mineralogy correlate with a decrease of the dredged matter in the harbours of Ostend and Nieuwpoort and an increase in the port of Zeebrugge since 2020 (Fettweis et al., 2024). In order to confirm if the changes in mineralogy are related to changes in weather type and if the changes in weather type result in an increase of the SPM concentration at Zeebrugge and a decrease in Nieuwpoort and Ostend, the following tasks are proposed in future research activities:

1) Building a mineralogical time series of the SPM by sampling at least once a year the mineralogical composition of the SPM at MOW1. These data will provide a follow up of mineralogical changes, an estimate of their variability and will allow to establish a link with climate conditions (indicator for climatic changes).

2) Analysing changes in the occurrence of weather types during the last decades and comparing it with a similar analysis (Fettweis et al., 2012) and new literature data on climate. The previous analysis has suggested that changes in weather type frequency

explain partially the observed changes in SPM concentration distribution and thus possibly also in SPM composition.

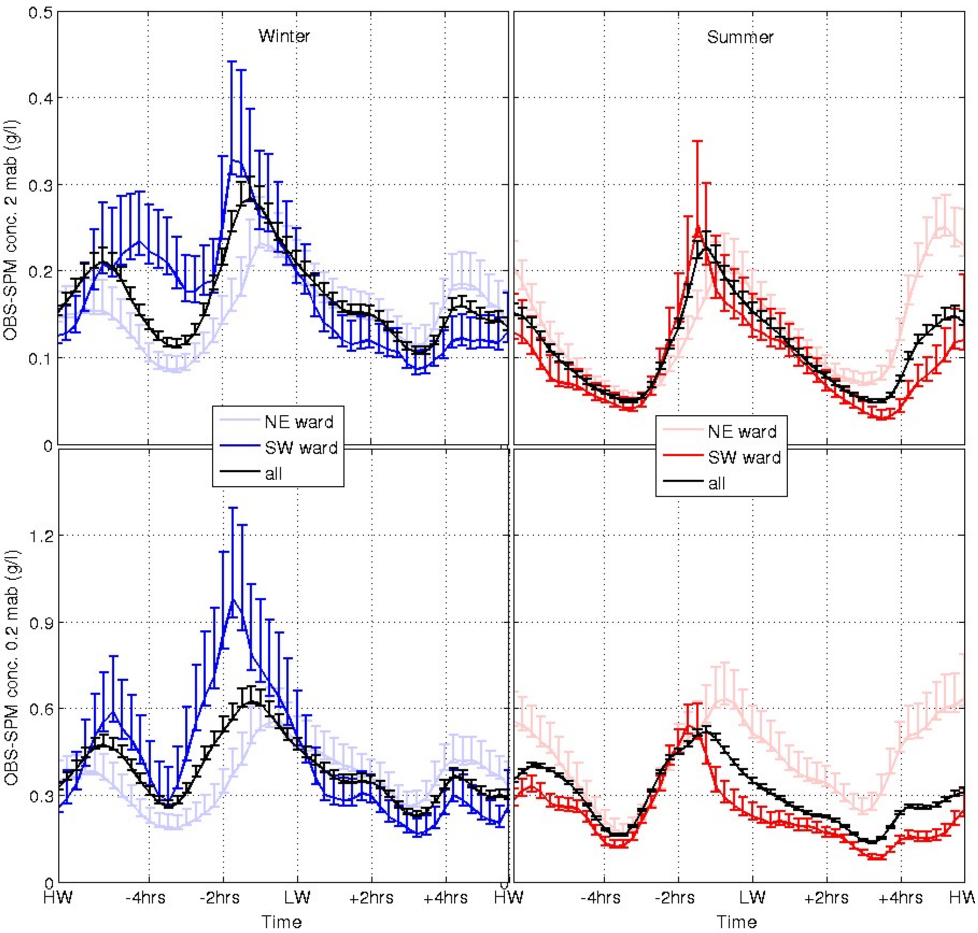

Figure 2.8: Ensemble averaged OBS-derived SPM concentration (MOW1) at 2 and 0.2 mab during a tidal cycle (g/L) in (left) winter and (right) summer for two different alongshore flows. The error bars are the standard errors (from Fettweis et al., 2015).

2.4. Conclusions

The SPM is composed of both mineral and organic particles that interact constantly. The organic fraction of the SPM is composed of labile and refractory material. To better understand these interactions on the North Sea shelf, we have analyzed at different locations the mineralogical composition of clays and have estimated the mineral SSA, which is correlated with the amount of adsorbed organic compounds. Assuming these mineral surfaces are always saturated with organic matter, we calculated the mineral-associated POC linked to the SPM concentration at each location. The resulting mineral-associated POC is consistently lower than the one estimated in a previous model study (Fettweis et al., 2022). This led us to consider three different fractions of POC, which are the $POC_{mineral}$, that is the organic molecules adsorbed onto mineral surfaces and thereby less exposed to degradation, the POC_{slow}, that is an intrinsically refractory fraction with variable rates of degradation, and the POC_{fresh}, that is an intrinsically labile fraction. The OC adsorbed onto mineral particles is dynamically exchanging with the DOC, and thus influencing its fate and concentration. However this process is not sufficient to explain the variation in POC/DOC ratio along the SPM concentration gradient, which is further explained by primary production, advection and diffusion, density gradients and seabed erosion.

3. Spatio-temporal variation in particulate and dissolved organic matter dynamics in the southern North Sea

Turbid coastal waters are dynamic systems where fine-grained sediments interact with organic matter, significantly influencing the fate of both the components. The subject of the study was the seasonal dynamics of particulate (POC) and dissolved (DOC) organic carbon pools along a suspended particulate matter (SPM) gradient from nearshore to offshore waters in the Belhian part of the North Sea based on data collected in the monitoring stations MOW1, W05 and W08, see Figure 3.1.

To assess temporal and spatial variations in POC composition, the relative contributions of phytoplankton (POC_{phyto}), heterotrophs (POC_{het}), detritus (POC_{det}), and mineral-associated organic matter ($POC_{mineral}$) to the bulk POC pool were quatified. In nearshore waters, frequent tidal resuspension and high SPM concentrations led to elevated POC_{det} and $POC_{mineral}$ fractions that masked the influence of POC_{phyto}, despite the higher primary productivity during the spring bloom. In contrast, offshore waters exhibited a greater relative contribution of POC_{phyto}, with seasonal POC increases corresponding to elevated chlorophyll a (Chl*a*) levels in spring and summer, similar to the open-ocean dynamics. These trends were further reflected in particulate organic carbon to nitrogen (POC:PON) ratios and POC:Chl*a* ratios, commonly used to assess sources and quality of organic matter. The cross-shore gradient in organic matter partitioning, with dominance of POC nearshore and that of DOC offshore, highlights the role of particle resuspension and phytoplankton production in controlling organic carbon distribution between the two pools. Overall, these findings underscore the complex interplay between biological production, nutrient cycling, hydrodynamic forces, and SPM in shaping the composition and fate of organic carbon and of SPM in turbid coastal systems.

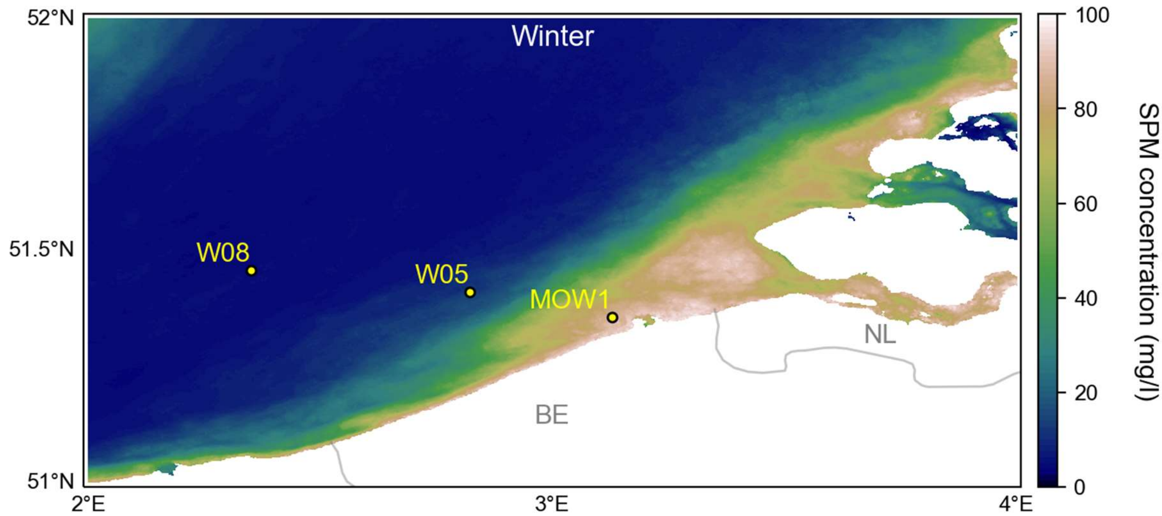

Figure 3.1: Map of sampling stations MOW1, W05 and W08. The background displays the averaged near surface SPM concentrations in the southern North Sea computed from satellite images taken by Sentinel-3/OLCI from November 2019 to March 2020.

4. Referenties

Abril G, Nogueira M, Etcheber H, Cabeçadas G, Lemaire E, Brogueira MJ. 2002. Behaviour of organic carbon in nine contrasting European estuaries. *Estuarine Coastal and Shelf Science.* 54, 241-62.

Adriaens R, Vandenberghe N, Elsen J, 2014. Natural clay-sized glauconite in the Neogene deposits of the Campine Basin (Belgium). *Clays and Clay Minerals* 62, 35–52.

Adriaens R, Zeelmaekers E, Fettweis M, Vanlierde E, Vanlede J, Stassen P, Elsen J, Środoń J, Vandenberghe N. 2018. Quantitative clay mineralogy as provenance indicator for recent muds in the southern North Sea. *Marine Geology* 398, 48–58.

Arndt S, Jørgensen BB, LaRowe DE, Middelburg JJ, Pancost RD, Regnier P. 2013. Quantifying the degradation of organic matter in marine sediments: A review and synthesis. *Earth Science Review* 123, 53-86.

Baltar F, Alvarez-Salgado XA, Arístegui J, Benner R, Hansell DA, Herndl GJ, Lønborg C. 2021. What is refractory organic matter in the ocean? *Frontiers in. Marine Science* 8, 642637.

Bianchi TS. 2011. The role of terrestrially derived organic carbon in the coastal ocean: A changing paradigm and the priming effect. *PNAS* 108, 19473–19481.

Blattmann TM, Liu Z, Zhang Y, Zhao Y, Haghipour N, Montlucon DB, Plötze M, Eglinton TI. 2019. Mineralogical control on the fate of continentally derived organic matter in the ocean. *Science 366*, 742–745.

Chen Y-M, Gao J-b, Yuan Y-Q, Ma J, Yu S. 2016. Relationship between heavy metal contents and clay mineral properties in surface sediments: Implications for metal pollution assessment. *Continental. Shelf Research.* 124, 125-133.

Dauwe B, Middelburg JJ, Herman PMJ, Heip CHR. 1999. Linking diagenetic alteration of amino acids and bulk organic matter reactivity. *Limnology & Oceanography* 44, 1809-1814.

Deng Z, Huang D, He Q, Chassagne C. 2022. Review of the action of organic matter on mineral sediment flocculation. *Frontiers in Earth Science* 10, 965919.

Desmit X, Schartau M, Terseleer N, Van der Zande D, Riethmüller R, Fettweis M. 2024. The transition between coastal and offshore areas in the North Sea unraveled by the suspended particle composition. *Science of the Total Environment* 915, 169966.

Drits VA, Lindgreen H, Sakharov BA, Salyn AL. 1997. Sequential structure transformation of illite-smectite-vermiculite during diagenesis of Upper Jurassic shales, North Sea. *Clay Minerals* 33, 351–371.

Ehrhardt M, Koeve W. 1999. Determination of particulate organic carbon and nitrogen. In K. Grasshoff, K. Kremling, and M. Ehrhardt (Eds.), Methods of seawater analysis (3rd ed., pp. 437–444). Wiley.

Etcheber H, Taillez A, Abril G, Garnier J, Servais P, Moatar F, Commarieu M-V. 2007. Particulate organic carbon in the estuarine turbidity maxima of the Gironde, Loire and Seine estuaries: origin and lability. *Hydrobiology* 588, 245–259.

Fettweis M, Monbaliu J, Nechad B, Baeye M, Van den Eynde D. 2012. Weather and climate related spatial variability of high turbidity areas in the North Sea and the English Channel. *Methods in Oceanography* 3-4, 25-39.

Fettweis M, Baeye M. 2015. Seasonal variation in concentration, size and settling velocity of muddy marine flocs in the benthic boundary layer. *Journal of Geophysical Research Oceans*, 120, 5648-5667.

Fettweis M, Schartau M, Desmit X, Lee BJ, Terseleer N, Van der Zande D, Parmentier K, Riethmüller R. 2022. Organic matter composition of biomineral flocs and its influence on suspended particulate matter dynamics along a nearshore to offshore transect. *Journal of Geophysical Research Biogeosciences* 127, e2021JG006332.

Fettweis M, De Witte B, Van Hoey, Seghers S, Vanermaete, Timmermanx S, Hermans L. 2024. Vooruitgangsrapport juni 2024 over de effecten op het mariene milieu van baggerspeciestortingen. MF/2024/10, 33pp.

Fripiat WF. 1964. Surface properties of alumino-silicates, p. 327-358. In: Bradley, W.F. (ed.), Clay and clay minerals, Proc. 12th Nat. Conf., Macmillan, New York.

Greene-Kelly R. 1962. The identification of montmorillonoids in clay. *Journal of Soil Science* 4, 233–237.

Hedges JI, Keil RG. 1995. Sedimentary organic matter preservation: an assessment and speculative synthesis. *Marine Chemistry* 49, 81-115.

Hemingway JD, Rothman DH, Grant KE, Rosengard SZ, Eglinton TI, Derry LA, Galy VV. 2019. Mineral protection regulates long-term global preservation of natural organic carbon. *Nature* 570, 228–231.

Herman PMJ, Heip CHR. 1999. Biogeochemistry of the Maximum Turbidity Zone of Estuaries (MATURE) Some Conclusions. *Journal of Marine Systems* 22, 89-104.

Irion G, Wunderlich F, Schwedhelm E. 1987. Transport of clay minerals and anthropogenic compounds into the German Bight and the provenance of fine-grained sediments SE of Helgoland. *Journal of the Geological Society* 144, 153 - 160.

Ittekkot V. 1988. Global trends in organic matter in river suspensions. *Nature* 332, 436–438.

Jackson, M.L., 1975. Soil chemical analysis. 2nd Ed. Parallel Press, University of Wisconsin, 895pp.

Jung AS, Bijkerk R, Van Der Veer HW, Philippart CJM. 2017. Spatial and temporal trends in order richness of marine phytoplankton as a tracer for the exchange zone between coastal and open waters. Journal of the Marine Biological Association of the United Kingdom 97, 477–489.

Keil RG, Montluçon DB, Prahl FG, Hedges JI. 1994. Sorptive preservation of labile organic matter in marine sediments. *Nature* 370, 549-52.

Keil RG, Mayer LM. 2014. 12.12 - Mineral Matrices and Organic Matter. Treatise on Geochemistry (2nd Edition), 12, 337-359.

Kohnke H. 1968. Soil physics. McGraw-Hill Book Co., New York.

Kleber M, Bourg IC, Coward EK, Myneni SCB, Nunan N. 2021. Dynamic interactions at the mineral–organic matter interface. *Nature Reviews Earth and Environment* 2, 402–421.

Lauwaert B, Fettweis M, De Witte B, Van Hoei G, Timmermans S, Hermans L. 2019. Vooruitgangsrapport (juni 2019) over de effecten op het mariene milieu van baggerspeciestortingen (Vergunningsperiode 01/01/2017 – 31/12/2021). RBINS-ILVO-AMT-CD rapport. BL/2019/01, 28pp.

Lauwaert B, De Witte B, Festjens F, Fettweis M, Hermans L, Lesuisse A, Le H-M, Seghers S, Timmermans S, Vanavermaete D, Van Hoey G. 2021. Synthesis report on the effects of dredged material dumping on the marine environment (licensing period 2017-2021). RBINS-ILVO-AMT-AMCS-FHR report BL/2021/10, 67pp.

Lee BJ, Fettweis M, Toorman E, Molz F. 2012. Multimodality of a particle size distribution of cohesive suspended particulate matters in a coastal zone. *Journal of Geophysical Research Ocean* 117, C03014.

Liu Z, Xue J. 2020. The Lability and Source of Particulate Organic Matter in the Northern Gulf of Mexico Hypoxic Zone. *Journal of Geophysical Research Biogeosciences* e2020JG005653.

Maggi F. 2009. Biological flocculation of suspended particles in nutrient-rich aqueous ecosystems. *Journal of Hydrology* 376, 116-125.

Macht F, Eusterhues K, Pronk GJ, Totsche KU. 2011. Specific surface area of clay minerals: Comparison between atomic force microscopy measurements and bulk-gas (N2) and -liquid (EGME) adsorption methods. *Applied Clay Science* 53, 20-26.

Mayer LM. 1994. Surface area control of organic carbon accumulation in continental shelf sediments. *Geochimica et Cosmochimica Acta* 58, 1271–1284.

Mayer LM. 1995. Sedimentary organic matter preservation: An assessment and speculative synthesis - a comment. *Marine Chemistry* 49, 123-126.

Middelburg JJ, Vlug T, Vandernat F. 1993. Organic-matter mineralization in marine systems. *Global Planetary Change* 8, 47-58.

Middelburg JJ, Meysman FJR. 2007. Burial at sea. *Science* 316, 1249-1295.

Mitchel, J.K., Soga, K., 2005. Fundamentals of Soil Behavior. John Wiley, 558pp.

Muylaert K, Gonzales R, Franck M, Lionard M, Van der Zee C, Cattrijsse A, Vyverman W. 2006. Spatial variation in phytoplankton dynamics in the Belgian coastal zone of the North Sea studied by microscopy, HPLC-CHEMTAX and underway fluorescence recordings. *Journal of Sea Research* 55, 253-265.

Nechad B, Ruddick KG, Park Y. 2010. Calibration and validation of a generic multisensor algorithm for mapping of total suspended matter in turbid waters. *Remote Sensing of*

Environment 114, 854-866.
Opdal AF, Lindemann C, Aksnes DL. 2019. Centennial decline in North Sea water clarity causes strong delay in phytoplankton bloom timing. *Global Change Biology* 25, 3946-3953.
Osterholz H, Kilgour DPA, Storey DS, Lavik G, Ferdelman TG, Niggemann J, Dittmar T. 2021. Accumulation of DOC in the South Pacific Subtropical Gyre from a molecular perspective. *Marine Chemistry* 231, 103955.
Pedersen T, Calvert S. 1990. Anoxia vs. productivity: What controls the formation of organic-carbon-rich sediments and sedimentary rocks? *AAPG Bulletin* 74. 454-466.
Postma H. 1984. Introduction to the symposium on organic matter in the Wadden Sea. Netherlands Institute of Sea Research - Publ. Ser. 10, 15–22.
Sakharov BA, Lindgreen H, Salyn AL, Drits VA. 1999. Determination of illite smectite structures using multispecimen X-ray diffraction profile fitting. *Clays and Clay Minerals* 47, 555–566.
Shen X, Toorman EA, Lee BJ, Fettweis M. 2018. Biophysical flocculation of suspended particulate matters in Belgian coastal zones. *Journal of Hydrology* 567, 238-252,
Singh M, Sarkar B, Biswas B, Churchman J, Bolan NS. 2016. Adsorption-desorption behavior of dissolved organic carbon by soil clay fractions of varying mineralogy. *Geoderma* 280, 47-56.
Środoń J, Drits VA, McCarty DK, Hsieh JCC, Eberl DD. 2001. Quantitative XRD analysis of clay-rich rocks from random preparations. *Clays and Clay Minerals* 49, 514–528.
Van den Eynde D, De Sutter R, Haerens P. 2012. Evolution of marine storminess in the Belgian part of the North Sea. *Natural Hazards and Earth System Sciences* 12, 305–312.
van der Zee C, Chou L. 2005. Seasonal cycling of phosphorus in the Southern Bight of the North Sea. *Biogeosciences 2*, 27–42.
White RE. 2005. Principles and Practice of Soil Science: The Soil as a Natural Resource, 4th Edition. Blackwell Publishing.
Zeelmaekers E. 2011. Computerized qualitative and quantitative clay mineralogy: Introduction and application to known geological cases. PhD thesis. KULeuven, Belgium.
Zeelmaekers E, Honty M, Derkowski A, Środoń J, De Craen M, Vandenberghe N, Adriaens R, Ufer K, Wouters L. 2015. Qualitative and quantitative mineralogical composition of the Rupelian Boom clay in Belgium. *Clay Minerals* 50, 249–272.
Zhang X, Stavn RH, Falster AU, Rick JJ, Gray D, Gould RW. 2017. Size distributions of coastal ocean suspended particulate inorganic matter: Amorphous silica and clay minerals and their dynamics. *Estuarine, Coastal and Shelf Science* 189, 243-251.
Zhao L, Gao L. 2019. Dynamics of dissolved and particulate organic matter in the Changjiang (Yangtze River) Estuary and the adjacent East China Sea shelf. *Journal of Marine Systems* 198, 103188.
Zhao T, Xu S, Hao F. 2023. Differential adsorption of clay minerals: Implications for organic matter enrichment. *Earth Science Reviews* 246, 104598.
Zhu X, Cai J, Song G, Ji J. 2015. Factors influencing the specific surface areas of argillaceous source rocks. *Applied Clay Sciences* 109–110, 83-94.

COLOPHON

Dit rapport werd voorbereid door de BMM in februari 2025
Zijn referentiecode is MOMO/10/MF/202502/NL/AR/6

De scheepstijd met de RV Belgica werd voorzien door BELSPO en KBIN-OD Natuur

Indien u vragen hebt of bijkomende copies van dit document wenst te verkrijgen, gelieve een e-mail te zenden naar mfettweis@naturalsciences.be, met vermelding van de referentie, of te schrijven naar:

Koninklijk Belgisch Instituut voor Natuurwetenschappen
OD Natuur – BMM
t.a.v. Michael Fettweis
Vautierstraat 29
B–1000 Brussel
België
Tel: +32 2 627 41 83

BEHEERSEENHEID VAN HET
MATHEMATISCH MODEL VAN DE NOORDZEE

APPENDIX 1

Bijdrage voor

Symposium on Advances in Marine Ecosystem Modelling Research, 8-11 July, Plymouth (UK)

A coupled phytoplankton-flocculation model to quantify suspended particulate matter dynamics on the Belgian shelf.

Nathan Terseleer, Michael Fettweis, Saumya Silori, Xavier Desmit, Auria Kallend, Luz Amadei Martinez, Koen Sabbe, Vyverman Wim, K., Byung Joon Lee, Onur Kerimoglu

Biological and mineral components of marine ecosystems are often studied and modelled separately. Yet, they interact and form an integrated dynamic system. In coastal waters, this is translated into highly variable suspended particulate matter (SPM) concentration. SPM comprises mineral particles, living organisms, detritus and extracellular organic matter. On time scales ranging from tide to year, SPM dynamics respond to interactions between physical, sedimentological and biological processes. Unravelling these dynamics needs more integrated models.

In this study, a biogeochemical 0D model simulating phytoplankton growth and production of different classes of organic matter, including transparent exopolymer particles (TEP), is coupled to a two-class population balance equation model of flocculation. TEP production follows the carbon overconsumption hypothesis, where TEP precursors are increasingly excreted at the end of the bloom under nutrient depletion. Flocculi and flocs interact following collision and breakage kinetics, primarily controlled by turbulence. The collision efficiency of mineral particles is affected by the TEP concentration, whose sticky properties enhance flocculation. Larger flocs are less constrained by water viscosity and settle faster. The coupled phytoplankton-flocculation model is applied in three intensely monitored stations on the Belgian shelf, investigating the complex SPM dynamics on time scales ranging from tide to season, and along a cross-shore transect from the high-turbid inshore to the low-turbid offshore waters. Especially in nearshore waters, observations show that SPM concentrations decrease from winter to summer while the median particle size increases with freshly produced TEP. This behaviour is simulated by the model, which indicates that biologically-induced flocculation over the bloom affects floc size and concentration to a greater extent than turbulence-induced changes over tidal time scales. In turn, the lower SPM concentration alters the light regime in the water column, though preliminary results suggest that the effect on photosynthesis and, consequently, on the bloom, remains limited. Altogether, depending on the relative importance of the mineral and organic fractions and on hydrological conditions in the distinct stations, SPM dynamics and fate quantitatively and qualitatively differ.

APPENDIX 2

Bijdragen voor

21st Physics of Estuaries and Coastal Seas Conference, 23-27 September, Bordeaux (France

On the effects of SPM composition on the inherent acoustic and optical particle properties of the SPM

Baeye M. [1], Fettweis M. [2], and Verney R. [3]

Keywords: mixed sediments, flocculation, turbidity, SPM, sensor sensitivity, in-situ water sampling.

Abstract

From high-resolution in-situ time series of calibrated optical and acoustic instruments, robust relationships that can be applied to SPM (suspended particulate matter) concentrations were aimed at as part of refining the SPM - POM (particulate organic matter) model (see Fettweis et al., 2022) for the North Sea and the English Channel. In 10 stations located along nearshore to offshore transects in the Belgian coastal zone, Seine Bay, German Bight and Thames plume have been sampled in spring and winter 2023 during a tidal cycle. The presence of mixed sediments in the seabed and/or strong currents and wave conditions may cause sandy material or particle with other erosion characteristics to be resuspended up to the detection volumes of acoustic and optical sensors (see e.g. Baeye et al., 2011). Sand grains do not contain mineral attached POM and the presence of them lowers the POM content of the SPM and thus increases the uncertainty of the SPM-POM model. The presence of mixed sediments in suspension influences also the acoustic and optical inherent particle properties and thus the SPM concentration derived from sensors (see e.g. Fettweis et al., 2019). If not considered, the SPM concentration output of optical and acoustic sensors will over- or underestimate the SPM concentration and thus also the derived POM proxies.

In Fig. 1, the relationship between the ADCP echo intensity and SPM concentration (following the method of Kim et al. 2004) when including all the stations yields a positive linear relationship. Although, when focusing on the different stations separately most of the slopes are somewhat weaker compared to the general one. This is likely due to the presence of mixed sediments (solid grains, flocs and phytoplankton) that are triggering the acoustic signal differently than the optical one.

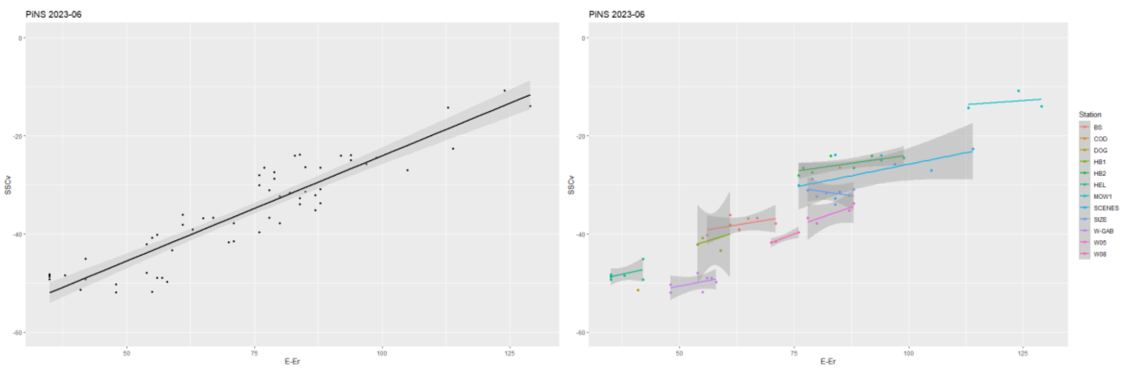

Figure 1 Left, relationship between SPM concentration (from filtration) and associated hull-mounted ADCP backscatter; right, station-based color-coded relationships between SPM concentration and ADCP echo intensity.

Concentration of SPM is recorded by the ADCP as shown for station Sizewell (southern coast of Suffolk, UK) in Fig.2, the corresponding current speed illustrates that the SPM is transported by a combination of advective process and locally re-suspended seafloor sediment.

[1] Institute of Natural Sciences, Brussels, Belgium.
[2] Institut Français de Recherche pour l'Exploitation de la Mer, France.

New insights into near-bed SPM concentration and sand/mud fraction in the use of Sediment Composition Index

Tran D. [1], Verney R. [2], and Fettweis M. [1]

Keywords: Sediment composition index, OBS, ADV, sand/mud fraction.

Abstract

Introduction

Optical turbidity and acoustic sensors have been widely used in laboratory experiments and field studies to investigate suspended particulate matter concentration over the last four decades. Both methods face a serious challenge as laboratory and in-situ calibrations are usually required. Furthermore, in coastal and estuarine environments, the coexistence of mud and sand often results in multimodal particle size distributions, amplifying erroneous measurements. This paper proposes a new approach of combining a pair of optical turbidity-acoustic sensors to estimate the total concentration and sediment composition of a sand/mud mixture in an efficient way without an extensive calibration. More specifically, we defined a Sediment Composition Index, such that

$$SCI = 10\log_{10}(OBS) - SNR \qquad (1)$$

where OBS is the signal measured by an Optical Backscatter Sensor (in NTU) and SNR is the signal measured by an ADV, Acoustic Doppler Velocimetry, sensor (in dB) (Pearson et al, 2021, Tran et al 2023). In this study, we empirically derived the SCI functions from laboratory experiments. Such SCI functions (Eq. 2 and 3), were then, applied to in-situ hydro-sedimentary dynamics data at the monitoring station MOW1 (Belgium) to investigate the impact of sand mining and beach nourishment activities in the region.

Approach

Based on Eq. 1 and a series of 60 experiments we were able to derive SCI functions for a pair of OBS and ADV which allows us to infer the sand/mud fraction, f_{sand}, and total concentration C, (Tran et al, 2023).

$$f_{sand} = -0.089 * SCI - 0.098 \qquad (2)$$

$$C = 10\text{^}(f_{sand} + Amp)/10) \qquad (3)$$

The lab-derived SCI functions (Fig. 1 and Eqs. 2, 3) were applied to field data with one more step of calibrating the coefficients with "pure mud" conditions. Pure mud conditions are calm periods, i.e., small waves and low current periods in a tidal cycle. During pure mud conditions, the measured concentrations should be equal to the SCI-predicted-concentrations (Fig. 2 the grey, vertical lines). The SCI functions with new coefficients were then applied to in-situ data at station MOW1, situated about 3 km offshore of Zeebrugge, Belgium. Data at MOW1 consists of hourly water samples, particle size distributions, turbidity, and hydrodynamic conditions for the year 2013 during 125 tidal cycles, providing one of the most comprehensive field data sets in the North Sea.

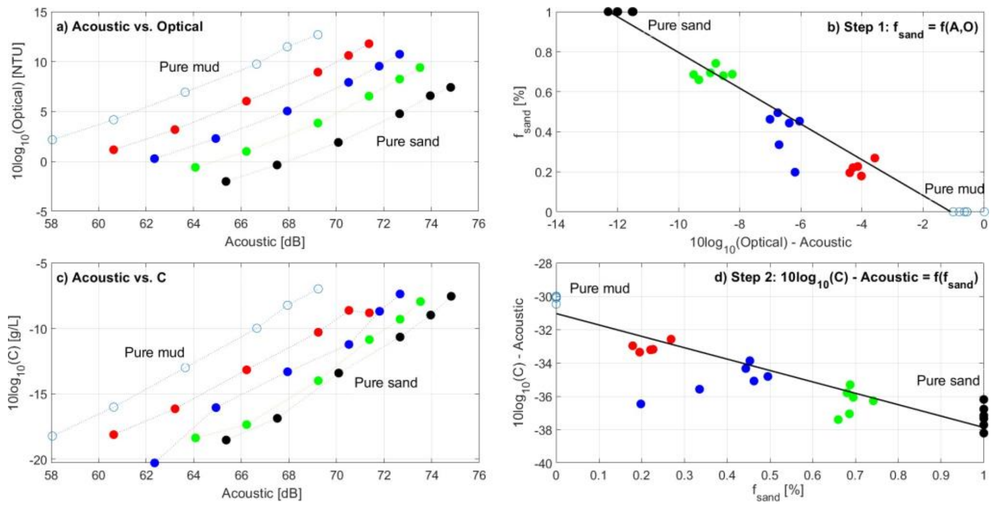

Figure 1. SCI functions obtained from laboratory experiments (b, d). Relationships between raw, uncalibrated optical and acoustic signals and total concentration (a, c). Pure sand: $f_{sand} = 1$ (or $f_{mud} = 0$) and vice versa. Reprinted from Tran et al (2023).

[1] Royal Belgian Institute of Natural Sciences, OD Nature, Brussels, Belgium, dtran@naturalsciences.be
[2] IFREMER, Laboratoire DHYSED, Plouzané, France

Results and conclusions

Overall, the application of the SCI method allows one to investigate near-bed sand/mud dynamics and SPM concentration directly from raw, uncalibrated OBS and ADV signals without the need for intensive gravimetric measurements of filtered water samples. Figure 2 shows that during spring tide the suspended sediment composition changed from muddy to sandy environment. The altitude data revealed that instead of local resuspension of sand, there was some deposition at the time, suggesting a possibility of advection transport of sand from adjacent areas. This observation was confirmed by comparing with the dredging and beach nourishment activities in the area (Kint et al, 2023). Application of SCI functions to other deployments in 2013 also showed a strong correlation between the fraction of sand/mud and total concentration with coastal engineering activities.

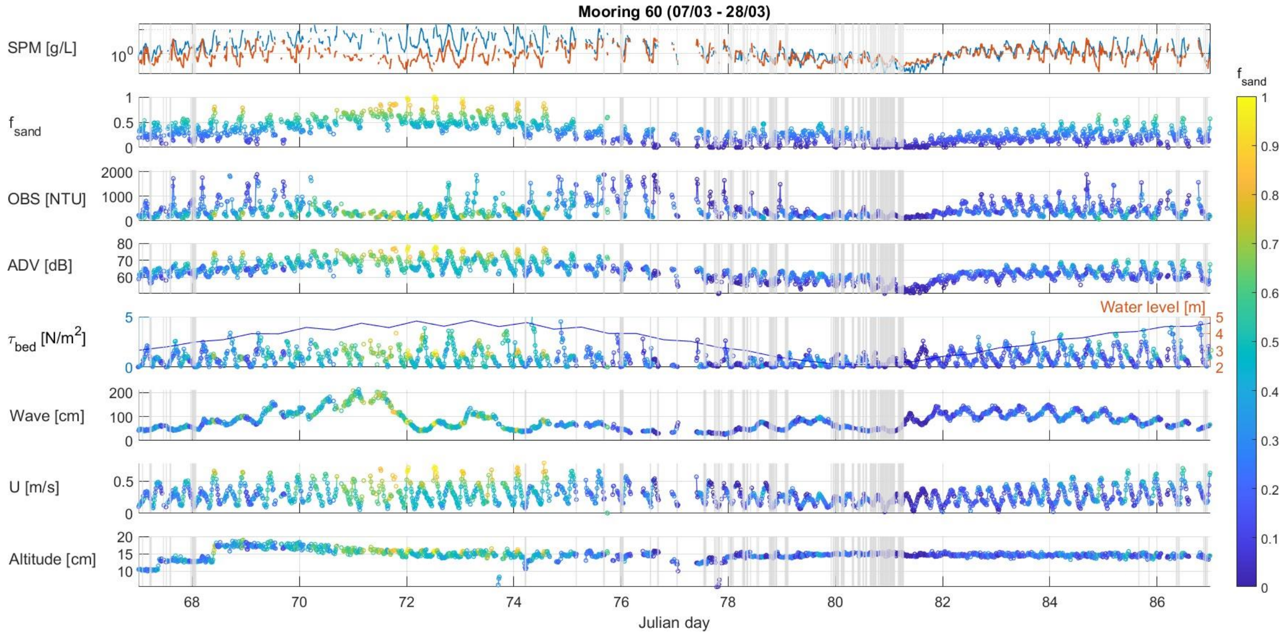

Figure 2. Time series of hydrodynamic conditions, f_{sand} and predicted concentrations. During spring tide, concentrations obtained from OBS measurements were significantly lower than concentrations computed from SCI functions. During neap tide, both concentrations from OBS and SCI method were similar. SCI method also provided information on sand/mud fraction.

In conclusion, results show that the application of SCI method to field data provides a deeper understanding of the sand/mud dynamics and/or concentration variations under different conditions. The results also suggest that the use of OBS alone leaves out important information and underestimates the near-bed concentration due to failure to capture the presence of sand. The SCI method is also applicable to different pairs of optical turbidity and acoustics sensors, providing flexibility and efficiency in either revisiting historical field data or for current/future long-term, high-frequency measurements. In the future, we will apply this method for acoustic profiler sensors to obtain more comprehensive information on the ratio of sand/mud and SPM concentrations in a water column.

Acknowledgments

This work is part of the research program “PiNS: Particle in the North Sea” funded by Federal Public Planning Service Science Policy and “EU_Sed” Marie Sklodowska-Curie Postdoctoral Fellowship (No 101067047).

References

Kint, L., Barette, F., Degrendele, K., Roche, M., Van Lancker, V., (2023). Sediment variability in intermittently extracted sandbanks in the Belgian part of the North Sea. Frontiers in Earth Science, 11:1154564, DOI: 10.3389/feart.2023.1154564.

Pearson, S., Verney, R., Prooijen, B., Tran, D., Hendriks, E., Jacquet, M., Wang, Z., (2021). Characterizing the composition of sand and mud suspensions in coastal and estuarine environments using combined optical and acoustic measurements. JGR: Ocean, 126(7), e2021JC017354.

Tran, D., Desmit, X., Verney, R., Fettweis, M., (2023). Application of sediment composition index to predict suspended particulate matter concentration in the North Sea. INTECOH 2023, South Korea.

APPENDIX 4

Huynh TT et al. 2024. Spatiotemporal dynamics of suspended particulate matter in the water environment: A review. Water 16, 3613

water

Review

Spatiotemporal Dynamics of Suspended Particulate Matter in Water Environments: A Review

Trung Tin Huynh [1,2], Jaein Kim [3], Sang Deuk Lee [4], Michael Fettweis [5], Qilong Bi [6], Sangsik Kim [7,*], Sungyun Lee [8], Yun Young Choi [8], Huu Son Nguyen [1,9], Trong Vinh Bui [9] and Byung Joon Lee [3,8,*]

[1] Bach Khoa Ho Chi Minh City Science Technology Joint Stock Company, Ho Chi Minh City University of Technology (HCMUT), VNU-HCM, Ho Chi Minh City 70000, Vietnam; httinvn@gmail.com (T.T.H.); nguyenhuuson@hcmut.edu.vn (H.S.N.)
[2] School of Advanced Science and Technology Convergence, Kyungpook National University, 2559 Gyeongsang-daero, Sangju 37224, Republic of Korea
[3] Energy Environment Institute, Kyungpook National University, 2559 Gyeongsang-daero, Sangju 37224, Republic of Korea; jikim1224@knu.ac.kr
[4] Nakdonggang National Institute of Biological Resources (NNIBR), Sangju 37242, Republic of Korea; diatom83@nnibr.re.kr
[5] Operational Directorate Natural Environment, Royal Belgian Institute of Natural Sciences, Rue Vautier 29, B-1000 Bruxelles, Belgium; mfettweis@naturalsciences.be
[6] Department of Ecosystems & Sediment Dynamics, Deltares, 2629HV Delft, The Netherlands; qilong.bi@deltares.nl
[7] Department of Energy Chemical Engineering, Kyungpook National University, 2559 Gyeongsang-daero, Sangju 37224, Republic of Korea
[8] Department of Environmental Safety Engineering, Kyungpook National University, 2559 Gyeongsang-daero, Sangju 37224, Republic of Korea; sungyunlee@knu.ac.kr (S.L.); yunchoi@knu.ac.kr (Y.Y.C.)
[9] Faculty of Geology and Petroleum Engineering, Ho Chi Minh City University of Technology (HCMUT), VNU-HCM, Ho Chi Minh City 70000, Vietnam; btvinh@hcmut.edu.vn
* Correspondence: sangsik@knu.ac.kr (S.K.); bjlee@knu.ac.kr (B.J.L.); Tel.: +82-54-530-1334 (S.K.); +82-54-530-1444 (B.J.L.)

check for updates

Citation: Huynh, T.T.; Kim, J.; Lee, S.D.; Fettweis, M.; Bi, Q.; Kim, S.; Lee, S.; Choi, Y.Y.; Nguyen, H.S.; Bui, T.V.; et al. Spatiotemporal Dynamics of Suspended Particulate Matter in Water Environments: A Review. *Water* **2024**, *16*, 3613. https://doi.org/10.3390/w16243613

Academic Editor: Xavier Durrieu de Madron

Received: 23 October 2024
Revised: 7 December 2024
Accepted: 12 December 2024
Published: 15 December 2024

Abstract: Suspended particulate matter (SPM) is an indispensable component of water environments. Its fate and transport involve various physical and biogeochemical cycles. This paper provides a comprehensive review of SPM dynamics by integrating insights from biogeochemical processes, spatiotemporal observation techniques, and numerical modeling approaches. It also explores methods for diagnosing SPM-mediated biogeochemical processes, such as the flocculation kinetics test and organic matter composition analysis. Advances in remote sensing, in situ monitoring, and high-resolution retrieval algorithms are discussed, highlighting their significance in detecting and quantifying SPM concentrations across varying spatial and temporal scales. Furthermore, this review examines integrated models that incorporate population balance equations on the basis of flocculation kinetics into multi-dimensional sediment transport models. The results from this study provide valuable insights into SPM dynamics, ultimately enhancing our knowledge of SPM behavior and transport in water environments. However, uncertainties remain due to limited field data on flocculation kinetics and the need for parameter optimization in numerical models. Addressing these gaps through enhanced fieldwork and model refinement will significantly improve our ability to predict and manage SPM dynamics, which is critical for sustainable aquatic ecosystem management in an era of rapid environmental change.

Keywords: suspended particulate matter; remote sensing; echosounder; population balance equation model; suspended particulate matter retrieval

1. Introduction

Suspended particulate matter (SPM) originates from various natural and anthropogenic sources, including terrigenous and autochthonous particles, as well as man-made products [1–3]. SPM is characterized by its biomineral composition, such as organics (e.g., transparent exopolymer particles (TEPs), particulate organic carbon (POC), and particulate organic nitrogen (PON)) and inorganics (e.g., mineral, metal or oil droplets, and engineered nanoparticulate). Climate and weather conditions regulate the variation in the organic and inorganic composition of SPM while participating in the hydrological and biogeochemical cycles [4–6]. Under extreme weather conditions, such as rising global temperatures, changes in the growing season length (GSL), or intense rainfall conditions, SPM dynamics often deteriorate aquatic ecosystems, alongside turbid water, siltation, and hypoxia [5,7].

As SPM travels from the upper reaches of rivers to estuaries, it undergoes various physical and biogeochemical processes. These dynamics are influenced by biogeochemical and hydrological factors, such as aquatic chemistry, currents, and turbulence. SPM dynamics are of great concern in water resources management because SPM with cohesive and colloidal properties causes substantial siltation in rivers, estuaries, harbors, and waterways, as well as the propagation or deposition of toxic pollutants [4,8–10]. Specifically, flocculation, defined as a combined process of SPM aggregation and breakage, scavenges particles into larger aggregates [5]. The flocculation of heterogeneous organic and inorganic particulates, such as microbial cells, debris, feces, clays, and metals, creates diverse floc structures that vary in size, density, and porosity [11]. Turbulent flow conditions influence floc structure and size. High turbulence promotes floc breakage, whereas moderate turbulence offers a favorable condition for aggregation [12]. This SPM-mediated process occurring on a minute scale ultimately controls the fate and transport of SPM on regional and global scales. A better understanding of the interactions and flocculation processes of the biomineral particles may clarify SPM dynamics in water environments. However, because most scientific findings of the SPM-mediated processes have been elucidated in well-controlled experiments, they remain uncertain under complex real-world conditions. Extensive efforts in the technological development of observation techniques and mathematical models have been made to bridge the gaps between scientific understanding and real-world conditions.

Traditional pointwise measurements have provided insights into SPM dynamics at specific times and locations. However, these measurements require intensive labor to monitor the spatiotemporal variation of SPM on a large scale [13]. Recently, remote sensing with satellite hyperspectral sensors has been employed to monitor the spatiotemporal distribution of SPM on a regional scale. For example, various sources of satellite hyperspectral images, such as Landsat [14,15], Sentinel [16,17], and MODIS [18–20], have been used to retrieve the spatiotemporal distribution of SPM concentrations. This image analysis utilizes a correlation formula to relate hyperspectral intensity to SPM concentration. Machine learning (ML) algorithms facilitate the retrieval of high-quality, high-resolution SPM dynamics [21,22]. Unmanned aerial vehicles (UAVs), portable flying objects equipped with hyperspectral image sensors, provide high-resolution images [23–25]. Recent advancements in hardware and software for remote sensing enable the instantaneous and continuous monitoring of SPM dynamics and water quality indices on regional and global scales.

With the advancement of SPM monitoring techniques, modern computer-aided prediction models have been developed to simulate complex SPM-mediated biogeochemical processes on regional and global scales. However, insufficient knowledge of these processes continues to result in significant errors in numerical calculations [26,27]. To improve mathematical models for SPM processes, substantial efforts have been made to integrate flocculation kinetics into large-scale sediment transport modeling systems [28,29], such as TELEMAC [30–32] and ROMS [33]. The incorporation of flocculation kinetics into sediment transport models adopts population balance equations (PBE) to form a mechanistic model [32,34,35].

Substantial efforts have been made to elucidate and predict SPM dynamics in water environments. A comprehensive understanding of SPM dynamics at both minute (i.e., molecular, nano, and micro) and regional scales is essential for the better management of estuaries, coasts, and water resources. Therefore, this paper summarizes the state-of-the-art knowledge on SPM-mediated biogeochemical processes, along with recent advancements in analytical and observation techniques and predictive models of SPM dynamics in water environments. The advanced analytical and monitoring methods and numerical models introduced in this research offer valuable insights into the fate and transport of SPM and SPM-associated pollutants in water environments. This helps us to establish the best management practices regarding SPM-mediated issues, such as turbid water, siltation, and water quality degradation, in the era of climate change.

2. Overview of the SPM-Mediated Aquatic Processes

2.1. Heterogeneous Components of Suspended Particulate Matter

Heterogeneous components of flocs include a variety of organics and minerals (Figure 1) [5,31,37]. Particulate organic matter includes living cells, such as bacteria, phytoplankton, and zooplankton, and non-living debris, such as fecal pellets, detritus, and decomposed products from microbial activities [3,5,38]. Conversely, particulate inorganic matter originates from anthropogenic, lithogenic, and biogenic sources. For example, quartz, feldspar, illite, and glauconite are the dominant mineral particles, whereas engineered nano- or microparticles and oil droplets are derived from human activities [36]. The interactions and flocculation of these heterogeneous organic and inorganic particles play a significant role in SPM dynamics and regulate biogeochemical cycles in water environments [5,36,39].

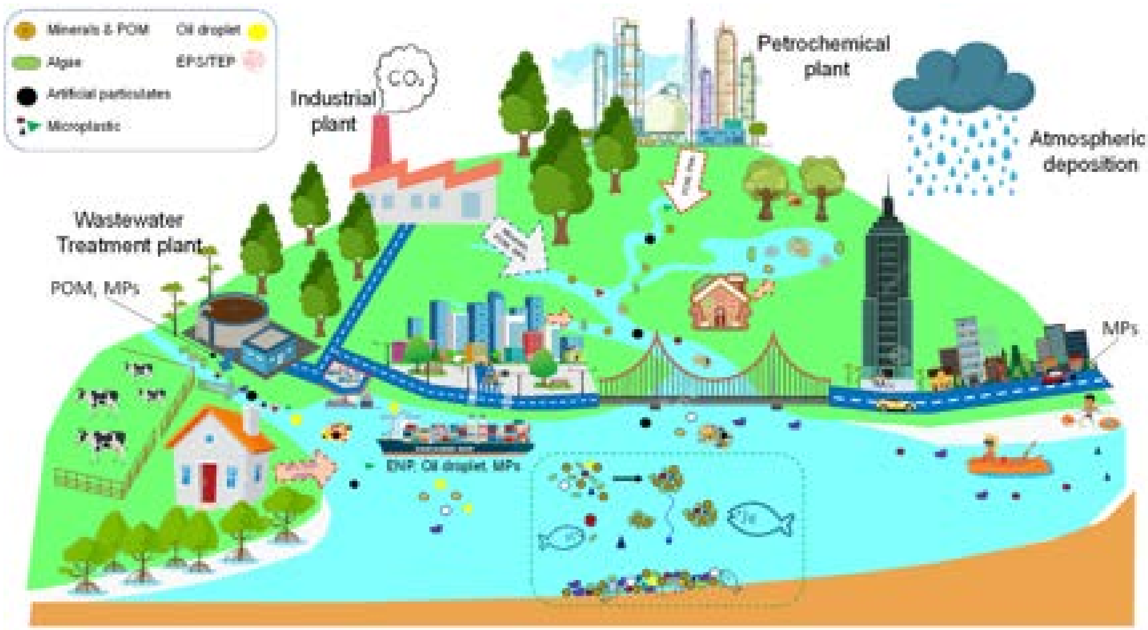

Figure 1. Sources, fate, and transport of flocs with heterogeneous composition.

Microorganisms and multicellular organisms often exhibit adhesive properties, aiding in the scavenging of SPM in water environments. For example, microalgae produce extracellular biopolymers in the form of slimes, spines, or hairs, which promote SPM aggregation. Additionally, aquatic microorganisms aggregate into SPM flocs, influencing their morphology (e.g., size, density, and porosity). Biopolymers produced by various aquatic organisms are commonly referred to as extracellular polymeric substances (EPS) or TEP [40]. EPS, together with cations such as Ca^{2+} and Mg^{2+}, enhance particle aggregation by forming polymeric bridges between microbial cells and other particles. TEPs, on the other hand, are particulate forms of biopolymers larger than 0.4 μm that remain suspended in water environments. Due to their adhesive nature, TEPs act as glue to enhance SPM aggregation [36]. In turbid water environments, TEPs bind to microbial cells and clay minerals, forming biomineral flocs with heterogeneous contents, which eventually undergo

fields leads to eutrophic conditions and phytoplankton bloom, in which microalgae become a major component of SPM flocs, thus altering SPM dynamics [36].

SPM generates composite flocs with a variety of organic and inorganic materials, such as clay particles, microbial cells and debris, and biopolymers. Their morphological properties help to develop unique floc structures. The structure of heterogeneous flocs depends highly on the organic matter fraction (i.e., cells, debris, biopolymers) within the flocs. The floc structure becomes more dense and compact with an abundance of inorganic particles (i.e., clay, silt), whereas it becomes less dense and more fluffy in biologically enriched conditions with higher organic matter content [51,52]. Biopolymers are especially crucial in constructing the floc structure. These mucilaginous biopolymers tend to combine heterogeneous components and develop large, porous flocs [53].

Figure 1. Sources, fate, and transport of flocs with heterogeneous composition.

2.2. Processes Controlling the Dynamics of Suspended and Benthic Particulate Matter

Complex biological and physicochemical processes, including flocculation, contribute to the formation of a highly concentrated sediment layer (HCSL) on the river, lake, or sea floor [4]. The aggregation of SPM into settleable flocs, and the subsequent formation of HCSL on the bed, depends on the hydrological and biogeochemical conditions of the near-bed layer, such as flow and turbulence intensity, organic matter (OM) content, and benthic populations. However, wave and current actions, as well as the biological actions of filter feeders, disturb and resuspend the HCSL [4,54]. Once developed, the HCSL regulates the near-bed ecosystem through fluid mud formation, carbon burial, or hypoxia. Conversely, the deformation and resuspension of SPM by the wave and current actions attenuate light intensity and primary production, leading to the clogging of feeding sources for benthic organisms [55,56].

The cohesive components of SPM help to form settleable flocs and enhance HCSL formation on the bed [36]. Among the heterogeneous components of SPM, OM, specifically biopolymers, plays a crucial role in flocculation by building polymeric bridges sedimentation and deposition on riverbeds or seabeds. Biopolymers and bio-mediated flocculation are also subject to seasonal variations in terms of quantity and quality while participating in biological cycles [41,42].

Human activities contribute a substantial amount of xenobiotic particles, such as microplastics (MPs), engineered nanoparticles (EPNs), and oil droplets, to floc formation in water environments (Figure 1) [36]. MP pollution has become a major threat to riverine, estuarine, and marine ecosystems [43–45]. MPs participate in the flocculation of SPM [46] as heterogeneous components due to their high affinity for solid surfaces [47,48]. Similarly, engineered nanoparticles (ENPs) produced by industrial activities (e.g., cosmetics, paintings, lubricants, or coating materials) are easily captured by EPS matrices of flocs. Oil droplets, which are hydrophobic particles discharged from oil spill sites, readily aggregate with biomineral particles to form oil–mineral aggregates (OMAs) or "clay–oil flocs". OMAs are typically small, stable, hydrophobic, and exhibit poor settling capability in the water column [49,50]. Furthermore, nutrient discharge from agricultural fields leads to eutrophic conditions and phytoplankton bloom, in which microalgae become a major component of SPM flocs, thus altering SPM dynamics [36].

Heterogeneous components of flocs include a variety of organics and minerals, such as clay particles, microbial cells and debris, and biopolymers. Their morphological properties help to develop unique floc structures. The structure of heterogeneous flocs depends highly on the organic matter fraction (i.e., cells, debris, biopolymers) within the flocs. The floc structure becomes more dense and compact with an abundance of inorganic particles (i.e., clay, silt), whereas it becomes less dense and more fluffy in biologically enriched conditions with higher organic matter content [51,52]. Biopolymers are especially crucial in constructing the floc structure. These mucilaginous biopolymers tend to combine heterogeneous components and develop large, porous flocs [53].

2.2. Processes Controlling the Dynamics of Suspended and Benthic Particulate Matter

Complex biological and physicochemical processes, including flocculation, contribute to the formation of a highly concentrated sediment layer (HCSL) on the river, lake, or sea floor [4]. The aggregation of SPM into settleable flocs, and the subsequent formation of HCSL on the bed, depend on the hydrological and biogeochemical conditions of the near-bed layer, such as flow and turbulence intensity, organic matter (OM) content, and benthic populations. However, wave and current actions, as well as the biological actions of filter feeders, disturb and resuspend the HCSL [4,54]. Once developed, the HCSL regulates the near-bed ecosystem through fluid mud formation, carbon burial, or hypoxia. Conversely, the deformation and resuspension of SPM by the wave and current actions attenuate light intensity and primary production, leading to the clogging of feeding sources for benthic organisms [55,56].

The cohesive components of SPM help to form settleable flocs and enhance HCSL formation on the bed [36]. Among the heterogeneous components of SPM, OM, specifically biopolymers, plays a crucial role in flocculation by building polymeric bridges between particles. Microalgae in eutrophic waters produce abundant biopolymers and enhance the flocculation of biomineral particles in fresh, brackish, or saline waters. Flocs with a high OM content are typically large and highly settleable, thus contributing to the formation of HCSL on the bed [4–6]. Biomineral flocs, consisting of organic and mineral particles, are known as "mucilaginous structures". These structures occur in biologically active and turbid waters, such as estuaries, and control SPM dynamics. The mucilaginous flocs, characterized by tight interparticle bindings and high settling velocity, tend to deposit on the river- or seabed [51,53]. Given that floc structures on a minute scale influence SPM dynamics on a large scale, understanding the microscopic interactions and processes of SPM is necessary to achieve the sustainable management of waterways, fisheries, and water resources [53,57].

SPM flocs with heterogeneous components scavenge a variety of natural and anthropogenic particles and transport them downward to river or lake beds. The flocs in influence SPM dynamics on a large scale, understanding the microscopic interactions and processes of SPM is necessary to achieve the sustainable management of waterways, fisheries, and water resources [53,57].

SPM flocs with heterogeneous components scavenge a variety of natural and anthropogenic particles and transport them downward to river or lake beds. The flocs in the benthic environment affect the biogeochemical cycles of various carbonaceous and mineral elements. For example, flocs with particulate organic carbon (POC) enhance the downward flux of carbon in the water column and carbon storage in river or lake beds. Excessive POC deposition on the bed may alter the redox conditions in benthic environments. The biodegradation of POC depletes dissolved oxygen and causes anaerobic conditions (Figure 2) [4,5,58]. Heavy metals and their composites adsorb on clays and integrate into flocs. The heavy metals in flocs tend to settle and deposit on river or lake beds. However, when particulate heavy metals are exposed to anaerobic conditions in the benthic layer, they tend to become dissolved and mobile, being released back into the water column [59]. Sulfur redox reactions also affect the mobility of heavy metals, with the formation of either particulate metal–sulfur composites in reduced conditions or dissolved metal ions in oxidative conditions [60]. Microplastics, as an emerging xenobiotic element, are also incorporated into flocs and hence tend to settle and deposit on river or lake beds [61]. Heavy metals and microplastics in flocs can be taken up or ingested by plants and animals in water and benthic environments, accumulating in the food web and threatening ecosystems and human beings.

the benthic environment affect the biogeochemical cycles of various carbonaceous and mineral elements. For example, flocs with particulate organic carbon (POC) enhance the downward flux of carbon in the water column and carbon storage in river or lake beds. Excessive POC deposition on the bed may alter the redox conditions in benthic environments. The biodegradation of POC depletes dissolved oxygen and causes anaerobic conditions (Figure 2) [4,5,58]. Heavy metals and their composites adsorb on clays and integrate into flocs. The heavy metals in flocs tend to settle and deposit on river or lake beds. However, when particulate heavy metals are exposed to anaerobic conditions in the benthic layer, they tend to become dissolved and mobile, being released back into the water column [59]. Sulfur redox reactions also affect the mobility of heavy metals, with the formation of either particulate metal–sulfur composites in reduced conditions or dissolved metal ions in oxidative conditions [60]. Microplastics, as an emerging xenobiotic element, are also incorporated into flocs and hence tend to settle and deposit on river or lake beds [61]. Heavy metals and microplastics in flocs can be taken up or ingested by plants and animals in water and benthic environments, accumulating in the food web and threatening ecosystems and human beings.

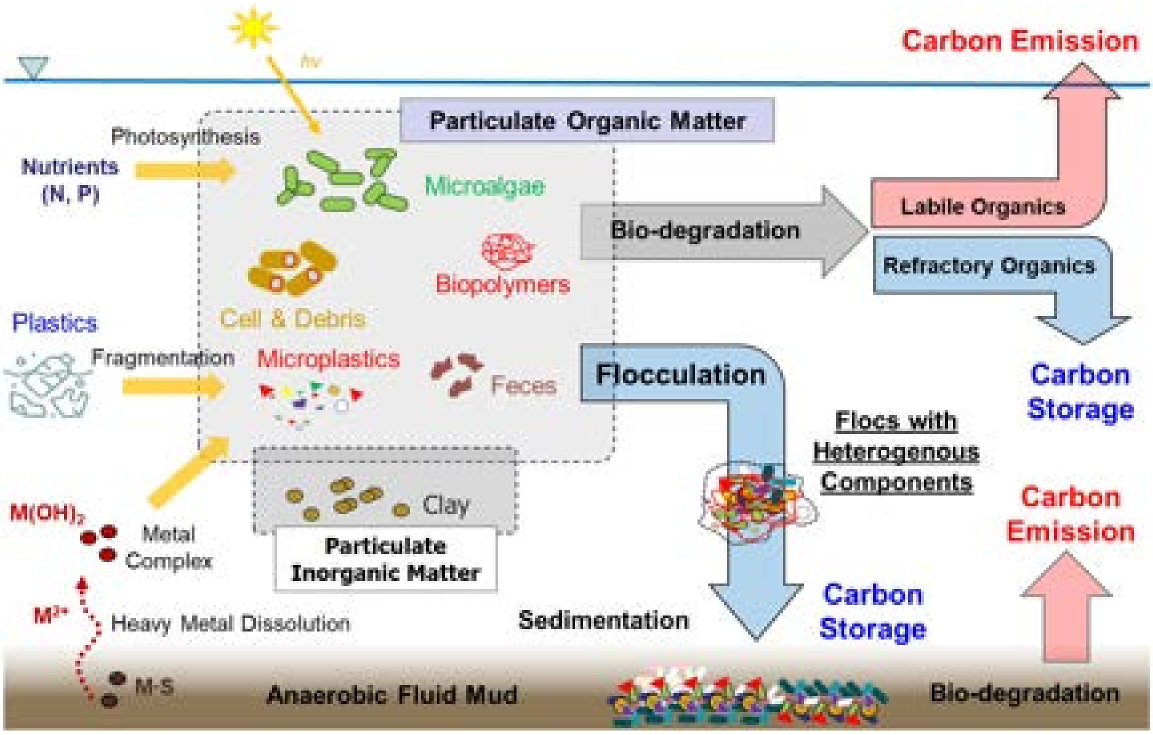

Figure 2. Schematic diagram of the biogeochemical cycle of carbonaceous materials mediated by flocculation with heterogeneous components in water and benthic environments.

Figure 2. Schematic diagram of the biogeochemical cycle of carbonaceous materials mediated by flocculation with heterogeneous components in water and benthic environments.

2.3. SPM Dynamics in the Era of Climate Change

2.3. SPM Dynamics in the Era of Climate Change

Global warming is associated with increasing atmospheric temperatures, sea level rise, and sea ice melting [62,63]. It also induces changes in the hydrological cycle and the heat content of oceans, leading to variations in SPM dynamics [63,64]. Warmer temperatures can increase precipitation intensity, hydrological variability, and GSL. Research indicates that an average increase of 1% in precipitation results in a 1.3% increase in water discharge and a 2% increase in sediment load [65]. Additionally, climate change accelerates soil weathering, which enhances the erosion of sediment fluxes from land to water resources. Climate change can also disrupt the SPM budget's equilibrium by altering the

Global warming is associated with increasing atmospheric temperatures, sea level rise, and sea ice melting [62,63]. It also induces changes in the hydrological cycle and the heat content of oceans, leading to variations in SPM dynamics [63,64]. Warmer temperatures can increase precipitation intensity, hydrological variability, and GSL. Research indicates that an average increase of 1% in precipitation results in a 1.3% increase in water discharge and a 2% increase in sediment load [65]. Additionally, climate change accelerates soil weathering, which enhances the erosion of sediment fluxes from land to water resources. Climate change can also disrupt the SPM budget's equilibrium by altering the biodiversity of riverine habitats [66,67]. Changes in the GSL, characterized by an earlier start of spring and a delayed onset of autumn, correlate with the biogeochemical cycles of the land–water continuum and SPM dynamics [68–70]. This alteration in GSL not only increases rainfall intensity in summer but also reduces soil moisture and streamflow during the dry season [71,72]. Additionally, warmer temperatures and higher nutrient discharge, combined with changes in GSL, promote microalgae proliferation and biopolymer production, thereby facilitating SPM flocculation and HCSL formation [5].

3. Diagnosis of the SPM-Mediated Biogeochemical Processes

3.1. Estimation of Flocculation Kinetics and Potential

Previous studies have performed well-controlled laboratory experiments to investigate flocculation mechanisms systematically. For example, a plume experiment was conducted to reveal the empirical correlation between settling velocity (or floc size) and suspended sediment concentration (SSC) [73]. A Couette-type reactor is frequently used to evaluate flocculation kinetics because it generates well-controlled laminar flow conditions, promoting either aggregation or breakage [74,75]. Besides reactor selection, scholars have adopted a camera-based system to observe changes in floc size and structure resulting from aggregation and breakage [11,12,76–80]. Specifically, LabSFLOC, a camera-based system developed by Manning and Dyer (2002), has been used for the continuous in situ observation of SPM dynamics [81,82]. Obtaining visual images of flocs is a key advantage of using a shear-controlled reactor equipped with a camera system [11,53,81,83]. On the other hand, a light-scattering particle size analyzer, such as the laser in situ scattering and transmissometry (LISST-200X; Sequoia Inc., Seatle, DC, USA) particle size analyzer, has been employed for the instantaneous and continuous monitoring of floc size growth (i.e., flocculation kinetics) [4,5,84,85]. The LISST analyzer enables the real-time monitoring of floc size distribution and the flocculation kinetics of SPM-containing suspensions [4]. However, its measurable floc size is limited to 500 µm, which may not be adequate for large biomineral flocs, such as rivers or marine snow (see Table 1) [4].

Table 1. Comparison of floc measurement techniques, regarding their pros and cons.

Techniques	Properties
LabSFLOC	▪ Camera-based method ▪ Applicability to large-size flocs up to 2000 µm (pros) ▪ Provision of real flocs images (pros) ▪ Time requirement for image analysis (cons) ▪ Limitation in floc size, with respect to image resolution (cons)
LISST-200X	▪ Light-scattering measurement technique ▪ Instantaneous, continuous measurement (pros) ▪ Robust in field measurement (pros) ▪ Incapability of obtaining floc structural images (pros) ▪ Limitation in floc size range (1~500 µm) (cons)

3.2. Analysis of Organic Matter Composition as a Biochemical Driver of Flocculation

OM content in waters or sediments, which usually vary under hydrodynamic forcing, biogeochemical processes, weather conditions, and human activities, significantly influences flocculation kinetics and floc structures [5,52,86,87]. OM either stems from aquatic fauna and flora (i.e., autochthonous) or is discharged from upstream watersheds (i.e., allochthonous). It comprises various organic compounds, such as polysaccharides, proteins, lipids, deoxyribonucleic acid (DNA), and humic substances. Microalgal proliferation during summer can maximize OM production. OM tends to adsorb onto SPM and alter its colloidal and surface properties, thereby controlling SPM dynamics [5,6,36,88]. As a matter of course, OM composition is a key factor in understanding the correlation between OM and SPM dynamics.

Liquid chromatography–organic carbon detection analysis (LC-OCD) classifies the subordinate fractions of OM on the basis of molecular weight. LC-OCD separates OM in a water sample into four major fractions: biopolymers (>20,000 Da), humic substances

(~10,000 Da), building blocks (300–500 Da), and low-molecular weights (<350 Da) [89]. Prior studies have reported that the abundance of biopolymers promotes the formation of polymeric bridges between particles and enhances flocculation kinetics in water environments [4,36]. The fluorescence emission excitation matrix (FEEM) measures the high-resolution fluorescence spectrum of an OM-containing water sample, and it classifies the OM into subgroups, including humic-like, tyrosine-like, and tryptophan-like organic compounds [88,90]. Humic- and fulvic-like fluorophores, characterized by FEEM, have been reported to reduce flocculation kinetics and potential because they modify colloidal and surface properties and cause steric stabilization [5]. Table 2 compares the analytical techniques for organic matter with respect to the advantages and limitations.

Table 2. Comparison of the analytical techniques for organic matter, regarding their pros and cons.

Techniques	Properties
LC-OCD	▪ Liquid chromatography—Organic Carbon Detector ▪ OM fractionation on the basis of its molecular weight ▪ Capability of measuring biopolymers (pros) ▪ Incapability of measuring particulate OM (cons)
FEEM	▪ Fluorescence Excitation–Emission Matrix ▪ OM fractionation on the basis of its fluorescence ▪ Capability of measuring humic substances (pros) ▪ Incapability of measuring biopolymers and POM (cons)

3.3. Field Observation of SPM Dynamics

Field observation using water samples and short- and long-term deployments of acoustic and optical sensors have been conducted to investigate the SPM dynamics under complex, variable environmental conditions, although it requires a substantial amount of equipment and labor costs. The optimal frequency of monitoring is imposed by the main variabilities of the aquatic system, imposed by seasonal, meteorological or tidal variabilities. Additional variations have lower (interannual variations) or higher frequencies (turbulence) or occur irregularly, such as variations caused by extreme weather events or human activities [91]. Examples of field observations are the in situ settling velocity (INSSEV) method, coupled with the Profile of Sediment Transport (POST), which have been broadly applied for in situ observation in European estuaries [82,92]. This combined system enables researchers to observe sediment dynamics under varying currents and turbulence in estuarine and coastal areas. Additionally, a moored tripod system equipped with a 5 MHz ADV Ocean velocimeter, a 3 MHz SonTek® Acoustic Doppler Profiler (ADP), two optical backscatter point sensors (OBS), a Sea-bird SBE37 CT, and a Sequoia Scientific Laser in situ Scattering and Transmissometer (LISST-100X) have been deployed in the Belgian sea to monitor seasonal variations in SPM concentration and settling velocity. The tripod system can conduct multiple observations on hydrodynamic and sediment parameters over extended periods during neap and spring tides or across seasons, including various meteorological events [6,93]. However, the quality of the observed data may deteriorate due to various causes, such as sensor saturation, the obstruction of the measuring window of the sensor by floating objects, and biofouling [94].

4. Regional Scale Observation of the SPM Dynamics

4.1. Aerial-Borne Remote Sensing for Retrieval of Suspended Particulate Matter Concentration

Multispectral image acquisition and analysis have been employed in the retrieval of chlorophyll-a (Chl-a) and SSC on the basis of reflectance at a 700 nm bandwidth of three-visible bands of Blue, Green, and Red (Figure 3) [95–97]. Multiple bandwidths allow for the better retrieval of SPM, chlorophyll-a, and colored dissolved OM concentrations. However, low spectral resolution and cloud cover can hinder the retrieval of SPM concentration. A low signal-to-noise ratio (SNR) can also increase uncertainty in the multispectral image analysis. Multispectral image acquisition and analysis provide a spatiotemporal distribution of SPM concentration on a regional scale, where pointwise sampling and monitoring are impractical. However, the resolution limit and weather obstruction should be considered in the application of multispectral image analysis and the retrieval of SPM concentrations in water bodies. Furthermore, hyperspectral imaging (HSI), on the basis of optical spectroscopy and imaging at various wavelengths, collects data in continuous spectral bands across the electromagnetic spectrum [98]. Airborne hyperspectral images with high spatial and spectral resolution are advantageous for the precise detection of water quality indices [98,99]. Recently, HSI has been widely applied in water resources management, often in conjunction with different retrieval methods, including empirical, semi-empirical, and artificial intelligence (AI) models [13].

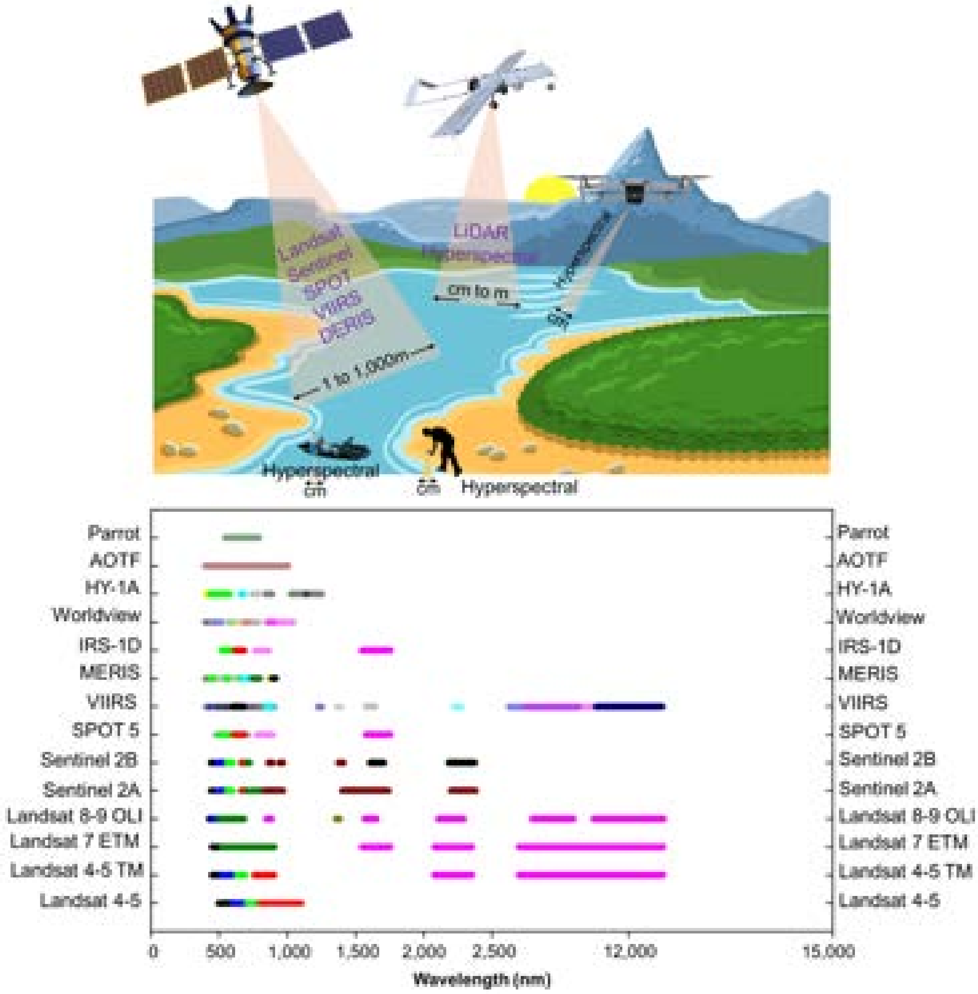

Figure 3. Schematic diagram of satellite-, aircraft-, and UAV-based remote sensing, and measurable spectral bands of satellites in operation [96].

The acquisition of high-resolution, multispectral spatiotemporal images with UAVs has become increasingly popular in water quality and resource management [100]. The UAV equipped with a high-resolution, multispectral image sensor can bridge the gap between satellite and aircraft-based remote sensing techniques (Figure 3). The UAV with a multispectral camera collects real-time data on water quality indices without mobility constraints [101]. For example, a UAV was employed to observe the spatiotemporal distribution of algal blooms in the Great Lake and coastal areas [23,24]. Additionally, an inversion model can establish the spatiotemporal distribution of SPM concentration in coastal areas [15]. UAV-based multispectral or hyperspectral image acquisition and analysis provide an opportunity to monitor the spatiotemporal distribution of SPM concentration with reduced mobility restrictions and lower costs. However, the deployment of small UAVs is constrained by adverse weather conditions (e.g., strong winds and heavy rainfall) and battery time for flight. Additionally, the skill level of the drone operator may influence the quality of hyperspectral images. The georeferencing and post-processing of a large volume of high-resolution images may incur extensive computational costs [13,101].

4.2. Retrieval Algorithm for Suspended Particulate Matter Concentration

Empirical models for assessing SPM concentration utilize the reflectance from spectral measurements or spectroradiometers, either in a single band or as a ratio of two bands. These models establish a correlation between the observed reflectance and the measured SPM concentration [96,102]. The underlying principle is that the reflectance of turbid water containing white or red clay is higher than that of clean water [103]. It is also acknowledged that the reflectance of turbid water depends on the size of the SPM [103,104]. The advantages of these empirical models include ease of use and flexibility in selecting multiple band ratios, allowing for refinement with widely available open-source datasets [13,105]. However, calibrating these empirical models is very tedious, as it requires a large number of pointwise measurements to cover the spatiotemporal distribution of SPM concentration [105]. Furthermore, these models are often difficult to compare in terms of performance because they are typically tuned to unique band positions and bandwidths [105].

Analytical models account for the interaction between bio-optical properties and radiation transmission, using the reflectance spectrum to predict the water quality indices [13]. Reflectance is dependent on the backscattering and absorption coefficients of water bodies [106,107]. Monte Carlo simulations are commonly employed to estimate the light reflectance of water bodies [107,108]. However, determining water reflectance is difficult due to the variability of optical characteristics and water quality indices [13,109]. Additionally, the inconsistency between reflection spectrum acquisition and in situ measurements presents numerous limitations in practical applications [110].

Semi-empirical models (SEM), which combine elements of analytical and empirical models, have demonstrated high performance in retrieving water quality indices, including SPM concentration. These comprehensive models could increase the prediction accuracy for both physical and biogeochemical parameters [111]. SEMs are particularly effective for monitoring highly concentrated suspended sediments with a red–green (R-G) band ratio and near-infrared (NIR) band [111]. In summary, SEMs have demonstrated better performance in retrieving water quality indices and more flexibility in practical applications than analytical and empirical models that rely solely on several specific wave bands. The properties of the empirical, analytical, and semi-empirical models of assessing SPM concentration are summarized in Table 3.

Table 3. Comparison of retrieval algorithms for suspended particulate matter concentration.

Models	Properties	Applications
Empirical Models	▪ Correlate reflectance (single band or band ratios) with observed SPM concentrations ▪ Easy to implement (pros) ▪ Widely applicable with accessible datasets (pros) ▪ Labor-intensive calibration (cons) ▪ Case specific due to unique band tuning (cons)	▪ Best suited for regional-scale data with extensive calibration data and consistent SPM characteristics
Analytical Models	▪ Adopt bio-optical properties and radiation transmission to predict water quality indices ▪ Incorporate bio-optical interactions and physical processes (pros) ▪ Predict multiple indices (pros) ▪ Complication in reflectance determination due to optical variability (cons) ▪ Inconsistencies with in situ data (cons)	▪ Ideal for applications needing robust, high-performance models for turbid water conditions or multiple water quality indices

Table 3. *Cont.*

Models	Properties	Applications
Semi-Empirical Models	▪ Combining empirical and analytical elements to improve prediction accuracy ▪ High accuracy for physical and biogeochemical parameters (pros) ▪ Flexibility in various scenarios (pros) ▪ Effective for highly concentrated sediments (pros) ▪ Complexity in calibration (cons) ▪ Necessity of integration of spectral and optical property data (cons)	• Ideal for applications needing robust, high-performance models for turbid water conditions or multiple water quality indices

ML has been adopted in multispectral or hyperspectral data analysis and model prediction [112,113]. Inspired by the structures of neurons, ML algorithms have been widely applied in the retrieval and prediction of water quality indices from the multispectral or hyperspectral data [13,114]. Among the various ML algorithms (see Table 4), artificial neural network (ANN) is one of the most commonly used models for this purpose. The ANN algorithm adopts neuron architectures to extract high-level features of multispectral and hyperspectral images (Figure 4) [115–117]. For instance, Hosseiny et al. (2023) developed an ANN algorithm to predict bed load sediment transport using 8117 measured datasets from 134 rivers [115]. The ANN algorithm is an effective retrieval and prediction tool for compensating pointwise in situ SPM monitoring, which does not entirely capture the spatiotemporal distribution of SPM concentration. However, the performance of ANN algorithms depends highly on users' competence and knowledge of numerical and computational algorithms.

	▪ Capability of intergration with other algorithm in a hybrid model ▪ Flexibility in modeling non-linear relationships	concentration, turbidity, salinity, water temperature, etc.
Convolutional Neural Networks (CNN)	▪ Enhancement in prediction efficiency ▪ Capability of simulating the multi-directional spatial models	

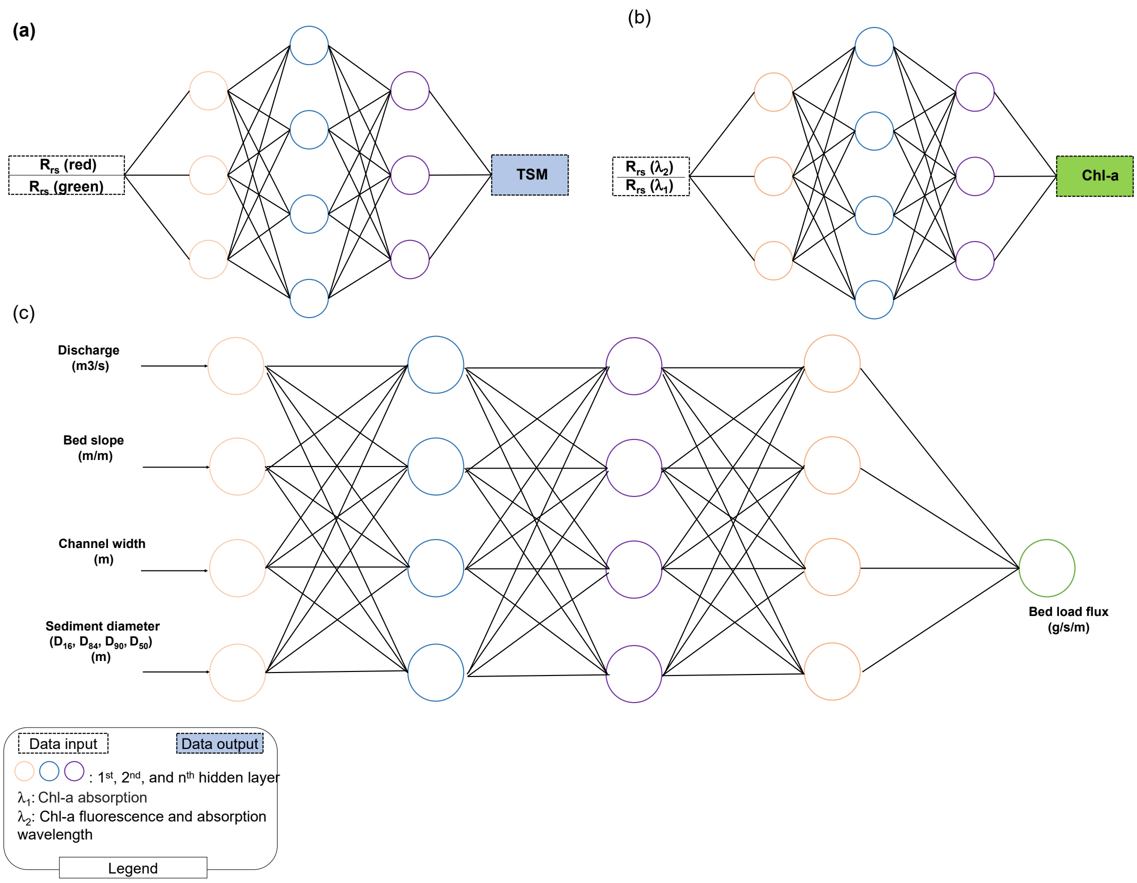

Figure 4. Basic structure for quantification of (a) total suspended matter (TSM), (b) Chlorophyll-a, and (c) bed load flux using the machine learning algorithms [20,115,118].

Figure 4. Basic structure for quantification of (a) total suspended matter (TSM), (b) Chlorophyll-a, and (c) bed load flux using the machine learning algorithms [20,115,118].

4.3. Observation Techniques on Highly Concentrated Sediment Layer

Traditional bed surveys utilize single beam echo sounding (SBES) of 50–200 kHz to identify the bathymetric profile of riverbeds or seabeds [119,120]. Since the 1960s, multi-beam echo sounding (MBES) instruments have been widely adopted for river and coastal

Table 4. Comparison of various AI-based models to retrieve SPM concentration in water environments.

Models	Properties	Applications
Artificial Neural Networks (ANNs)	▪ Capability of modeling complex, non-linear relationships that traditional models cannot handle ▪ Adaptablility in various water environments	▪ Suspended sediment load, wave generation, chlorophyll-a concentration, turbidity, salinity, water temperature, etc.
Random Forest (RF)	▪ Retrieval of highly variable SSC data, ranging up to six orders of magnitude ▪ Capability of intergration with other algorithm in a hybrid model ▪ Flexibility in modeling non-linear relationships	
Convolutional Neural Networks (CNN)	▪ Enhancement in prediction efficiency ▪ Capability of simulating the multi-directional spatial models	

4.3. Observation Techniques on Highly Concentrated Sediment Layer

Traditional bed surveys utilize single beam echo sounding (SBES) of 50–200 kHz to identify the bathymetric profile of riverbeds or seabeds [119,120]. Since the 1960s, multi-beam echo sounding (MBES) instruments have been widely adopted for river and coastal bathymetry surveying [121]. The MBES instruments distinguish the respective signals returned from the top surface of the soft (i.e., fluid) mud and the underlying surface of the consolidated layer, depending on the difference in the acoustic reflection characteristics of the two layers [122]. Recent studies have introduced dual-frequency scanning, combining low-frequency (15–38 kHz) and high-frequency echo soundings (180–220 kHz) to detect fluid mud atop the consolidated bed (Figure 5) [119,123–125]. However, the MBES with the low-frequency echo sounding does not clearly detect the fluid mud when the mud exhibits a weak density gradient [10,119,124]. Additionally, the acoustic signal of the fluid mud can be weakened by organic particles, density, viscosity, and penetration depth [126–128]. These limitations of MBES should be considered in practical applications.

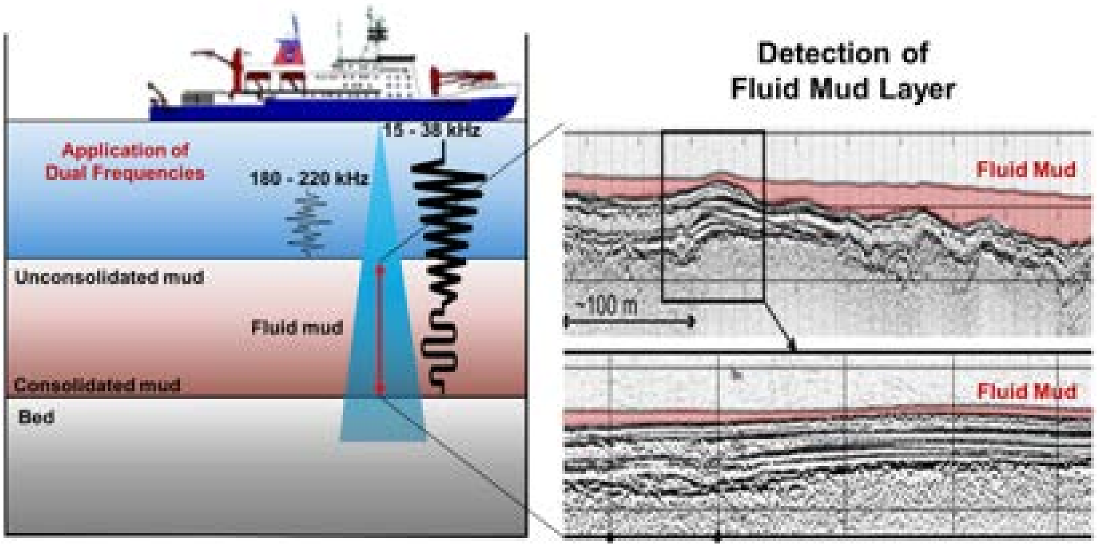

Figure 5. Conceptual schematic of dual frequency echosounder on fluid mud detection with high-frequency (180–220 kHz) and low-frequency (15–38 kHz) ranges [129].

Figure 5. Conceptual schematic of dual frequency echosounder on fluid mud detection with high-frequency (180–220 kHz) and low-frequency (15–38 kHz) ranges [129].

5. Integrated Models of SPM Dynamics, Combining Micro- and Macro-Processes

5.1. Flocculation Kinetic Model, Based on Population Balance Equations

SPM undergoes flocculation (i.e., aggregation and breakage), which alters floc size depending on the biogeochemical conditions of water environments. In formulating floc-

5. Integrated Models of SPM Dynamics, Combining Micro- and Macro-Processes

5.1. Flocculation Kinetic Model, Based on Population Balance Equations

SPM undergoes flocculation (i.e., aggregation and breakage), which alters floc size depending on the biogeochemical conditions of water environments. In formulating flocculation kinetics, Winterwerp introduced a single-class population balance equation (SCPBE), assuming that SPM contains homogeneous flocs with uniform properties, including size, density, and fractal dimension. The SCPBE formulates the aggregation and breakage kernels, which have been further modified by other researchers for improved prediction [130,131]. Subsequently, Lee et al. introduced the two-class population balance equation (TCPBE), assuming that SPM consists of size-fixed flocculi (i.e., building blocks) and size-varying flocs (i.e., buildings). The TCPBE effectively simulates the interactions and flocculation of flocculi and flocs in estuarine and coastal areas [35]. Shen et al. (2018) expanded the model to a three-class population balance equation (3-CPBE), which incorporates biomineral megaflocs alongside flocculi and flocs (Figure 6) [32]. Although complex flocculation kinetics models with multiple floc size classes have been developed and applied [132–134], the TCPBE proved to be one of the simplest and most effective models for simulating SPM dynamics in estuarine and coastal areas [28].

5.2. Integration of Flocculation Kinetics into Multi-Dimensional Sediment Transport Models

Traditional numerical models for cohesive sediment transport rely on empirical correlations between settling velocity, turbulence, salinity, and SSC [135–137]. In integrating mechanistic models of flocculation kinetics (e.g., population balance equations) into a cohesive sediment transport model, Lee et al. implemented the TCPBE to a 1-dimensional vertical sediment transport model and simulated the interactions and flocculation of flocculi and flocs of cohesive sediments in an estuarine and coastal site [28].

Large-scale, multi-dimensional sediment transport models, such as TELEMAC [138], MIKE 21 [139], DELFT3D [140,141], ECOMSED, and ROMS [142,143], are required to balance computing efficiency with model complexity, especially when incorporating the complex processes of cohesive sediments. Earlier multi-dimensional sediment transport models, relying on less computational power, adopted a simple empirical approach while disregarding the complex flocculation kinetics (see Section 1). However, a lack of knowledge of flocculation kinetics may cause substantial errors when dealing with spatiotemporal variations in cohesive sediments [26,138].

When the PBE-based flocculation kinetic models are integrated into a large-scale, multi-dimensional sediment transport model, their applicability and performance should be considered. Some flocculation kinetic models are highly realistic and require substantial computational resources, while others are more approximate and involve relatively fewer computations [28]. A multi-class PBE is effective for simulating the flocculation of various particle and floc size groups but is mathematically complex, involving many coupled differential equations. Conversely, a single-class PBE is mathematically simple and robust, involving only one aggregate size group; however, it cannot simulate flocculation that involves multimodal floc size distributions, hereinafter referred to as multimodal flocculation. As briefly discussed earlier, the two- or three-class PBE is appropriate for integration into a large-scale, multi-dimensional sediment transport model, regarding applicability and performance [32,35].

Recently, Bi and colleagues integrated a PBE-based flocculation kinetic model (MCPBE) into the TELEMAC system. The flocculation kinetics module in the TELEMAC-MCPBE system solves the aggregation and breakage kinetics of cohesive sediments and updates the floc size and settling velocity. The other modules then utilize the updates of flocculation kinetics and floc properties to calculate sediment transport and bed morphological changes at each time step in the numerical calculation. The TELECMAC-MCPBE system has demonstrated great potential for producing realistic and rigorous simulations of the flocculation kinetics of fine-grained cohesive sediments [30–32]. Furthermore, Sherwood et al. (2018) developed a comprehensive simulation system for cohesive sediment transport

MCPBE system solves the aggregation and breakage kinetics of cohesive sediments and updates the floc size and settling velocity. The other modules then utilize the updates of flocculation kinetics and floc properties to calculate sediment transport and bed morphological changes at each time step in the numerical calculation. The TELECMAC-MCPBE system has demonstrated great potential for producing realistic and rigorous simulations of the flocculation kinetics of fine-grained cohesive sediments [30-32]. Furthermore, Sherwood et al. (2018) developed a comprehensive simulation system for cohesive sediment transport by integrating PBE-based flocculation kinetics [78] and bed evolution models [144] into the Regional Ocean Modelling System (ROMS) [143]. The ROMS-PBE system could perform more realistic and accurate simulations of cohesive sediment transport in estuarine and coastal areas than earlier versions of the ROMS. However, the ROMS-PBE model may not be applicable to extreme turbulent conditions, which cause the abrupt destruction of flocs and fluid mud layers. Additionally, the selection of fitting parameters for flocculation kinetics poses challenges in practical applications of both the ROMS-PBE and TELEMAC-MCPBE systems [33].

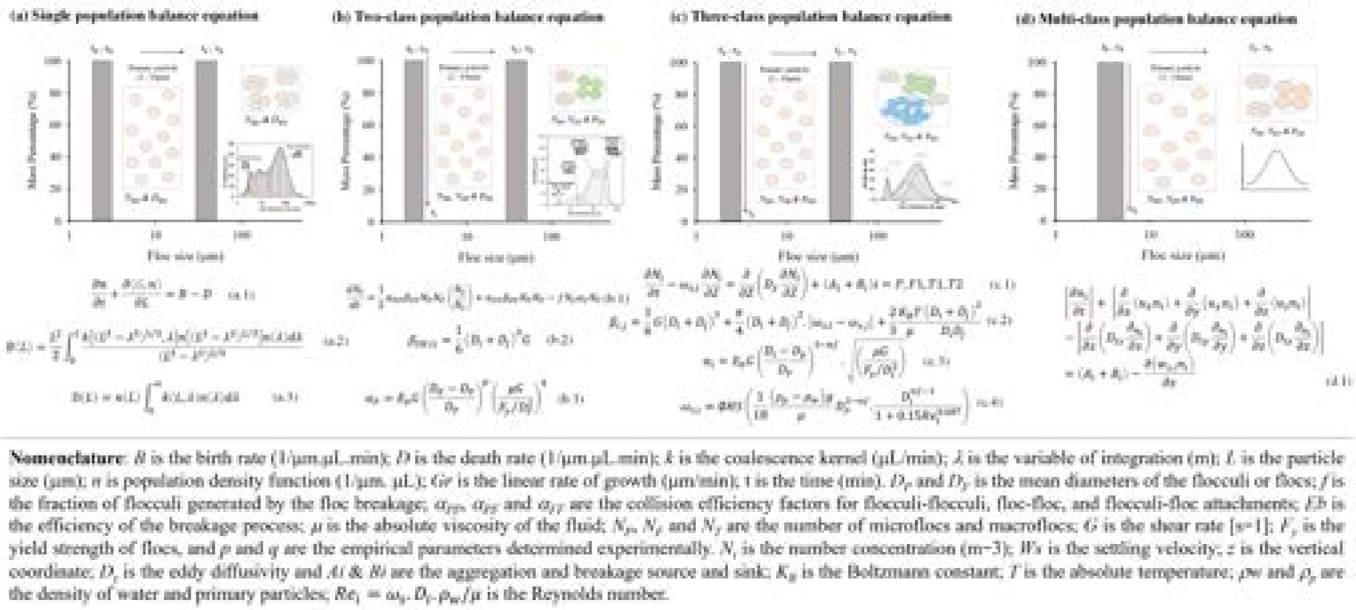

Figure 6. Comparison of (**a**) single−class population balance equation, (**b**) two−class population balance equation, (**c**) three−class population balance equation, and (**d**) multi−class population balance equation models [32,35,145,146].

Furthermore, a realistic, comprehensive biogeochemical model may be developed by integrating flocculation kinetics with heterogeneous components. The PBE-based flocculation kinetic model proposed in this study serves as a foundation for such a realistic, comprehensive biogeochemical model, as its mathematical formulation is theory-based (i.e., not empirical) and easily adaptable to other biogeochemical processes. For example, biologically mediated flocculation, which combines biological and mineral particles, has been formulated based on the PBE-based flocculation kinetic model [34]. Integrating the PBE-based flocculation model into a large-scale, multi-dimensional water quality (i.e., ecological) model will allow for the realistic prediction of the biogeochemical cycles of leading elements in water and benthic environments [33]. This model can also be extended to predict the behaviors of emerging contaminants, such as heavy metals and microplastics. The realistic, comprehensive biogeochemical model with flocculation kinetics may be used to diagnose and predict the way that the weather, hydrological, ecological, and anthropogenic drivers affect the biogeochemical cycles of the leading elements in the era of climate change.

6. Conclusions

SPM is an essential element in water environments, and SPM-mediated processes regulate numerous environmental issues, such as water quality, ecology, siltation, and bank erosion. Understanding SPM dynamics requires comprehensive investigation into biophysicochemical processes (e.g., flocculation, sedimentation, and consolidation), measurement techniques (e.g., remote sensing and echo-sounding surveys), and numerical models.

These investigations provide valuable insights into the diagnosis, analysis, detection, and simulation of the SPM dynamics. The findings of this review are summarized below:

- SPM flocs contain heterogeneous components and develop various floc structures. These compositional and structural properties of SPM flocs can be used as a knowledge basis to regulate SPM dynamics in biogeochemical cycles.
- Advances in multispectral and hyperspectral image acquisition and analysis enable the identification and quantification of long-term, large-scale spatiotemporal SPM dynamics. Machine learning (ML) algorithms for retrieving SPM concentration can also be employed as big data analysis tools for predicting the spatiotemporal distribution of SPM concentration.
- The PBE-based flocculation kinetic model, integrated into a large-scale, multi-dimensional sediment transport model, can be used for realistic and rigorous simulations of SPM dynamics on regional or global scales. A realistic, comprehensive biogeochemical model with PBE-based flocculation kinetics can further be used to diagnose and predict SPM dynamics and biogeochemical cycles in the era of climate change.

However, the lack of field investigations into flocculation kinetics and SPM dynamics may increase uncertainty in these applications. Additionally, estimating the fitting parameters of numerical models is essential for their practical applications.

Author Contributions: Conceptualization, T.T.H., T.V.B. and B.J.L.; methodology, T.T.H., J.K., S.D.L., M.F., Q.B. and B.J.L.; writing—original draft preparation, T.T.H. and B.J.L.; writing—review and editing, S.K., T.V.B. and B.J.L.; visualization, S.K., S.L., Y.Y.C., H.S.N., T.V.B. and B.J.L.; supervision, T.V.B. and B.J.L.; project administration, J.K. and T.T.H. All authors have read and agreed to the published version of the manuscript.

Funding: This research was funded by the Basic Science Research Program through the National Research Foundation of Korea (NRF) (Grant No. RS-2023-00239875 and NRF-2020R1I1A3A04036895) and Nakdonggang National Institute of Biological Resources (Grant No. NNIBR20242104).

Data Availability Statement: Data will be made available on request.

Acknowledgments: Scientific input from Michael Fettweis is integrated in the research programs, be PiNS (contract nr RV/21/PiNS) supported by the Belgian Science Policy (BELSPO), and MOMO, supported by the Maritime Access Division of the Flemish Ministry of Mobility and Public Works. We acknowledge Ho Chi Minh City University of Technology (HCMUT), VNU-HCM for supporting this study.

Conflicts of Interest: Author Trung Tin Huynh was employed by the company Bach Khoa Ho Chi Minh City Science Technology Joint Stock. The remaining authors declare that the research was conducted in the absence of any commercial or financial relationships that could be construed as a potential conflict of interest.

Abbreviations

EPN	Engineered Nanoparticles
EPS	Extracellular Polymeric Substances
FEEM	Fluorescence emission excitation matrix
GSL	Growing Season Length
HCSL	Highly Concentrated Sediment Layer
LC-OCD	Liquid Chromatography–Organic Carbon Detection Analysis
MP	Microplastic
OM	Organic Matter
OMA	Oil–Mineral Aggregates
PBE	Population Balance Equation
POC	Particulate Organic Carbon
PON	Particulate Organic Nitrogen
SPM	Suspended Particulate Matter
SSC	Suspended Sediment Concentration

TEP	Transparent Exopolymer Particles
TSM	Total Suspended Matter
UAV	Unmanned Aerial Vehicle

References

1. Dyer, K. Sediment processes in estuaries: Future research requirements. *J. Geophys. Res. Ocean.* **1989**, *94*, 14327–14339. [CrossRef]
2. Shin, H.; Portela, L.; Schaerer, C.; Mangiavacchi, N. Dynamics of suspended sediment transport: A Direct Numerical Simulation study. *Int. J. Multiph. Flow* **2022**, *155*, 104165. [CrossRef]
3. Wang, Y.; Gao, L. Sources and dynamics of suspended particulate matter in a large-river dominated marine system: Contributions from terrestrial sediments, biological particles, and flocculation. *J. Mar. Syst.* **2022**, *225*, 103648. [CrossRef]
4. Huynh, T.; Kim, J.; Kim, W.; Hur, J.; Ho, Q.; Bi, Q.; Bui, T.; Kim, J.; Lee, S.; Choi, Y. Dynamics of suspended particulate matter in an impounded river under dry and wet weather conditions. *Water Resour. Res.* **2023**, *59*, e2022WR033629. [CrossRef]
5. Lee, B.; Kim, J.; Hur, J.; Choi, I.; Toorman, E.; Fettweis, M.; Choi, J. Seasonal dynamics of organic matter composition and its effects on suspended sediment flocculation in river water. *Water Resour. Res.* **2019**, *55*, 6968–6985. [CrossRef]
6. Fettweis, M.; Baeye, M. Seasonal variation in concentration, size, and settling velocity of muddy marine flocs in the benthic boundary layer. *J. Geophys. Res. Ocean.* **2015**, *120*, 5648–5667. [CrossRef]
7. Siddha, S.; Sahu, P. Impact of climate change on the river ecosystem. In *Ecological Significance of River Ecosystems*; Madhav, S., Kanhaiya, S., Srivastav, A., Singh, V., Singh, P., Eds.; Elsevier: Amsterdam, The Netherlands, 2022; pp. 79–104.
8. Li, J.; He, Q.; Xiang, W.; Wan, X.; Shen, H. Fluid mud transportation at water wedge in the Changjiang Estuary. *Sci. China Ser. B Chem.* **2001**, *44*, 47–56. [CrossRef]
9. Vinzon, S.B.; Mehta, A.J. Lutoclines in high concentration estuaries: Some observations at the mouth of the Amazon. *J. Coast. Res.* **2003**, *19*, 243–253.
10. Kirby, R. High Concentration Suspension (Fluid Mud) Layers in Estuaries. In *Physical Processes in Estuary*; Leussen, J.D.W.v., Ed.; Springer: London, UK, 1988; pp. 463–485.
11. Wheatland, J.A.; Bushby, A.J.; Spencer, K.L. Quantifying the structure and composition of flocculated suspended particulate matter using focused ion beam nanotomography. *Environ. Sci. Technol.* **2017**, *51*, 8917–8925. [CrossRef]
12. Tran, D.; Kuprenas, R.; Strom, K. How do changes in suspended sediment concentration alone influence the size of mud flocs under steady turbulent shearing? *Cont. Shelf Res.* **2018**, *158*, 1–14. [CrossRef]
13. Yang, H.; Kong, J.; Hu, H.; Du, Y.; Gao, M.; Chen, F. A Review of Remote Sensing for Water Quality Retrieval: Progress and Challenges. *Remote Sens.* **2022**, *14*, 1770. [CrossRef]
14. Doxaran, D.; Froidefond, J.-M.; Castaing, P. Remote-sensing reflectance of turbid sediment-dominated waters. Reduction of sediment type variations and changing illumination conditions effects by use of reflectance ratios. *Appl. Opt.* **2003**, *42*, 2623–2634. [CrossRef] [PubMed]
15. Wei, L.; Huang, C.; Zhong, Y.; Wang, Z.; Hu, X.; Lin, L. Inland Waters Suspended Solids Concentration Retrieval Based on PSO-LSSVM for UAV-Borne Hyperspectral Remote Sensing Imagery. *Remote Sens.* **2019**, *11*, 1455. [CrossRef]
16. Sánchez-Espinosa, A.; Schröder, C. Land use and land cover mapping in wetlands one step closer to the ground: Sentinel-2 versus landsat 8. *J. Environ. Manag.* **2019**, *247*, 484–498. [CrossRef]
17. Peterson, K.T.; Sagan, V.; Sidike, P.; Cox, A.L.; Martinez, M. Suspended sediment concentration estimation from landsat imagery along the lower missouri and middle Mississippi Rivers using an extreme learning machine. *Remote Sens.* **2018**, *10*, 1503. [CrossRef]
18. Tian, Q.; Xu, K.; Wang, Y.; Liang, C. Dam impacts on seasonality of water and sediment transport in intensively managed river basins: A case study of the Yangtze River. *J. Geophys. Res. Earth Surf.* **2022**, *127*, e2021JF006573. [CrossRef]
19. Shi, K.; Zhang, Y.; Zhu, G.; Qin, B.; Pan, D. Deteriorating water clarity in shallow waters: Evidence from long term MODIS and in-situ observations. *Int. J. Appl. Earth Obs. Geoinf.* **2018**, *68*, 287–297. [CrossRef]
20. Chen, J.; Quan, W.; Cui, T.; Song, Q. Estimation of total suspended matter concentration from MODIS data using a neural network model in the China eastern coastal zone. *Estuar. Coast. Shelf Sci.* **2015**, *155*, 104–113. [CrossRef]
21. Kitsikoudis, V.; Sidiropoulos, E.; Hrissanthou, V. Assessment of sediment transport approaches for sand-bed rivers by means of machine learning. *Hydrol. Sci. J.* **2015**, *60*, 1566–1586. [CrossRef]
22. Bhattacharya, B.; Price, R.K.; Solomatine, D.P. Machine Learning Approach to Modeling Sediment Transport. *J. Hydraul. Eng.* **2007**, *133*, 440–450. [CrossRef]
23. Becker, R.H.; Sayers, M.; Dehm, D.; Shuchman, R.; Quintero, K.; Bosse, K.; Sawtell, R. Unmanned aerial system based spectroradiometer for monitoring harmful algal blooms: A new paradigm in water quality monitoring. *J. Great Lakes Res.* **2019**, *45*, 444–453. [CrossRef]
24. Cheng, K.; Chan, S.N.; Lee, J.H. Remote sensing of coastal algal blooms using unmanned aerial vehicles (UAVs). *Mar. Pollut. Bull.* **2020**, *152*, 110889. [CrossRef] [PubMed]
25. Ying, H.; Xia, K.; Huang, X.; Feng, H.; Yang, Y.; Du, X.; Huang, L. Evaluation of water quality based on UAV images and the IMP-MPP algorithm. *Ecol. Inform.* **2021**, *61*, 101239. [CrossRef]
26. Droppo, I.G. Suspended sediment transport–flocculation and particle characteristics. In *Encyclopedia of Hydrological Sciences*; John Wiley & Sons, Ltd.: Hoboken, NJ, USA, 2006. [CrossRef]

27. Merritt, W.S.; Letcher, R.A.; Jakeman, A.J. A review of erosion and sediment transport models. *Environ. Model. Softw.* **2003**, *18*, 761–799. [CrossRef]
28. Lee, B.J.; Toorman, E.; Fettweis, M. Multimodal particle size distributions of fine-grained sediments: Mathematical modeling and field investigation. *Ocean Dyn.* **2014**, *64*, 429–441. [CrossRef]
29. Escobar, S.; Bi, Q.; Fettweis, M.; Wongsoredjo, S.; Monbaliu, J.; Toorman, E. A dynamic 2DH flocculation model for coastal domains. *Ocean Dyn.* **2023**, *73*, 333–358. [CrossRef]
30. Bi, Q.; Vanlede, J. Implementation of multi-class flocculation model in TELEMAC modelling system: Sub report 1. The code development. *FHR Rep.* **2022**, *VIII*, 40 + 48 p. [CrossRef]
31. Bi, Q.; Lee, B.J.; Shen, X.; Toorman, E.A.; Smolders, S.; Vanlede, J. Implementing MCPBE flocculation module in TELEMAC and investigating its influence on large-scale sediment transport. In Proceedings of the Abstract book of INTERCOH 2019, Istanbul, Turkey, 13–17 October 2019; pp. 116–118.
32. Shen, X.; Lee, B.J.; Fettweis, M.; Toorman, E.A. A tri-modal flocculation model coupled with TELEMAC for estuarine muds both in the laboratory and in the field. *Water Res.* **2018**, *145*, 473–486. [CrossRef]
33. Sherwood, C.R.; Aretxabaleta, A.L.; Harris, C.K.; Rinehimer, J.P.; Verney, R.; Ferré, B. Cohesive and mixed sediment in the regional ocean modeling system (ROMS v3. 6) implemented in the Coupled Ocean–Atmosphere–Wave–Sediment Transport Modeling System (COAWST r1234). *Geosci. Model Dev.* **2018**, *11*, 1849–1871. [CrossRef]
34. Shen, X.; Toorman, E.A.; Lee, B.J.; Fettweis, M. An approach to modeling biofilm growth during the flocculation of suspended cohesive sediments. *J. Geophys. Res. Ocean.* **2019**, *124*, 4098–4116. [CrossRef]
35. Lee, B.J.; Toorman, E.; Molz, F.J.; Wang, J. A two-class population balance equation yielding bimodal flocculation of marine or estuarine sediments. *Water Res.* **2011**, *45*, 2131–2145. [CrossRef]
36. Ho, Q.N.; Fettweis, M.; Spencer, K.L.; Lee, B.J. Flocculation with heterogeneous composition in water environments: A review. *Water Res.* **2022**, *213*, 118147. [CrossRef] [PubMed]
37. Yao, Q.; Wang, X.; Jian, H.; Chen, H.; Yu, Z. Behavior of suspended particles in the Changjiang Estuary: Size distribution and trace metal contamination. *Mar. Pollut. Bull.* **2016**, *103*, 159–167. [CrossRef] [PubMed]
38. Walch, H.; von der Kammer, F.; Hofmann, T. Freshwater Suspended Particulate Matter–Key Components and Processes in Floc Formation and Dynamics. *Water Res.* **2022**, *220*, 118655. [CrossRef] [PubMed]
39. Maggi, F. Flocculation Dynamics of Cohesive Sediment. Ph.D. Dissertation, Delft University of Technology, Delft, The Netherlands, 2005.
40. Kim, J.I.; Lee, B.J. Investigation on Flocculi-floc Interaction and Flocculation in Extracellular Polymeric Substances, Ionic Species and Clay-containing Suspension. *J. Korean Soc. Water Environ.* **2020**, *36*, 185–193. [CrossRef]
41. Nguyen, H.D.; Nurhayati, M.; Pham, T.T.T.; Lee, B.J.; Park, J.; Shon, H.K.; Lee, S. Updated measurement method for transparent exopolymer particles (TEPs) and their precursors with insights into efficient monitoring. *Desalination* **2024**, *591*, 117975. [CrossRef]
42. Villacorte, L.O.; Ekowati, Y.; Winters, H.; Amy, G.L.; Schippers, J.C.; Kennedy, M. Characterisation of transparent exopolymer particles (TEP) produced during algal bloom: A membrane treatment perspective. *Desalination Water Treat.* **2013**, *51*, 1021–1033. [CrossRef]
43. Ivar do Sul, J.A.; Costa, M.F. The present and future of microplastic pollution in the marine environment. *Environ. Pollut.* **2014**, *185*, 352–364. [CrossRef] [PubMed]
44. Dusaucy, J.; Gateuille, D.; Perrette, Y.; Naffrechoux, E. Microplastic pollution of worldwide lakes. *Environ. Pollut.* **2021**, *284*, 117075. [CrossRef] [PubMed]
45. Mani, T.; Primpke, S.; Lorenz, C.; Gerdts, G.; Burkhardt-Holm, P. Microplastic pollution in benthic midstream sediments of the Rhine River. *Environ. Sci. Technol.* **2019**, *53*, 6053–6062. [CrossRef] [PubMed]
46. Joest Andersen, T.; Rominikan, S.; Stuhr Laursen, I.; Hofer Skinnebach, K.; Zaza Grube, N.; Jedal, S.R.; Nyboe Laursen, S.; Fruergaard, M. Flocculation of microplastic and cohesive sediment in natural seawater. In Proceedings of the EGU General Assembly Conference Abstracts, Sharing Geoscience Online, Virtual, 4–8 May 2020; p. 13617.
47. Lapointe, M.; Farner, J.M.; Hernandez, L.M.; Tufenkji, N. Understanding and improving microplastic removal during water treatment: Impact of coagulation and flocculation. *Environ. Sci. Technol.* **2020**, *54*, 8719–8727. [CrossRef]
48. Cai, L.; Wang, J.; Peng, J.; Wu, Z.; Tan, X. Observation of the degradation of three types of plastic pellets exposed to UV irradiation in three different environments. *Sci. Total Environ.* **2018**, *628*, 740–747. [CrossRef] [PubMed]
49. Lee, K.; Stoffyn-Egli, P. Characterization of oil-mineral aggregates. *Int. Oil Spill Conf.* **2001**, *2001*, 991–996. [CrossRef]
50. Wood, P.; Lunel, T.; Daniel, F.; Swannell, R.; Lee, K.; Stoffyn-Egli, P. Influence of oil and mineral characteristics on oil-mineral interaction. In Proceedings of the Arctic and Marine Oilspill Program Technical Seminar, Environment Canada, Ottawa, ON, Canada, 10–12 June 1998; pp. 51–77.
51. Fettweis, M.; Lee, B.J. Spatial and seasonal variation of biomineral suspended particulate matter properties in high-turbid nearshore and low-turbid offshore zones. *Water* **2017**, *9*, 694. [CrossRef]
52. Fettweis, M.; Schartau, M.; Desmit, X.; Lee, B.J.; Terseleer, N.; Van der Zande, D.; Parmentier, K.; Riethmüller, R. Organic matter composition of biomineral flocs and its influence on suspended particulate matter dynamics along a nearshore to offshore transect. *J. Geophys. Res. Biogeosciences* **2022**, *127*, e2021JG006332. [CrossRef]
53. Spencer, K.L.; Wheatland, J.A.; Bushby, A.J.; Carr, S.J.; Droppo, I.G.; Manning, A.J. A structure–function based approach to floc hierarchy and evidence for the non-fractal nature of natural sediment flocs. *Sci. Rep.* **2021**, *11*, 14012. [CrossRef] [PubMed]

54. Conde-Frias, M.; Ghisalberti, M.; Lowe, R.J.; Abdolahpour, M.; Etminan, V. The Near-Bed Flow Structure and Bed Shear Stresses Within Emergent Vegetation. *Water Resour. Res.* **2023**, *59*, e2022WR032499. [CrossRef]
55. Glover, H.E.; Ogston, A.S.; Miller, I.M.; Eidam, E.F.; Rubin, S.P.; Berry, H.D. Impacts of Suspended Sediment on Nearshore Benthic Light Availability Following Dam Removal in a Small Mountainous River: In Situ Observations and Statistical Modeling. *Estuaries Coasts* **2019**, *42*, 1804–1820. [CrossRef]
56. Herman, P.M.J.; Middelburg, J.J.; Heip, C.H.R. Benthic community structure and sediment processes on an intertidal flat: Results from the ECOFLAT project. *Cont. Shelf Res.* **2001**, *21*, 2055–2071. [CrossRef]
57. Stone, M.; Collins, A. A Review of Literature on Cohesive Sediment Transport Processes, Methodological Frameworks and Management Strategies in Relation to the North Saskatchewan and Other Alberta Rivers. Alberta Environment: Edmonton, AB, Canada, 2010. Available online: https://open.alberta.ca/dataset/review-of-literature-on-cohesive-sediment-transport-processes#summary (accessed on 6 December 2024).
58. Mehta, A.J. *An Introduction to Hydraulics of Fine Sediment Transport*; World Scientific: Hackensack, NJ, USA, 2014; Volume 38, p. 1060.
59. TT, H.; Hur, J.; Lee, B. Formation and Deformation of the Fluid Mud Layer on Riverbeds under the Influence of the Hydrological Property and Organic Matter Composition. *J. Korean Soc. Water Environ.* **2024**, *59*, 79–88. [CrossRef]
60. Cho, Y.-H.; Baek, J.-W.; An, S.-U.; Yoo, H.-J.; Baek, H.-M.; Choi, J.Y.; Kim, T.H.; Kim, K.-T.; Lee, J.S.; Kim, S.-H. Benthic Respiration and Heavy Metal Benthic Fluxes in Artificial Shihwa Lake: Approaching In Situ Measurement. *J. Mar. Sci. Eng.* **2023**, *11*, 2186. [CrossRef]
61. Wu, Y.; Leng, Z.; Li, J.; Yan, C.; Wang, X.; Jia, H.; Chen, L.; Zhang, S.; Zheng, X.; Du, D. Sulfur mediated heavy metal biogeochemical cycles in coastal wetlands: From sediments, rhizosphere to vegetation. *Front. Environ. Sci. Eng.* **2022**, *16*, 102. [CrossRef]
62. Wu, N.; Grieve, S.W.; Manning, A.J.; Spencer, K.L. Flocs as vectors for microplastics in the aquatic environment. *Nat. Water* **2024**, *2*, 1082–1090. [CrossRef]
63. Christiansen, D.E.; Markstrom, S.L.; Hay, L.E. Impacts of climate change on the growing season in the United States. *Earth Interact.* **2011**, *15*, 1–17. [CrossRef]
64. Douglas, B.C.; Peltier, W.R. The puzzle of global sea-level rise. *Phys. Today* **2002**, *55*, 35–41. [CrossRef]
65. Church, J.A.; Godfrey, J.S.; Jackett, D.R.; McDougall, T.J. A model of sea level rise caused by ocean thermal expansion. *J. Clim.* **1991**, *4*, 438–456. [CrossRef]
66. Lu, X.; Ran, L.; Liu, S.; Jiang, T.; Zhang, S.; Wang, J. Sediment loads response to climate change: A preliminary study of eight large Chinese rivers. *Int. J. Sediment Res.* **2013**, *28*, 1–14. [CrossRef]
67. de Oliveira Fagundes, H.; de Paiva, R.C.D.; Brêda, J.P.L.F.; Fassoni-Andrade, A.C.; Borrelli, P.; Fan, F.M. An assessment of South American sediment fluxes under climate changes. *Sci. Total Environ.* **2023**, *879*, 163056. [CrossRef] [PubMed]
68. Li, D.; Li, Z.; Zhou, Y.; Lu, X. Substantial Increases in the Water and Sediment Fluxes in the Headwater Region of the Tibetan Plateau in Response to Global Warming. *Geophys. Res. Lett.* **2020**, *47*, e2020GL087745. [CrossRef]
69. Linderholm, H.W. Growing season changes in the last century. *Agric. For. Meteorol.* **2006**, *137*, 1–14. [CrossRef]
70. Robeson, S.M. Increasing growing-season length in Illinois during the 20th century. *Clim. Chang.* **2002**, *52*, 219–238. [CrossRef]
71. Galen, C.; Stanton, M.L. Responses of snowbed plant species to changes in growing-season length. *Ecology* **1995**, *76*, 1546–1557. [CrossRef]
72. Tavakoli, M.; De Smedt, F. Impact of Climate Change on Streamflow and Soil Moisture in the Vermilion Basin, Illinois. *J. Hydrol. Eng.* **2012**, *17*, 1059–1070. [CrossRef]
73. Erler, A.R.; Frey, S.K.; Khader, O.; d'Orgeville, M.; Park, Y.-J.; Hwang, H.-T.; Lapen, D.R.; Peltier, W.R.; Sudicky, E.A. Evaluating Climate Change Impacts on Soil Moisture and Groundwater Resources Within a Lake-Affected Region. *Water Resour. Res.* **2019**, *55*, 8142–8163. [CrossRef]
74. Krone, R.B. *Flume Studies of the Transport of Sediment in Estuarial Shoaling Processes: Final Report*; Hydraulic Engineering Laboratory and Sanitary Engineering Research Laboratory: Berkeley, CA, USA, 1962; p. 110.
75. Tsai, C.-H.; Iacobellis, S.; Lick, W. Flocculation of Fine-Grained Lake Sediments Due to a Uniform Shear Stress. *J. Great Lakes Res.* **1987**, *13*, 135–146. [CrossRef]
76. Lick, W.; Huang, H. Flocculation and the physical properties of flocs. *Nearshore Estuar. Cohesive Sediment Transp.* **1993**, *42*, 21–39. [CrossRef]
77. Mikkelsen, O.A.; Hill, P.S.; Milligan, T.G. Single-grain, microfloc and macrofloc volume variations observed with a LISST-100 and a digital floc camera. *J. Sea Res.* **2006**, *55*, 87–102. [CrossRef]
78. Mietta, F.; Chassagne, C.; Manning, A.J.; Winterwerp, J.C. Influence of shear rate, organic matter content, pH and salinity on mud flocculation. *Ocean Dyn.* **2009**, *59*, 751–763. [CrossRef]
79. Verney, R.; Lafite, R.; Claude Brun-Cottan, J.; Le Hir, P. Behaviour of a floc population during a tidal cycle: Laboratory experiments and numerical modelling. *Cont. Shelf Res.* **2011**, *31*, S64–S83. [CrossRef]
80. Tran, D.; Strom, K. Suspended clays and silts: Are they independent or dependent fractions when it comes to settling in a turbulent suspension? *Cont. Shelf Res.* **2017**, *138*, 81–94. [CrossRef]
81. Ye, L.; Penaloza-Giraldo, J.; Manning, A.; Holyoke, J.; Hsu, T.-J. Biophysical flocculation reduces variability of cohesive sediment settling velocity. *Commun. Earth Environ.* **2023**, *4*, 138. [CrossRef]

82. Manning, A.J.; Dyer, K.R. The use of optics for the in situ determination of flocculated mud characteristics. *J. Opt. A Pure Appl. Opt.* **2002**, *4*, S71. [CrossRef]
83. Manning, A.; Dyer, K. Mass settling flux of fine sediments in Northern European estuaries: Measurements and predictions. *Mar. Geol.* **2007**, *245*, 107–122. [CrossRef]
84. Spencer, K.; Wheatland, J.; Carr, S.; Manning, A.; Bushby, A.; Gu, C.; Botto, L.; Lawrence, T. Quantification of 3-dimensional structure and properties of flocculated natural suspended sediment. *Water Res.* **2022**, *222*, 118835. [CrossRef]
85. Lee, B.J.; Schlautman, M.A. Effects of polymer molecular weight on adsorption and flocculation in aqueous kaolinite suspensions dosed with nonionic polyacrylamides. *Water* **2015**, *7*, 5896–5909. [CrossRef]
86. Ho, Q.N.; Fettweis, M.; Hur, J.; Desmit, X.; Kim, J.I.; Jung, D.W.; Lee, S.D.; Lee, S.; Choi, Y.Y.; Lee, B.J. Flocculation kinetics and mechanisms of microalgae-and clay-containing suspensions in different microalgal growth phases. *Water Res.* **2022**, *226*, 119300. [CrossRef]
87. Fettweis, M.; Francken, F.; Pison, V.; Van den Eynde, D. Suspended particulate matter dynamics and aggregate sizes in a high turbidity area. *Mar. Geol.* **2006**, *235*, 63–74. [CrossRef]
88. Eisma, D. Flocculation and de-flocculation of suspended matter in estuaries. *Neth. J. Sea Res.* **1986**, *20*, 183–199. [CrossRef]
89. Villacorte, L.O.; Ekowati, Y.; Neu, T.R.; Kleijn, J.M.; Winters, H.; Amy, G.; Schippers, J.C.; Kennedy, M.D. Characterisation of algal organic matter produced by bloom-forming marine and freshwater algae. *Water Res.* **2015**, *73*, 216–230. [CrossRef]
90. Huber, S.A.; Balz, A.; Abert, M.; Pronk, W. Characterisation of aquatic humic and non-humic matter with size-exclusion chromatography–organic carbon detection–organic nitrogen detection (LC-OCD-OND). *Water Res.* **2011**, *45*, 879–885. [CrossRef] [PubMed]
91. Coble, P.G. Characterization of marine and terrestrial DOM in seawater using excitation-emission matrix spectroscopy. *Mar. Chem.* **1996**, *51*, 325–346. [CrossRef]
92. Fettweis, M.; Riethmüller, R.; Van der Zande, D.; Desmit, X. Sample based water quality monitoring of coastal seas: How significant is the information loss in patchy time series compared to continuous ones? *Sci. Total Environ.* **2023**, *873*, 162273. [CrossRef] [PubMed]
93. Manning, A.; Baugh, J.; Soulsby, R.; Spearman, J.; Whitehouse, R. Cohesive sediment flocculation and the application to settling flux modelling. In *Sediment Transport*; Intech: Rijeka, Croatia, 2011; pp. 91–116. [CrossRef]
94. Manning, A.J.; Bass, S.J.; Dyer, K.R. Preliminary findings from a study of the upper reaches of the Tamar Estuary, UK, throughout a complete tidal cycle: Part II. In-situ floc spectra observations. In *Estuarine and Coastal Fine Sediment Dynamics—Proceedings in Marine Science 8*; Sanford, J.M.L., Schoellhamer, D., Eds.; Elsevier: Amsterdam, The Netherlands, 2006; pp. 15–33.
95. Fettweis, M.; Riethmüller, R.; Verney, R.; Becker, M.; Backers, J.; Baeye, M.; Chapalain, M.; Claeys, S.; Claus, J.; Cox, T.; et al. Uncertainties associated with in situ high-frequency long-term observations of suspended particulate matter concentration using optical and acoustic sensors. *Prog. Oceanogr.* **2019**, *178*, 102162. [CrossRef]
96. Liew, S.C.; Saengtuksin, B.; Kwoh, L.K. Monitoring turbidity and suspended sediment concentration of coastal and inland waters using satellite data. In Proceedings of the 2009 IEEE International Geoscience and Remote Sensing Symposium, Cape Town, South Africa, 12–17 July 2009; pp. II-837–II-839.
97. Qu, L. Remote Sensing Suspended Sediment Concentration in the Yellow River. Ph.D. Dissertation, University of Connecticut, Storrs, CT, USA, 2014.
98. Oxford, M. Remote sensing of suspended sediments in surface waters. *Photogramm. Eng. Remote Sens.* **1976**, *42*, 1539–1545.
99. Giardino, C.; Bresciani, M.; Valentini, E.; Gasperini, L.; Bolpagni, R.; Brando, V.E. Airborne hyperspectral data to assess suspended particulate matter and aquatic vegetation in a shallow and turbid lake. *Remote Sens. Environ.* **2015**, *157*, 48–57. [CrossRef]
100. Pyo, J.; Duan, H.; Baek, S.; Kim, M.S.; Jeon, T.; Kwon, Y.S.; Lee, H.; Cho, K.H. A convolutional neural network regression for quantifying cyanobacteria using hyperspectral imagery. *Remote Sens. Environ.* **2019**, *233*, 111350. [CrossRef]
101. Mishra, V.; Avtar, R.; Prathiba, A.; Mishra, P.K.; Tiwari, A.; Sharma, S.K.; Singh, C.H.; Chandra Yadav, B.; Jain, K. Uncrewed Aerial Systems in Water Resource Management and Monitoring: A Review of Sensors, Applications, Software, and Issues. *Adv. Civ. Eng.* **2023**, *2023*, 3544724. [CrossRef]
102. Acharya, B.S.; Bhandari, M.; Bandini, F.; Pizarro, A.; Perks, M.; Joshi, D.R.; Wang, S.; Dogwiler, T.; Ray, R.L.; Kharel, G.; et al. Unmanned Aerial Vehicles in Hydrology and Water Management: Applications, Challenges, and Perspectives. *Water Resour. Res.* **2021**, *57*, e2021WR029925. [CrossRef]
103. Ritchie, J.C.; McHenry, J.R.; Schiebe, F.R.; Wilson, R.B. Relationship of reflected solar radiation and the concentration of sediment in the surface water of reservoirs. *Remote Sens. Earth Resour.* **1975**, *3*, 57–71.
104. Novo, E.; Hansom, J.; Curran, P. The effect of sediment type on the relationship between reflectance and suspended sediment concentration. *Remote Sens.* **1989**, *10*, 1283–1289. [CrossRef]
105. Holyer, R.J. Toward universal multispectral suspended sediment algorithms. *Remote Sens. Environ.* **1978**, *7*, 323–338. [CrossRef]
106. Ligi, M.; Kutser, T.; Kallio, K.; Attila, J.; Koponen, S.; Paavel, B.; Soomets, T.; Reinart, A. Testing the performance of empirical remote sensing algorithms in the Baltic Sea waters with modelled and in situ reflectance data. *Oceanologia* **2017**, *59*, 57–68. [CrossRef]
107. Gould Jr, R.; Arnone, R.; Sydor, M. Absorption, scattering, and, remote-sensing reflectance relationships in coastal waters: Testing a new inversion algorithm. *J. Coast. Res.* **2001**, *17*, 328–341.

108. Gordon, H.R.; Brown, O.B.; Jacobs, M.M. Computed relationships between the inherent and apparent optical properties of a flat homogeneous ocean. *Appl. Opt.* **1975**, *14*, 417–427. [CrossRef] [PubMed]
109. Reif, R.; A'Amar, O.; Bigio, I.J. Analytical model of light reflectance for extraction of the optical properties in small volumes of turbid media. *Appl. Opt.* **2007**, *46*, 7317–7328. [CrossRef] [PubMed]
110. Preisendorfer, R.W. Application of radiative transfer theory to light measurements in the sea. *Union Geod. Geophys. Inst. Monogr.* **1961**, *10*, 11–30.
111. Palmer, S.C.; Kutser, T.; Hunter, P.D. Remote sensing of inland waters: Challenges, progress and future directions. *Remote Sens. Environ.* **2015**, *157*, 1–8. [CrossRef]
112. Lathrop, R.G.; Lillesand, T.M. Monitoring water quality and river plume transport in Green Bay, Lake Michigan with SPOT-1 imagery. *Photogramm. Eng. Remote Sens.* **1989**, *55*, 349–354.
113. LeCun, Y.; Bengio, Y.; Hinton, G. Deep learning. *Nature* **2015**, *521*, 436–444. [CrossRef] [PubMed]
114. Mas, J.F.; Flores, J.J. The application of artificial neural networks to the analysis of remotely sensed data. *Int. J. Remote Sens.* **2008**, *29*, 617–663. [CrossRef]
115. Singh, K.P.; Basant, A.; Malik, A.; Jain, G. Artificial neural network modeling of the river water quality—A case study. *Ecol. Model.* **2009**, *220*, 888–895. [CrossRef]
116. Hosseiny, H.; Masteller, C.C.; Dale, J.E.; Phillips, C.B. Development of a machine learning model for river bed load. *Earth Surf. Dynam.* **2023**, *11*, 681–693. [CrossRef]
117. Chebud, Y.; Naja, G.M.; Rivero, R.G.; Melesse, A.M. Water quality monitoring using remote sensing and an artificial neural network. *Water Air Soil Pollut.* **2012**, *223*, 4875–4887. [CrossRef]
118. Faruk, D.Ö. A hybrid neural network and ARIMA model for water quality time series prediction. *Eng. Appl. Artif. Intell.* **2010**, *23*, 586–594. [CrossRef]
119. Lunetta, R.S.; Schaeffer, B.A.; Stumpf, R.P.; Keith, D.; Jacobs, S.A.; Murphy, M.S. Evaluation of cyanobacteria cell count detection derived from MERIS imagery across the eastern USA. *Remote Sens. Environ.* **2015**, *157*, 24–34. [CrossRef]
120. Balan, M.S.; Das, C.D.A.; Khandelwal, M.; Chaudhari, P. Review of various technologies for depth measurement in estimating reservoir sedimentation. *Int. J. Eng. Res. Technol.* **2013**, *2*, 223–228.
121. Dorokhov, D.; Dudkov, I.; Sivkov, V. Single beam echo-sounding dataset and digital elevation model of the southeastern part of the Baltic Sea (Russian sector). *Data Brief* **2019**, *25*, 104123. [CrossRef] [PubMed]
122. Fenster, M.; FitzGerald, D. Morphodynamics, stratigraphy, and sediment transport patterns of the Kennebec River estuary, Maine, USA. *Sediment. Geol.* **1996**, *107*, 99–120. [CrossRef]
123. Abraham, D.D.; Pratt, T. *Quantification of Bed-Load Transport on the Upper Mississippi River Using Multibeam Survey Data and Traditional Methods*; Coastal and Hydraulics Lab, Engineer Research and Development Center: Vicksburg, MS, USA, 2002.
124. Amiri-Simkooei, A.; Snellen, M.; Simons, D.G. Riverbed sediment classification using multi-beam echo-sounder backscatter data. *J. Acoust. Soc. Am.* **2009**, *126*, 1724–1738. [CrossRef]
125. Mehta, A.J.; Samsami, F.; Khare, Y.P.; Sahin, C. Fluid mud properties in nautical depth estimation. *J. Waterw. Port Coast. Ocean Eng.* **2014**, *140*, 210–222. [CrossRef]
126. Kirichek, A.; Rutgers, R.; Nipius, K.; Ohle, N.; Meijer, H.; Ties, T.; Smits, J. Current surveying strategies in ports with fluid mud layers. In Proceedings of the Hydro18 Conference and Trade Exhibition, Sydney, Australia, 30 October–1 November 2018.
127. Buchanan, L.A. Using a Dual Frequency Echo Sounder for the Determination of Suspended Sediment in the Water Column. In Proceedings of the Western Dredging Association 25th Annual Dredging Conference, New Orleans, LA, USA, 19–23 June 2005; p. 5.
128. Bux, J.; Peakall, J.; Rice, H.P.; Manga, M.S.; Biggs, S.; Hunter, T.N. Measurement and density normalisation of acoustic attenuation and backscattering constants of arbitrary suspensions within the Rayleigh scattering regime. *Appl. Acoust.* **2019**, *146*, 9–22. [CrossRef]
129. Carneiro, J.C.; Gallo, M.N.; Vinzón, S.B. Detection of fluid mud layers using tuning fork, dual-frequency echo sounder, and chirp sub-bottom measurements. *Ocean Dyn.* **2020**, *70*, 573–590. [CrossRef]
130. Schrottke, K.; Becker, M.; Bartholomä, A.; Flemming, B.W.; Hebbeln, D. Fluid mud dynamics in the Weser estuary turbidity zone tracked by high-resolution side-scan sonar and parametric sub-bottom profiler. *Geo-Mar. Lett.* **2006**, *26*, 185–198. [CrossRef]
131. Winterwerp, J.C. A simple model for turbulence induced flocculation of cohesive sediment. *J. Hydraul. Res.* **1998**, *36*, 309–326. [CrossRef]
132. Kuprenas, R.; Tran, D.; Strom, K. A shear-limited flocculation model for dynamically predicting average floc size. *J. Geophys. Res. Ocean.* **2018**, *123*, 6736–6752. [CrossRef]
133. Shen, X.; Maa, J.P.Y. Modeling floc size distribution of suspended cohesive sediments using quadrature method of moments. *Mar. Geol.* **2015**, *359*, 106–119. [CrossRef]
134. Shen, X.; Maa, J.P.Y. A camera and image processing system for floc size distributions of suspended particles. *Mar. Geol.* **2016**, *376*, 132–146. [CrossRef]
135. Maggi, F. Biological flocculation of suspended particles in nutrient-rich aqueous ecosystems. *J. Hydrol.* **2009**, *376*, 116–125. [CrossRef]
136. Mehta, A.J. Depositional Behavior of Cohesive Sediments. Ph.D. Dissertation, University of Florida, Gainesville, FL, USA, 1973.

137. Lick, W. Entrainment, deposition, and transport of fine-grained sediments in lakes. In *Sediment/Freshwater Interaction*; Springer: Dordrecht, The Netherlands, 1982; pp. 31–40.
138. Van Rijn, L.C. *Principles of Sediment Transport in Rivers, Estuaries and Coastal Seas*; Aqua Publications: Amsterdam, The Netherlands, 1993; Volume 1006.
139. Villaret, C.; Hervouet, J.-M.; Kopmann, R.; Merkel, U.; Davies, A.G. Morphodynamic modeling using the Telemac finite-element system. *Comput. Geosci.* **2013**, *53*, 105–113. [CrossRef]
140. Warren, I.; Bach, H.K. MIKE 21: A modelling system for estuaries, coastal waters and seas. *Environ. Softw.* **1992**, *7*, 229–240. [CrossRef]
141. Lesser, G.; Van Kester, J.; Roelvink, J. *On-Line Sediment Transport Within Delft3D-FLOW*; Deltares (WL): Delft, The Netherlands, 2000.
142. Lesser, G.R.; Roelvink, J.A.; van Kester, J.A.T.M.; Stelling, G.S. Development and validation of a three-dimensional morphological model. *Coast. Eng.* **2004**, *51*, 883–915. [CrossRef]
143. Blumberg, A.F.; Mellor, G.L. A description of a three-dimensional coastal ocean circulation model. *Three-Dimens. Coast. Ocean Models* **1987**, *4*, 1–16.
144. Warner, J.C.; Sherwood, C.R.; Signell, R.P.; Harris, C.K.; Arango, H.G. Development of a three-dimensional, regional, coupled wave, current, and sediment-transport model. *Comput. Geosci.* **2008**, *34*, 1284–1306. [CrossRef]
145. Sanford, L.P. Modeling a dynamically varying mixed sediment bed with erosion, deposition, bioturbation, consolidation, and armoring. *Comput. Geosci.* **2008**, *34*, 1263–1283. [CrossRef]
146. Winterwerp, H. On the Dynamics of High-Concentrated Mud Suspensions. Ph.D. Dissertation, Delft University, Delft, The Netherlands, 1999.

APPENDIX 3

Bijdrage voor

AGU Meeting", 9-13 December, Washington DC (USA).

New insights into near-bed SPM concentration and sand/mud fraction in the use of Sediment Composition Index

Duc Tran[1], Romaric Verney[2], Michael Fettweis[1]

Introduction and Approach

This study aims to propose a new approach of combining a pair of optical-acoustic sensors to estimate the total concentration and sediment composition of a sand/mud mixture in an efficient way without an extensive calibration. Specifically, we defined a Sediment Composition Index, such that

$$SCI = 10\log_{10}(OBS) - SNR \qquad (1)$$

where OBS is the signal measured by an Optical Backscatter Sensor and SNR is the signal measured by an ADV, Acoustic Doppler Velocimetry (Pearson et al, 2021). Based on Eq. 1 and a series of 60 experiments, we empirically derived the SCI functions, which allows us to infer the sand/mud fraction, f_{sand}, and total concentration, C.

$$f_{sand} = -0.089*SCI - 0.098 \qquad (2)$$
$$C = 10\text{^}((f_{sand} + SNR)/10) \qquad (3)$$

Such SCI functions (Eq. 2 and 3), were then, applied to in-situ hydro-sedimentary dynamics data at the station MOW1 (3 km offshore of Zeebrugge, Belgium) to investigate the impact of sand mining and beach nourishment activities in the region.

Results and Conclusions

Figure 1 shows that from neap tide towards spring tide the suspended sediment composition changed from more muddy to more sandy. The altitude data revealed that instead of local resuspension of sand, there was some deposition at the time, suggesting a possibility of advection transport of sand from adjacent areas. This observation was confirmed by comparing with the dredging and beach nourishment activities in the area (Kint et al, 2023). Application of SCI functions to other deployments in 2013 also showed a strong correlation between the fraction of sand/mud and total concentration with coastal engineering activities.

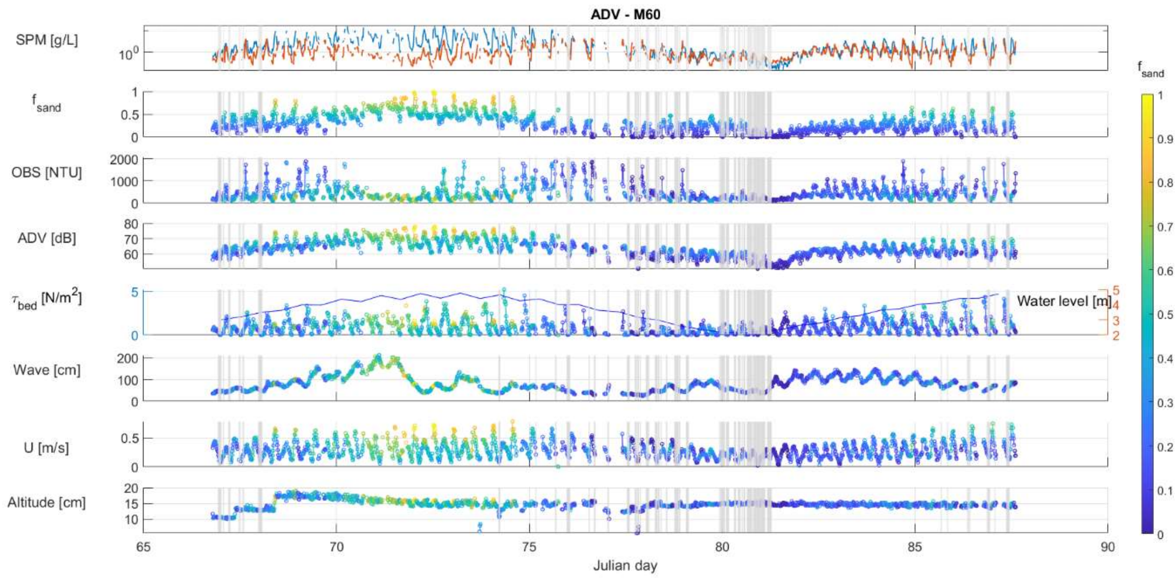

Figure 1. Time series of hydrodynamic conditions, f_{sand} and C. During spring tide, C obtained from OBS were lower than C computed from SCI functions. During neap tide, both Cs from OBS and SCI functions were similar.

In conclusion, results suggest that the use of OBS alone leaves out important information and underestimates the near-bed concentration due to its low sensitivity to sand. SCI lab-based functions is applicable to field data, providing flexibility and efficiency in either revisiting historical field data or for current/future long-term, high-frequency measurements.

References

Kint, L., Barette, F., Degrendele, K., Roche, M., Van Lancker, V., (2023). Sediment variability in intermittently extracted sandbanks in the Belgian part of the North Sea. Frontiers in Earth Science, 11:1154564, DOI: 10.3389/feart.2023.1154564.

Pearson, S., Verney, R., Prooijen, B., Tran, D., Hendriks, E., Jacquet, M., Wang, Z., (2021). Characterizing the composition of sand and mud suspensions in coastal and estuarine environments using combined optical and acoustic measurements. JGR: Ocean, 126(7), e2021JC017354.

Tran, D., Desmit, X., Verney, R., Fettweis, M., (2023). Application of sediment composition index to predict suspended particulate matter concentration in the North Sea. INTECOH 2023, South Korea.